TEHNIČKI GLASNIK

TECHNICAL JOURNAL

TEHNIČKI GLASNIK / TECHNICAL JOURNAL – GODIŠTE / VOLUME 11 – BROJ / NUMBER 1-2

SIJEČANJ-LIPANJ 2017 / JANUARY-JUNE 2017 – STRANICA / PAGES 1-66

/

SVEUČILIŠTE SJEVER / UNIVERSITY NORTH – CROATIA – EUROPE

ISSN 1846-6168 (PRINT) / ISSN 1848-5588 (ONLINE)

TEHNIČKI GLASNIK

TECHNICAL JOURNAL

ISSN 1846-6168 (Print) ISSN 1848-5588 (Online)

TEHNIČKI GLASNIK
TECHNICAL JOURNAL

Znanstveno-stručni časopis Sveučilišta Sjever
Scientific professional journal of University North

Godište (Volume) 11 Broj (Number) 1-2
Varaždin, siječanj-lipanj (January-June) 2017. Stranica (Pages) 1–66

Adresa uredništva (Address of Editorial Office):
Sveučilište Sjever – Tehnički glasnik
Sveučilišni centar Varaždin
104. brigade 3, 42000 Varaždin, Hrvatska;
Tel. ++385/ 42/ 493 328, Fax.++385/ 42/ 493 333
e-mail: tehnickiglasnik@unin.hr
http://tehnickiglasnik.unin.hr
http://www.unin.hr/djelatnost/izdavastvo/tehnicki-glasnik/
http://hrcak.srce.hr/tehnickiglasnik

Osnivač i izdavač (Founder and Publisher):
Sveučilište Sjever

Tisak:
Centar za digitalno nakladništvo, Sveučilište Sjever

Svi objavljeni članci u časopisu su recenzirani (All papers published in journal have been reviewed)
Časopis je besplatan i izlazi u četiri broja godišnje (The journal is free and published four issues per year)

Naklada (Circulation): 100 primjeraka (issues)

Časopis je referiran u (Journal is reffered in):
EBSCOhost Academic Search Complete, EBSCOhost – One Belt, One Road Reference Source Product, ERIH PLUS, CITEFACTOR – Academic Scientific Journals
Hrčak - Portal znanstvenih časopisa RH

Rukopisi se ne vraćaju (Manuscripts are not returned)

Registracija časopisa (Registration of journal):
Časopis "Tehnički glasnik" upisan je u Upisnik HGK o izdavanju i distribuciji tiska 18. listopada 2007. godine pod rednim brojem 825.

Uređenje zaključeno (Preparation ended):
lipanj (June) 2017.

CONTENT

Note from the Editor-in-Chief

Dear readers,

It is my pleasure to present this year's double issue of the journal **Tehnički Glasnik-Technical Journal**, number 1-2, year 11. Precisely, we are in the 11th year of regular publishing. Unfortunately, the second year in a row we did not manage to accomplish the planned dynamic of publishing four issues annually. Thus, we are forced to publish a double issue instead of numbers 1 and 2. Perhaps that is not so terrible since we are trying to retain the quality of published works on a level that will enable the journal to be included in significant databases.

It is my opinion, much like of many others, that databases should not be glorified and mystified because the criteria for the acceptance of journals are largely of solely formal nature; i.e., what is valued by the databases is the number of published works per volume, the number of published original scientific articles, the presence on the Internet, etc. Moreover, it is worth noting, and it can be read in **The San Francisco Declaration on Research Assessment** (**DORA**) (http://www.ascb.org/dora/), that the impact factor is calculated according to the Thomson Reuters Corporation, the owner of estimated bibliographical databases Current Contents, Web of Science, and Journal Citation Reports. It was initially created to make it easier for the libraries to recognize articles to be purchased, i.e., it was not created with the purpose of evaluating scientific quality of articles in journals. However, since everyone is trying to become a member of the community of journals which are in these databases, we will continue along that path as well.

With great devotion, both the authors' and the reviewers', we have managed to complete this double issue of our journal with ten chosen articles that were edited by the authors upon the reviewers' comments into the shape that lies in front of you. Since the first decade of publishing is behind us, at the beginning of the new decade, we have decided to change the journal front cover design, its format, and the template of the articles. The author of the cover is Assoc. Prof. Mario Tomiša, Ph.D., whom we thank warmly for the solution.

In the end, as always, we welcome you, our dear readers, to use your input to contribute to our joint work and permanent endeavor to retain the quality of our joint journal.

Best wishes,

Full. Prof. Milan Kljajin, Ph.D.
Editor-in-Chief
Tehnički Glasnik-Technical Journal

ISSN 1846-6168 (Print), ISSN 1848-5588 (Online)
ID: TG-20161002131245

Original scientific article

EFFECT OF SOIL PROPERTIES ON RC WALL RESPONSES

Widad BOUROUAIAH, Salah KHALFALLAH, Dhahbia GUERDOUH

Abstract: All reinforced concrete structures and buildings in contact with soil are directly affected by the interaction between the soil foundation and the structure. In this work, a nonlinear analysis of wall and flexible foundations under monotonous loading is investigated. The plasticity theory using the finite element concept is used to simulate the structure and the soil media responses. This work integrates the behavior of the soil and the structure to obtain the whole structure response. The fixed base assumption does not reflect the real behavior of the structure, but soil properties show an influence on the system response. As conclusion, vertical displacements are significant through the foundation space but horizontal ones are very important in deep levels of soil.

Keywords: soil-structure interaction, soil-properties, plasticity, nonlinear analysis, soil-wall system, monotonic loadings.

1 INTRODUCTION

In reality, all reinforced concrete structures often in contact with the soil require the integration of the behavior of the interface between the structure and the soil. For this reason, the behavior of the entire structure depends on the structure itself, the soil foundation, and the continuum interface between them. The structure and the soil contribute together against the external loadings. This phenomenon is known as the soil-structure interaction (SSI), which is generally neglected in the design codes of civil buildings. However, for structures and buildings resting on soft soils, the effect of the soil-structure interaction becomes a very significant factor [1].

In civil construction calculations, the assumption of fixed base is often considered. This consideration neglects the flexibility of the resting soil. In reality, supporting soil influences the structural response by permitting movement to some extent due to its natural ability to deform. The soil-structure interaction effect enables designers to evaluate real displacements of the soil-structure system under static and/or seismic loading.

In the literature, numerous studies have been published taking into account the effect of soil-structure interaction under static loading [2]. Some of these works have been elaborated with simplified models for several reasons [3-6] showing that the stiffness of the soil has an important effect on the distribution of internal actions in the structure. Moreover, numerous studies have been conducted to estimate internal forces in structural members. Zolghadr et al. [7] investigated the modeling of coupled soil-structure interaction using the decomposition technique. Chore et al. [6] studied the effect of soil-structure interaction of a single storey having two bay space frames resting on a group of piles.

The soil-structure interaction has been studied using analytical models [8], numerical models [9], and nonlinear models [10]. In this concept, Rajashekhar et al. [11] modeled soil-structure interaction of a 3D-frame resting on deformable foundation to study the interaction elements between the mat foundation and the soil; they concluded that the interface elements do not have an effect on the member end actions of the building but can highly affect the displacement field.

The interaction phenomenon has become a very important task in the design phase. Until now, the soil structure interaction has been taken into account only in research [12-14]. In this study, the influence of soil nature basing on the soil mechanical properties is established.

The soil behavior is different from traditional materials such as steel or concrete. The mechanical behavior of soil can be considered linear when deformations are not too large. However, mechanical properties of soils are often strongly nonlinear with plastic deformations during loading and unloading process. Additionally, the inhomogeneous structure of soil and the mechanical behavior are hard to predict the real response of soil and structure.

Important publications in the last three decades showed that most of the investigators take into account the effect of soil structure interaction. In this field, Toutanji [15] presented a simplified procedure based on the continuum approach for static analysis of regular structures combined with shear walls and frames and investigated the effect of flexibility of foundation using Winkler spring model. Badie et al. [16] presented a new method for analyzing wall-structures built on elastic foundations. Here, the soil is modeled using three-nodded elements including the vertical sub grade reaction and soil shear stiffness.

Baknahad et al. [17] and Nadjai et al. [18] investigated the importance of base flexibility on the elastic behavior of planar shear walls subjected to lateral loading. Oztorun et al. [19] presented a 3D finite element analysis of multi-story building structures composed of opening shear walls and flat plates. Boroschek et al. [20] developed a simple analytical model considering basic assumptions that were used to compare with recorded responses.

For these objectives, Tabatabaiefar et al. [21] studied the responses of frame under lateral seismic loading. This work leads to the conclusion that the dynamic soil-structure

interaction plays a considerable role in seismic behavior of frames including large lateral deflections and inter-storey drifts.

Finally, this work is the first one that must be established before initiating the nonlinear dynamic analysis of the soil-structure interaction.

2 MODELING OF THE SOIL STRUCTURE SYSTEM

Many methods have been already developed to study the soil-structure interaction. In this work, the direct method is employed, where the entire soil-structure system is modeled in a unique step. The use of the direct method required the development of a numerical program, which can treat the behavior of both soil and structure with identical rigidities [22]. The structure is submitted to external loads, which can be static and/or dynamic loadings (Fig. 1).

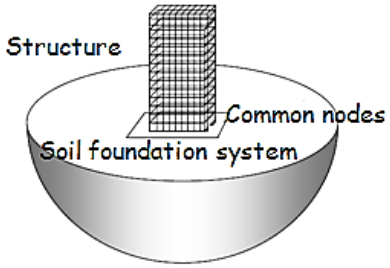

Figure 1 Idealization of soil-structure system

To obtain desired results, a numerical program was developed to simulate the nonlinear soil-structure behavior. The structure is a reinforced concrete wall resisting on soil media. The structure and the soil are discretized into two-dimensional quadrilateral finite elements. Each element behaves according to the prescribed nonlinear stress-strain law.

Two-dimensional plane strain and plane stress elements are used to model the soil medium and the wall structure, respectively. Along the frontier, fixed boundaries are used to represent the bed rock and quiet boundaries to avoid horizontal displacements.

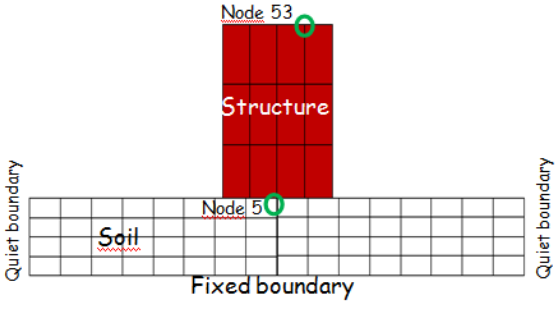

Figure 2 2D Soil-wall system

3 CONSTITUTIVE MODELING

In this section, the elasto-plastic model is considered. The constitutive laws governing the elasto-plastic behavior of 2D-dimensionnel solid elements are described by the plastic potential, the normality condition, plastic flow, and the hardening of the material. The mathematical theory of plasticity leads to provide the constitutive relationship between stress and strain vectors. The plastic behavior of materials is characterized by an irreversible straining, which depends on the level of stress that has been reached.

The external loading is applied in monotonous manner to describe the material behavior and the interface continuum. In general, (1) a relationship between stress and strain must be formulated to describe the elastic material behavior, (2) a yield criterion must be chosen to differentiate between elastic and elasto-plastic behaviors, and (3) a relationship between stress and strain must be described in the post yielding range.

3.1 Material elastic behavior

Before the initial yielding surface, the relationship between stress and strain obeys the linear elastic expression.

$$\sigma_{ij} = D_{ijkl}\varepsilon_{kl} \tag{1}$$

σ_{ij} and ε_{kl} are stress and strain components, respectively, and D_{ijkl} is the elastic tensor.

3.2 Yielding criterion

A surface function must be defined to delimit the elastic and the elasto-plastic behaviors. When the yielding curve is reached, then the material changes its behavior. In the elasto-plastic behavior range, the permanent deformation appears and is considered as an indicator of the beginning of elasto-plastic region. The criterion is defined in stress space by:

$$f(\sigma_{ij}) = K(k) \tag{2}$$

where f is a stress function and K is a material parameter describing the hardening phenomenon. In this study, the Von Mises criterion is adopted in the analysis.

3.3 Strain hardening

After initial yielding, the stress level depends on the plastic hardening. Thus, the yield surface varies with the plastic deformation. In this work, the actual yield surfaces are obtained by a uniform expansion of the initial yield surface "isotropic hardening". In this work, the total work hardening is postulated as the total work during the plastic strain.

$$W_P = \int_0^{\varepsilon_p} \sigma_{ij} d\varepsilon_{ij}^P \tag{3}$$

$d\varepsilon_{ij}^{P}$ is the plastic stain vector.

In this study, the hardening parameter is assumed to be defined as the equivalent plastic strain.

$$K = \sqrt{\frac{2}{3}} \quad (d\varepsilon_{ij}^{P})^{t}.(d\varepsilon_{ij}^{P}) \tag{4}$$

3.4 Elasto-plastic stress-strain relationship

The total strain can be divided into an elastic part and a plastic part.

$$d\varepsilon_{ij} = d\varepsilon_{ij}^{e} + d\varepsilon_{ij}^{p} \tag{5}$$

The plastic strain increment is proportional to the stress gradient of plastic potential using the associated plasticity. Then, it can be written as:

$$d\varepsilon_{ij}^{p} = d\lambda \frac{\partial f}{\partial \sigma_{ij}} \tag{6}$$

where $d\lambda$ is the plastic multiplier.

In the elasto-plastic region, the stress-strain relationship can be written as:

$$d\sigma_{ij} = D_{ijkl}^{ep}\varepsilon_{kl}^{e} \tag{7}$$

where D_{ijkl}^{ep} is the elasto-plastic tensor that can be expressed by:

$$D_{ijkl}^{ep} = D_{ijkl}^{e} - \frac{D_{ijkl}^{e}\cdot\frac{\partial f}{\partial \sigma_{ij}}.(\frac{\partial f}{\partial \sigma_{ij}})^{t} D_{ijkl}^{e}}{-\mathrm{A}+(\frac{\partial f}{\partial \sigma_{ij}})^{t}.D_{ijkl}^{e}\cdot\frac{\partial f}{\partial \sigma_{ij}}} \tag{8}$$

The hardening parameter A is neglected for elasto-perfectly plastic behavior.

4 NUMERICAL EXAMPLES

The proposed approach has been applied to analyze the behavior of a wall-structure combined with the soil media. The geometrical data of the structure, the soil media and loading are presented in Fig. 3.

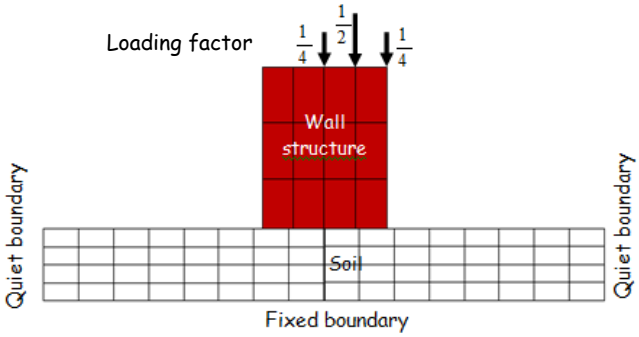

Figure 3 Geometry and loading of wall-structure system

To establish this investigation, the following finite element mesh was arranged (Fig. 3) considering:

- Non-interactive model.
- Interactive nonlinear material model for the wall and the soil media.
- To investigate the effect of different soil stiffness, three types of soil have been selected. The material properties of the soil media are adopted covering the general idea.
- To pronounce the behavior of the interface, horizontal and vertical displacements are deducted.
- Finally, the influence of the wall height on the interface level is established.

The Tab. 1 regroups the mechanical properties of materials used in this work.

Table 1 Properties of materials used

Material	Young's modulus (MPa)	Poisson's ratio	Width (m)	Yielding stress (MPa)	Friction	Hardening
Concrete	207.E+7	0.20	0.30	18.E+6	0.00	0.00
Soil	0.7E+6	0.40	12.0	0.1E+5	0.00	0.00

The dimensions of wall-structure and the soil media are:

- The wall-structure is (1): 4×9×0.3 m, (2): 4×18×0.3 m and (3): 4×27×0.3 m)
- The soil media is 12×5×12 m
- The weight of the structure is neglected and only the external load is applied monotonically.

5 RESULTS AND DISCUSSION

RC walls are largely used in buildings as main element of stiff buildings. Walls present an important aptitude to resist to vertical and horizontal loading, indifferently. In this section, the approach was applied to soil-wall system to quantify the response of the structure and the interface between super-structure and soil response.

5.1 Negligence of soil flexibility

In this case, the wall-structure is fixed at its base level.

The applied load vs. the vertical displacement at the node A (Fig. 5) is plotted. This case shows a performance and a strong aptitude of the wall-structure when the rigid base is considered. The curve can be composed into two

branches reflecting the linear and elasto-plastic behavior of the wall, respectively. Fig. 5 presents load versus displacement of the node A.

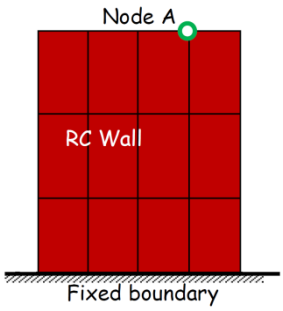

Figure 4 The wall structure fixed at base level

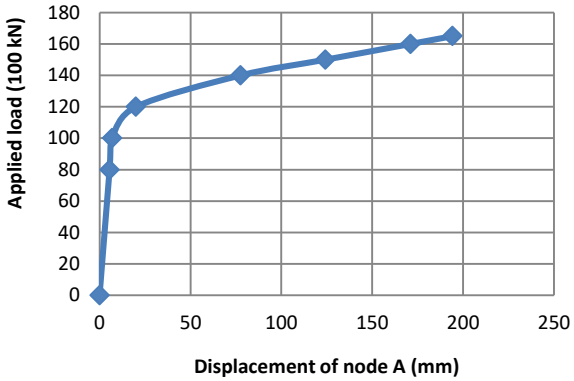

Figure 5 Load versus displacement of fixed wall

5.2 Linear and elasto-plastic analyses

Figs. 6 and 7 plot the linear and elasto-plastic analyses of wall-structure node (Fig. 6) and of interface node (Fig. 7), respectively. For small load values, analyses show concordance between linear and nonlinear analyses until 35% of the limit load. The interface node explains an important deflection compared to the wall node one. In figures (6-7), elasto-plastic curves concave due to the plastic behavior of materials that interprets mechanical degradation corresponding to this level of loading.

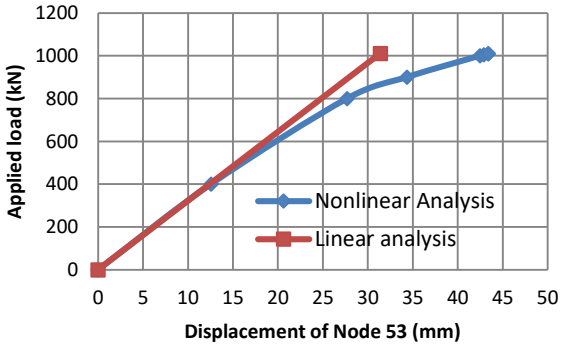

Figure 6 Linear and elasto-plastic analyses of wall node

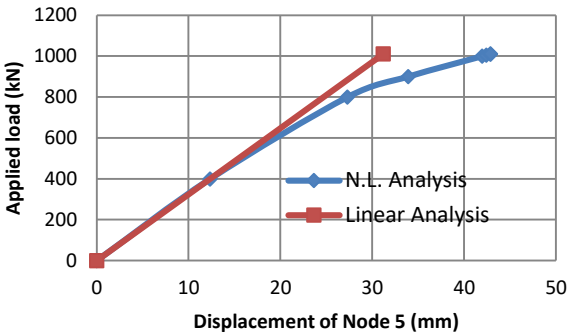

Figure 7 Linear and elasto-plastic analyses of interface node

5.3 Influence of soil properties

For different soil properties, Figs. 8 and 9 show the super-structure node behavior and the interface node behavior, respectively. They present a decrease of mechanical properties of the super-structure and of the soil media in function of the Young's modulus. The vertical displacements are very important in the super-structure node and in the interface level according to the feebleness of Young's modulus values.

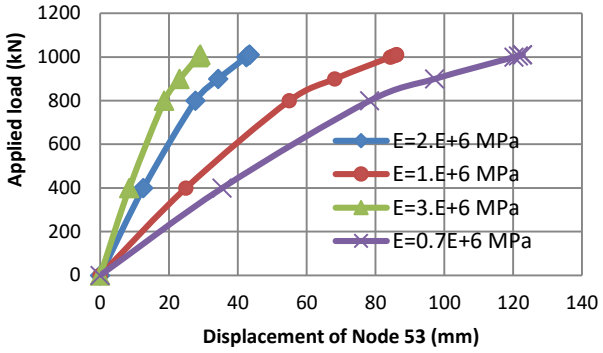

Figure 8 Soil effect on the super-structure node

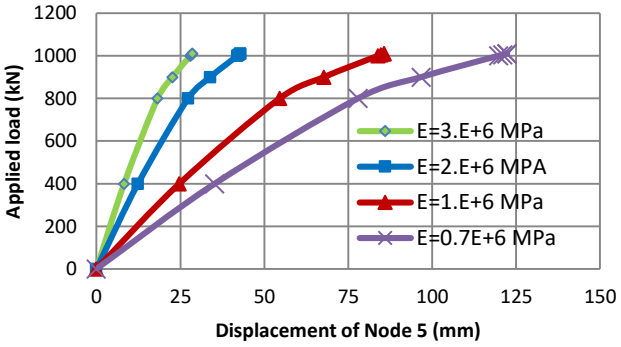

Figure 9 Soil effect on the interface node

5.4 Interface medium responses

Vertical displacements of different deepness are plotted in Fig. 10. The interface medium presents a considerable displacement and apprising far from the contact space between super-structure and soil. The deep level shows a

small vertical displacement and neglected apprising for from the foundation (Fig. 10).

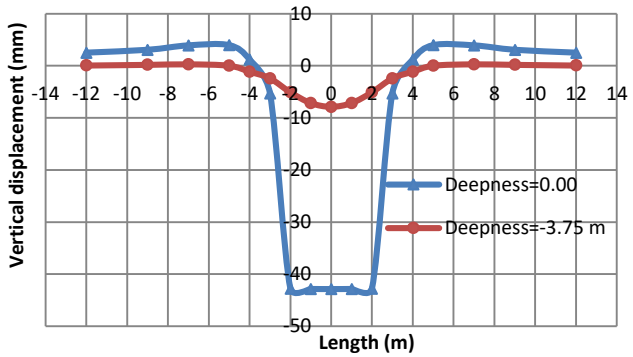

Figure 10 Vertical displacement of different deepness

Opposite to the above conclusions, horizontal displacements are very important if the deepness level is so important in the region under the foundation but they become important for weak deepness far from the foundation. Also, horizontal displacements under foundation are very small at near levels of the foundation (Fig. 11). The horizontal displacements present reciprocal effects for different deepness.

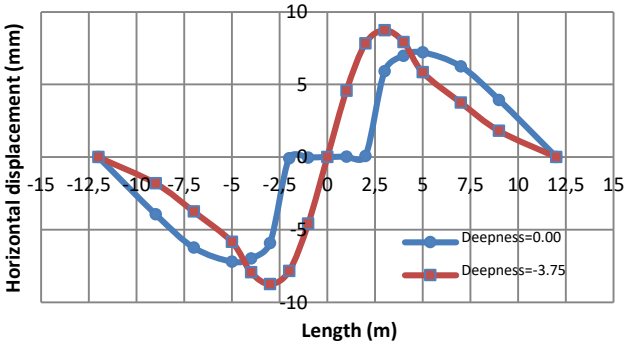

Figure 11 Horizontal displacement of different deepness

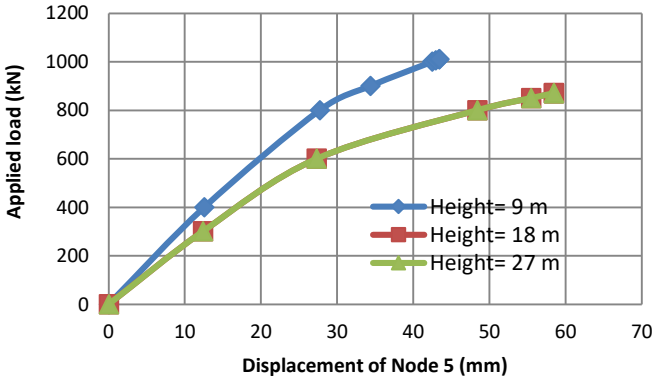

Figure 12 Influence of the wall height

5.5 Interface of the wall height

Only in this case, the wall height does not have an effect on interface continuum from high walls are grater then 18 m (Fig. 12). It seems that soil has been fully sustained a satisfactory and becomes apt to applied loads with very weak deformations.

6 CONCLUSION

Based on obtained results using this approach, the following conclusions can be drawn:

- The fixed base of building presents a performance and an attenuation of structures but this hypothesis is not valid in reality as soon as the bond nature between the structure and the soil.
- Nonlinear analysis of the structure and the soil reproduces faithfully the behavior of the structure. An increase of 15 % of displacement compared to the linear analysis is observed.
- The soil mechanical properties influence primordially on the response of the structure and the interface continuum. In this case, the displacements become important passing from E_s = 300 GPa to E_s = 100 GPa and become very important when E_s = 70 GPa. So, it is recommended to improve the mechanical properties of the soil.
- Vertical displacements are remarkable in the zone localized under the foundation region. These displacements decrease with the increase of the deepness.
- Horizontal displacements are pondering at deep levels under the foundation and become very weak at contact levels.
- In this example, the stability of the interface media behavior is well notable for the wall height (18 m). Probably, it seems that soil has been sustained a satisfactory and becomes apt to support vertical loadings with very weak deformations.

7 REFERENCES

[1] Wolf J. (1985), Dynamic Soil-Structure Interaction. Prentice-Hall International Series in Civil Engineering and Engineering Mechanics. Prentice-Hall.

[2] Dalili S. M., Huat B. B. K., JaafarM. S. and Alkarni, A., (2013), Review of static soil-framed structure interaction. Interaction and Multi-scale Mechanics, Vol. **6(1)**, pp. 51-81.

[3] Lee I. K. and Harrison H. B. (1970), Structure and foundation interaction theor, J. Struct. Div. - ASCE, **96**, pp. 177-197.

[4] King G. J. W. and Yao Z. E. (1983), Simplified interactive analysis of long framed building on raft foundation, J. Struct. Eng., **61B(3)**, pp. 62-67.

[5] Kumar A., Walia B. J. S. H. and Saran S. (2005), Pressure–settlement characteristics of rectangular

footings on reinforced sand, Geotech. Geolog. Eng., **23**, pp. 469-481.

[6] Chore H. S., Ingle R. K. and Sawant V. A. (2010), Building frame – pile foundation –soil interactive analysis: a parametric study, Interact. Multi-scale Mech., **3(1)**, pp. 55-79.

[7] Zolghadr J. H., Izzuddin B. A. and Zdravkovic L. (2007), Partitioned analysis of nonlinear soil-structure interaction using iterative coupling, Interact. Multi-scale Mech., **1(1)**, pp. 33-51.

[8] Teodoru I.-B. (2009), Beams on elastic foundation: The simplified continuum approach. Bulletin of the Polytechnic Institute of Jassy, Constructions, Architechture Section, **55**, pp. 37-45.

[9] Colasanti R. J. and Horvath J. S. (2010), Practical sub-grade model for improved soil-structure interaction analysis: software implementation. Practice Periodical on Structural Design and Construction, **15(4)**, pp. 278-286.

[10] Mazzoni S., Sinclair M. (2013), Modeling of Nonlinear Soil-Foundation-Structure Interaction in Response History Analysis-An Existing-Building Evaluation Case Study. Paper presented at the Structures Congress.

[11] Rajashekhar S. H. M., Krishnamoorthy A., Prabakhara D. L. and Bhavikatti S. S. (2011), Relevance of interface elements in soil structure interaction analysis of three dimensional multi-scale structure on raft foundation, Electron. J. Geotech. Eng., **16B**, pp. 199-218.

[12] Shoaei D., Huat B. B. K., Jaafar M. S., Elkarni A. (2015), Soil- framed interaction analysis – A new interface element. Latin American Journal of Solids and Structures.**12**, pp. 226-249.

[13] Bezih K., Alaa C., Kalla M., Bacconnet C. (2015), Effect of soil structure interaction on the reliability of reinforced concrete bridges. Ain Shams Engineering Journal, **6(3),** pp. 755-766.

[14] Rougui M., Boubel H., Elmarabet O. (2015), Study of the fundamental impact of soil-structure interaction on response of reinforced concrete bridges. 3rd Turkish conference on earthquake and seismology, October 14-16, Izmir, Turkey.

[15] Toutanji H. A. (1997), The effect of foundation flexibility on the interaction between shear walls and frame, Engineering Structures, **19(12)**, pp. 1036 – 1042.

[16] Badie S. S. and Salmon D. C. (1996), A quadratic order elastic foundation finite element, Computers & Structures, **58(3)**, pp. 435-443.

[17] Paknahad M., Noorzaei J., Jaafar M. S., Waleed A. Thanoon (2008), Non-linear soil structure interaction of shear wall system with super element, The 12th International Conference of International Association for Computer Methods and Advances in Geomechanics, 1-6 october 2008, Goa, India.

[18] Nadjai A., Johnson D. (1998), Elastic and Elasto-plastic analysis of planar coupled shear walls with flexible base, Computers and Structures, **68**, pp. 213-229.

[19] Oztorun N. K., Citipitioglu E., Akkas N. (1998),Three-dimensional finite element analysis of shear wall buildings, Computers and Structures, **68**, pp. 41-55.

[20] Boroschek R. L., Fernando, Yanez V. (2000), Experimental verification of basic analytical assumptions used in the analysis of structural wall buildings, Engineering Structures, **22**, pp. 657-669.

[21] Tabatabaiefar S. H. R, Fatahi B. and Samali B. (2013),Lateral seismic response of building frames considering dynamic soil-structure interaction effects, Structural Engineering and Mechanics, **45(3)**, pp. 311-321.

[22] Kramer S. L. (1996), Geotechnical Earthquake Engineering, Prentice Hall Civil Engineering and Engineering Mechanics Series.

Authors' contacts:

Widad BOUROUAIAH,
Laboratoire de Génie Civil et Environnement (LGCE),
Université de Jijel, Jijel, Algérie

Salah KHALFALLAH,
(Corresponding author)
Ecole Nationale Polytechnique de Constantine, Algérie
khalfallah_s25@yahoo.com

Dhahbia GUERDOUH
Laboratoire de Génie Civil et Environnement (LGCE),
Université de Jijel, Jijel, Algérie

ISSN 1846-6168 (Print), ISSN 1848-5588 (Online)
ID: TG-20170126230213

Original scientific article

MATLAB SIMULATION MODEL FOR DYNAMIC MODE OF THE LITHIUM-ION BATTERIES TO POWER THE EV

Ivan BABOSELAC, Željko HEDERIĆ, Tin BENŠIĆ

Abstract: The paper presents a simulation model for the electric vehicles (EV) drive with Lithium-Ion batteries. Explanations of all the input parameters are given. Analysis of the dynamic characteristics of Lithium-Ion batteries was carried out through simulations on standardized driving regime (urban and highway drive cycles). Finally, recuperation of breaking energy of EV is explained.

Keywords: simulation model, Lithium-Ion battery, EV drive, driving cycle

1 INTRODUCTION

Despite the known problems [1, 2] and the development of alternative solutions [3, 4, 5], the development of batteries with increased use of EV has a strong upward trend [6]. Market growth brought lower production rates leading to increased investment in the development of EV. Solutions for the autonomy and longer travel range problems are mainly done in three ways: 1) the design of batteries with a greater energy density [7]; 2) reduction of battery weight; 3) optimization of dynamic modes of charging and discharging the battery [8, 9, 10].

Lithium-Ion battery compared to other battery types has a number of advantages [11]:

- greater efficiency and energy density,
- increased nominal voltages,
- lower specific weight,
- increased lifetime,
- faster and more efficient charging,
- smaller size,
- no need for maintenance,
- greater resistance to external conditions.

One of the disadvantages of Lithium-Ion batteries is that they must not be completely discharged. This shortens their lifetime. Also, discharging a battery with high currents is not recommended since it can cause damage. These disadvantages are commonly avoided by using electronic circuits for protection and for management of charging and discharging the battery.

Dynamic characteristics of Lithium-Ion battery operating in various modes are described and the change of EV operating parameters during charging and discharging of the battery are observed in this paper.

2 MODELLING OF LITHIUM-ION BATTERIES

For the purpose of modelling of the battery, the battery packs and EV drives in different driving modes, the MatLab software is used.

In the MatLab graphical editor Simulink a generic model of Lithium-Ion battery according to Shepherd's model is developed and verified (Fig. 1) [12]. It is modelled as a controlled voltage source dependent on the actual state of the battery charge (SOC).

Idea of this design is the use of a simple procedure to obtain the input parameters for the battery model (shown in Fig. 2) from the battery manufacturer's catalogue data. Within the model, depending on the operating modes, there are different functions for dependency of battery voltage.

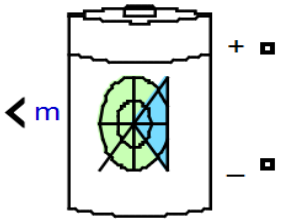

Figure 1 The block mask of Lithium-Ion battery model (SimPowerSystems) [12]

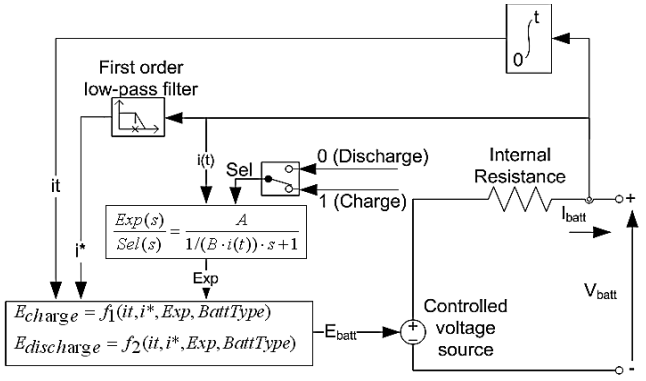

Figure 2 The battery model - block diagram of subsystems within the MATLAB Simulink, which in itself implements a generic model of Lithium-Ion battery [12, 13].

Fig. 3 shows the typical discharge characteristics of Lithium-Ion battery. The characteristics can be separated into three areas. The exponential area that represents battery voltage overshoot above the nominal value. The operating point of the battery is in this area during a period of

establishing a stationary value of discharge current after no-load battery mode.

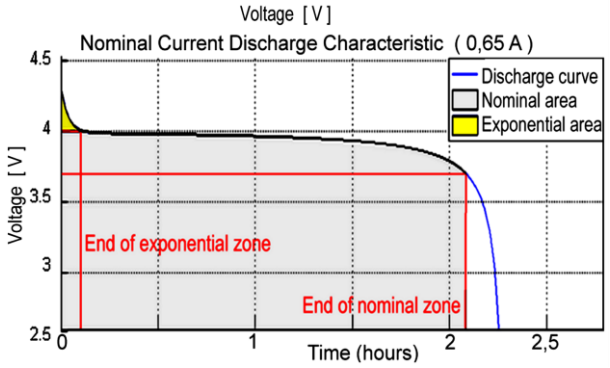

Figure 3 Discharge of the Lithium-Ion battery at nominal discharge current

In the nominal area of the battery operation, during the discharge mode, the voltage is slightly changed. When the nominal capacity of battery power is discharged, it is followed by the third area of operation in which the battery voltage rapidly decreases.

Battery discharge curve, shown as a blue line in Fig. 3, has a nonlinear characteristic and is described by the Eq. (1) in the Shepherd model [11], where the charging current is positive (i^*> 0):

$$f_1\left(i_t, i^*, i\right) = E_0 - K\frac{Q}{Q-i_t}\cdot i^* - K\frac{Q}{Q-i_t}\cdot i_t + \\ + A\cdot exp\left(-B\cdot i_t\right) \qquad (1)$$

where: E_0 − Constant voltage (V), K − Polarization resistance (Ω), i^* − Low frequency current dynamics (A), i − Battery current (A), i_t − Extracted capacity (Ah), Q − Maximum battery capacity (Ah), A − Exponential voltage (V), B − Exponential capacity (Ah^{-1}).

Second member of the equation (1) is the polarization voltage, presented as a product of the polarization resistance and the battery current, describes the behavior of batteries in the unloaded state. In Fig. 4 the changes of the discharge characteristics at different currents are presented.

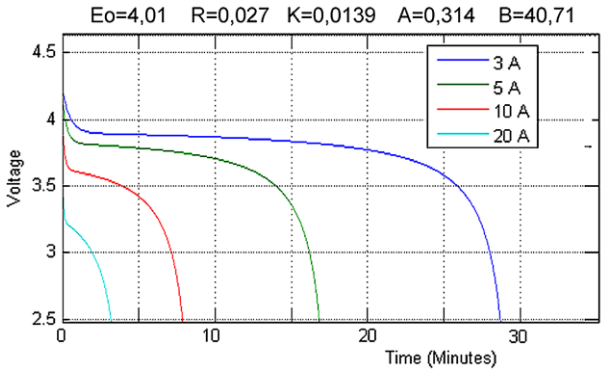

Figure 4 Discharge of the battery at different currents (nominal discharge current is 0.65 A)

Fig. 5 shows the charging curve of the battery and is described by the Eq. (2). It nominally has the inverse shape form of the discharge curve (initially from the empty battery state, through a period of rapid establishment of the nominal voltage, followed by a period of charging at nominal voltage, and finally the exponential area when the no-load voltage is restored).

$$f_2\left(i_t, i^*, i\right) = E_0 - K\frac{Q}{i_t + 0.1Q}\cdot i^* - K\frac{Q}{Q-i_t}\cdot i_t + \\ + A\cdot exp\left(-B\cdot i_t\right) \qquad (2)$$

Since the charging current has an opposite sign (i^*< 0), the resistance of polarization is changing, so the function of charging voltage is slightly different. The effect of temperature on operation of the Lithium-Ion battery is not taken into consideration in this paper [12].

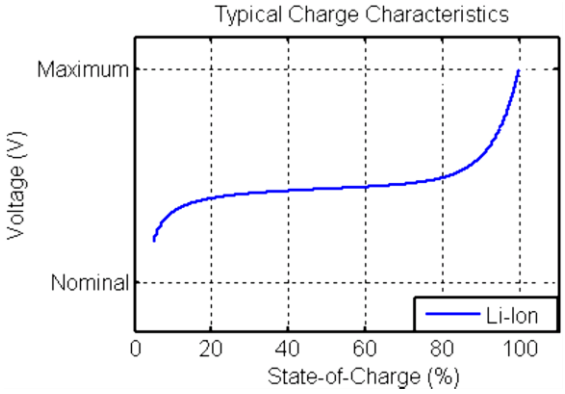

Figure 5 The typical discharge curve of Lithium-Ion battery and indicated characteristic areas

It should be noted that operation of the Lithium-Ion battery, in the areas where a rapid voltage changes are present (the initial exponential area and the area of rapid loss of capacity), requires the use of complex power electronic systems in order to protect the battery from overheating and destruction.

For the analysis of EV drive it is essential to consider all the assumptions of the model presented [14]:

- Internal resistance, considering operating mode of charging or discharging is unchanging, and the amount of battery current does not affect it,
- Hysteresis feature of the battery voltage curve is negligible,
- Battery capacity does not change in respect to amount of the charging current,
- The temperature dependences of battery parameters are neglecting,
- The possibility of self-discharge of the battery is ignored,
- The battery has no memory effect.

Since the simulations give away only discrete states of battery, the following restrictions on battery model with concentrated parameters are introduced [14]:

- Battery voltage and capacity cannot have negative values (in a state of total discharge the battery voltage is equal to zero)
- In the case of overcharging the battery, the maximum SOC may be over 100%.

For verification of the model, input parameters of EV Mitsubishi i-MiEV were selected. In this regard, the base of the battery pack in model is a battery cell with nominal voltage 3.75 V. By using these parameters within MATLAB program the curves of battery discharge for different currents (Fig. 5) can be obtained. The parameters obtained from the catalogue of the manufacturer, according to the method described above, are shown in Fig. 5.

3 EV DRIVE PARAMETERS SETTING

EV design is comparable when crossing a certain distance, according to predefined driving dynamics, starting with the full capacity of the battery. Multiple standardized driving cycles exist [15], and in this paper two are selected:

1. Urban Dynamometer Driving Schedule UDDS (Fig. 6, total distance 12 km, total time 1380s=23 min, average driving speed 36.6 km/h)
2. EPA Highway Fuel Economy Test HWFET (Fog. 7, total distance 16.5 km, total time 780s=13 min, average driving speed 77.6 km/h)

The initial parameter setting is done according to the UDDS driving cycles, followed by a simulation verification of the model carried out on the combined driving cycles (UDDS 10 km + HWFET 30 km).

In order to calculate the dynamics of the battery through a simulation, it is necessary to define all the parameters of EV that affect the dynamics of the battery.

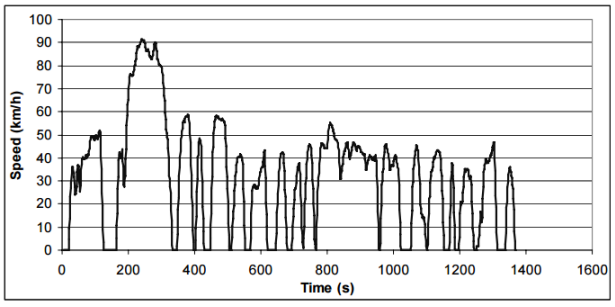

Figure 6 Urban Dynamometer Driving cycles UDDS

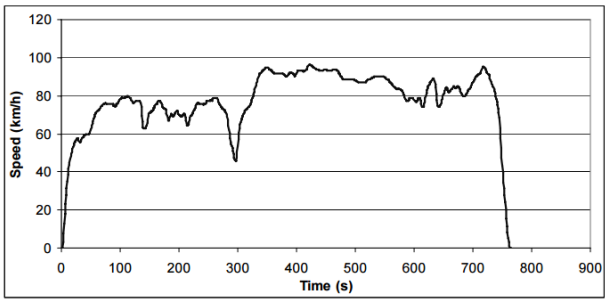

Figure 7 EPA Highway Fuel Economy Test HWFET

The calculation of the necessary energy is carried out - it is energy that mechanically burdens the EV drive, based on the driving mode and the basic parameters of the EV. This energy is transferred through electric drive and is considered as the electrical load of the battery (*discharge* - acceleration and driving, *charge* - recovery of braking energy).

For simplicity, this paper does not take into account any losses of energy within the vehicle (losses of control electronics, transmission losses or losses of the electric motor) which in real case may reach up to 20%. Also, a standard route is taken into calculation, possible changes of inclination of the vehicle (driving uphill - downhill) were not taken into account.

The total mechanical power is equal to the sum of the product of the total resistance force of vehicle movement and speed of the same at a given time [16]:

$$P_{\text{meh}} = \sum F \cdot v \tag{3}$$

The total resistance force of the vehicle movement consists of three components: rolling resistance, air resistance, and gradients resistance [14, 17]. Each component is individually modelled in the Simulink. Afterwards, they were united in a shared subsystem called "UDDS load". The mentioned subsystem and its structure can be seen in Fig. 8.

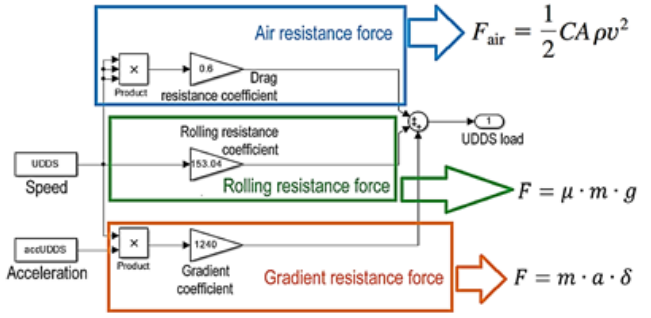

Figure 8 The simulation block "UDDS load"

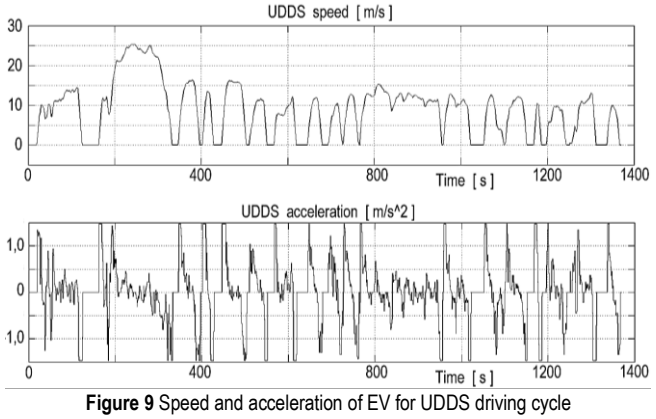

Figure 9 Speed and acceleration of EV for UDDS driving cycle

The value of C (drag coefficient: 0.0425) and A (an area of the front side of the vehicle) are taken from Mitsubishi i-MiEV that is based vehicle model in this paper.

The same is valid for the value of air density (1.2 kg/m3), the coefficient of rolling friction (0.013), and transmission coefficient (1.03) [17].

Input parameters in the MATLAB model of EV are vehicle speed (according to the selected driving cycles) and acceleration (derivation of the vehicle speed). Fig. 9 shows the change in speed and acceleration of EV for UDDS driving cycles.

Finally, by multiplying related force that opposes the movement of vehicles according to (3), with associated speed, function of the mechanical load of the DC motor that drives EV is obtained. The simulation output from the DC motor block that represents the electric energy demand provided by battery pack, is shown in Fig. 10.

Calculations of the EV model are based on the i-MiEV vehicle, where nominal voltage value battery pack is equal to 330 V. The battery pack is composed of 11 series-connected modules with the 8 battery cells in parallel with a nominal voltage of 3.75 V. Model of battery pack is shown in Fig. 11.

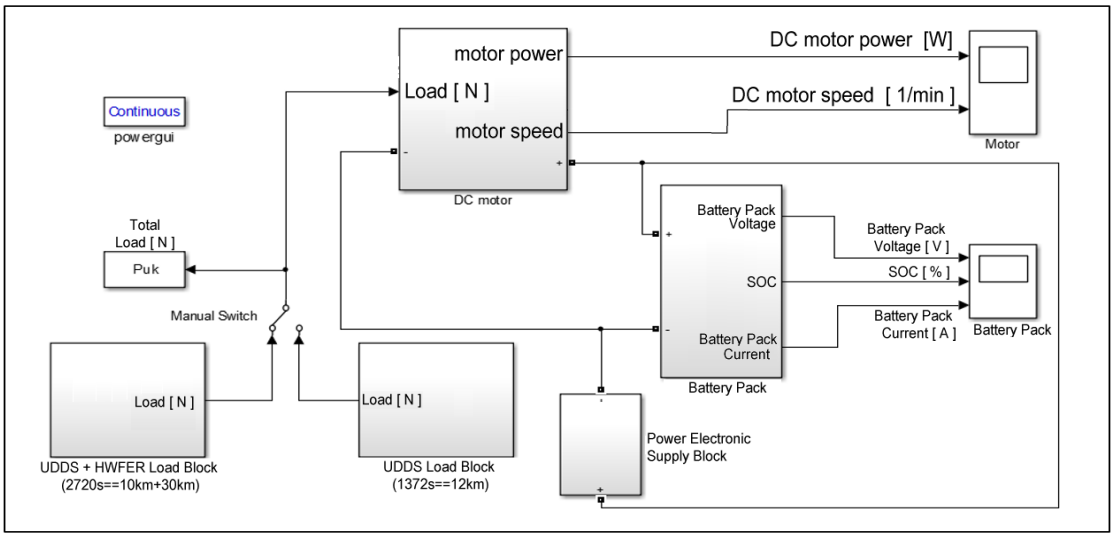

Figure 10 Simulink model of electric vehicles powered for driving cycle UDDS and HWFET

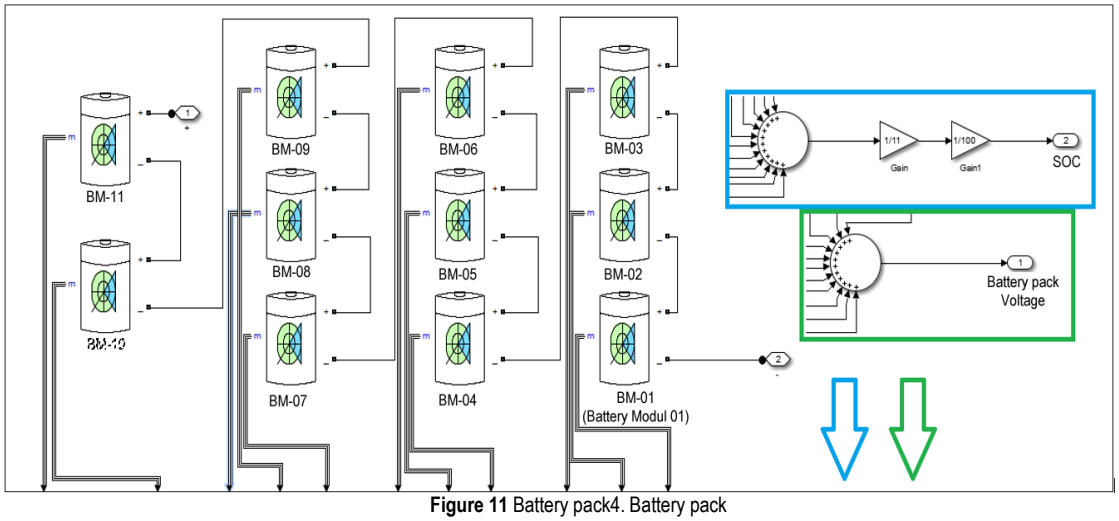

Figure 11 Battery pack4. Battery pack

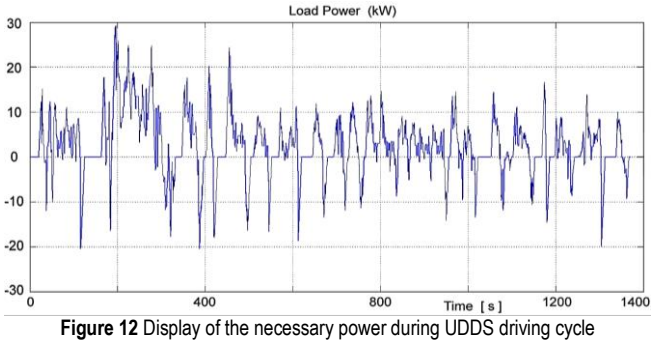

Figure 12 Display of the necessary power during UDDS driving cycle

The diagram in Fig. 12 provides an overview of changes in power that EV drive must provide for UDDC drive cycle.

The power of the DC motor is determined by the maximum calculated value of power, shown in diagram in Fig. 12, which is rounded up to the first higher value according to the standard determined power. Maximum power of 29.2 kW appears in diagram at 196 s, which leads to 30 kW selected power of the DC motor for the EV drive [18]. Periods of negative power that occur during the deceleration can be seen in Fig. 12. In these intervals, when

energy flow is directed from the block DC motor to the battery pack, process of regenerative braking is being carried out.

By integration of the function of power in time, the energy required for EV drive during the drive cycle is calculated.

To determine the capacity of battery pack, from demanded energy at certain voltage, the following relation is used:

$$C = \frac{W}{3600 \cdot U} \tag{4}$$

where: C - capacity of battery pack (Ah), W - total energy required for the drive cycles (J), U - nominal voltage of battery pack (V).

The calculation of energy for the simulated driving cycle, by summing the function of power in time, the total electrical energy to be stored in the battery is obtained (W_{TOTAL} = 40.1 MJ). Since Lithium-Ion batteries work in capacity range 25% – 95%, with regard to the safe use of the batteries, only 70% of theoretical capacity is available. The calculated value of total energy that battery has to provide must be divided by 0.7 in order to get correct values [16]. It follows that the required theoretical capacity of the battery is about 47 Ah.

5 SIMULATION RESULTS AND ANALYSIS

By setting the parameters of all relevant parts of EV, based on the initial selection of the structural elements of the well-known model of EV i-Miev, and adjusting other parts of a drive according to UDDC drive cycles, verification of the model can be initiated.

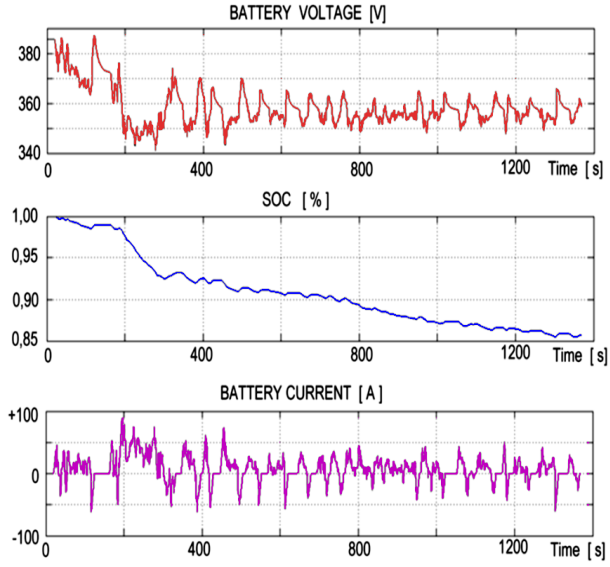

Figure 13 Change of the battery pack parameters for UDDC drive cycles

Confirmation that the modelled EV can provide drive distance, according to UDDC drive cycles, is the first step in model verification. The dynamic characteristics of the battery pack, at loads caused by UDDS driving cycles, are shown in Fig. 13.

The output from the block DC motor is speed and power of the DC motor for driving EV. Figure 14 shows that speed of the DC motor follows the default speed of the vehicle according to UDDC drive cycles.

In Fig. 14, red marks the intervals when the battery is discharged and green marks a period of braking energy recovery. By analyzing power in time shown in Fig.14, it can be seen that during acceleration of the EV motor power ranges from 70 to 95%, which represents about 20% of drive cycles.

These are the intervals with the maximum battery load and the largest discharge current (Fig. 13). In periods when the EV is driving with the cruise speed, engine power ranges from 30% to 40%, which represents about 55% of drive cycles [17]. In these intervals, the discharge current of the batteries is almost twice lower, and stress of the batteries is reduced. Since the duration of the discharge lasts longer, more intense changes of the SOC are shown in the diagram in Fig. 13.

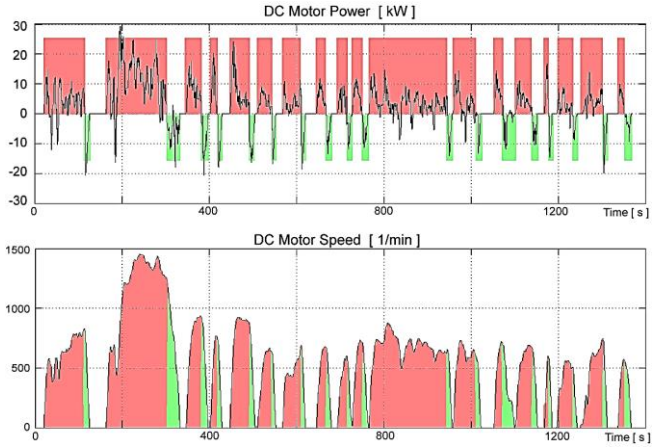

Figure 14 The speed and power of the DC motor during UDDC drive cycles

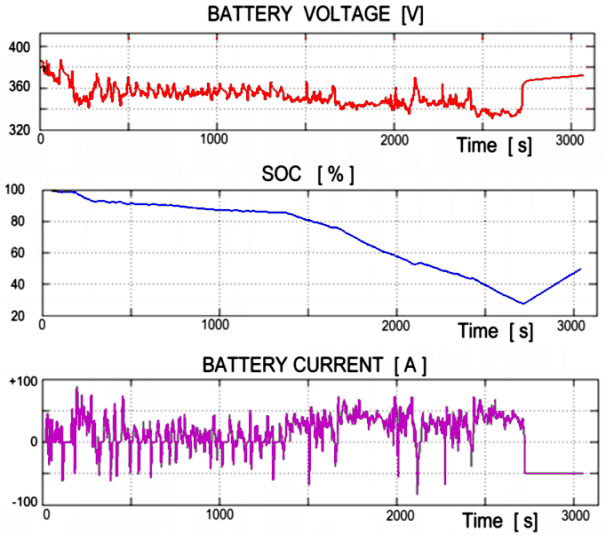

Figure 15 Change parameters battery pack for UDDS + HWFET drive cycles

The second phase of the simulation is to test a model through the combined driving (10 km UDDC + 30 km HWFET). This simulation lasts for 3760 seconds.

The first 1370 seconds (*distance of 10 km*) the vehicle is moving towards urban driving cycle (*UDDS*), and from 1370 to 2720 seconds (*distance of 30 km*) it is moving according to highway driving cycles (*HWFET*).

After 2720 seconds the vehicle arrives at the destination, and the battery is charged for 1040 seconds with a constant current of 50 A. Figure 15 shows the dynamic characteristics of battery pack; SOC, voltage and current for UDDS + HWFET drive cycle. The power and the engine speed are shown in Fig. 16.

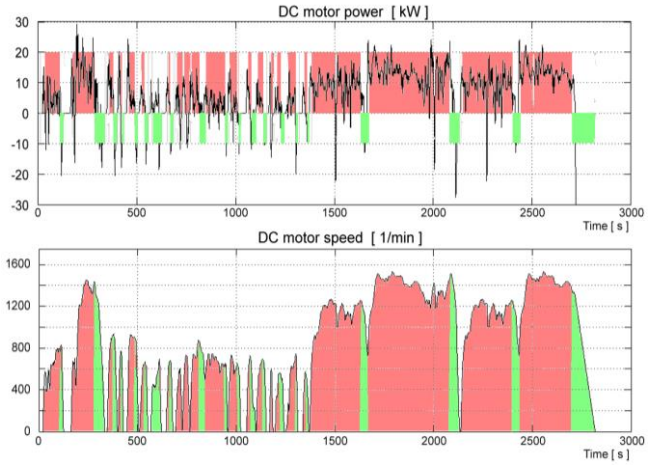

Figure 16 The speed and power of DC motor for a combined UDDC + HWFET drive cycles.

The analysis shows that, during the first 10km (*UDDC drive cycles*), the vehicle has numerous stops and energy recovery is achieved. Therefore, SOC has a slower decrease (Fig.15). However, switching to highway driving (HWFET *drive cycles*), discharge current of batteries is substantially increased; there is practically no recovery, which is why the SOC decreases twice as fast.

Also, at the end of the cycle, the battery pack is not discharged below the 25%, which was the intention of the design.

6 CONCLUSION

This paper shows the parameterization of the EV drive using the Matlab-Simulink. The emphasis of the paper was on studying the dynamic characteristics of the Lithium-Ion battery during various charge and discharge regimes.

Essential parts of modelling process for the EV have been shown. The way to determine the parameters for Lithium-Ion battery from catalogue data producers has been presented. From the base drive cycle data, the parameters of the model have been selected and the EV drive required power has been calculated. Based on this power and the drive cycle data battery capacity has been selected.

Explanations of the model simplification, as well as limitations of the model have been given. In further research the model can be upgraded so it includes all the parameters that describe realistic EV which ultimately reduces the distance range of the EV.

Based on these simulations and analysis of results the boundary areas of the Lithium-Ion battery, operation in EV may be defined. Also, the measuring signals for control electronics can be selected.

7 REFERENCES

[1] Jianwu, W.; Yan, Y.; Chunhua, C. A Review on Lithium-Ion Batteries Safety Issues: Existing Problems and Possible Solutions. // Materials Express, 2, 3(2012), pp. 197-212.

[2] Taylor, W.; Krithivasan, G.; Nelson, J. System safety and ISO 26262 compliance for automotive Lithium-Ion batteries. // 2012 IEEE Symposium on Product Compliance Engineering Proceedings, (2012), pp. 1-6.

[3] Felgenhauera, M. F.; Pellowb, M. A.; Bensonb, S. M.; Hamachere, T. Evaluating co-benefits of battery and fuel cell vehicles in a community in California. // Energy, 114, 1(2016), pp. 360-368.

[4] Park, K. H.; Hong, K.Y.; Kang, J. All-graphene-battery: bridging the gap between supercapacitors and lithium ion batteries. // Scientific Reports 4, Num. 5278 (2014), DOI: 10.1038/srep05278

[5] Wasbaria, F.; Bakara, A.; Gana, M.; Tahirb, M.; Yusofb, A. A review of compressed-air hybrid technology in vehicle system. // Renewable and Sustainable Energy Reviews, Vol. 67, January 2017, pp. 935-953

[6] Mwasilu, F.; Justo, J. J.; Kim, E. K.; Do, T. D.; Jung, J. W. Electric vehicles and smart grid interaction: A review on vehicle to grid and renewable energy sources integration. // Renewable and Sustainable Energy Reviews, vol. 34, (2014), pp. 501-516.

[7] Sikkabut, S.; Mungporn, P.; Ekkaravarodome, C.; Bizon, N.; Tricoli, P.; Nahid-Mobarakeh, B.; Pierfederici, S.; Davat, B.; Thounthong, P. Control of High-Energy High-Power Densities Storage Devices by Li-ion Battery and Supercapacitor for Fuel Cell/Photovoltaic Hybrid Power Plant for Autonomous System Applications. // IEEE Transactions on Industry Applications, 52, 5(2016), pp. 4395-4407.

[8] Imai, T.; Yamaguchi, H. Dynamic battery charging voltage optimization for the longer battery runtime and lifespan. // 2013 IEEE 2nd Global Conference on Consumer Electronics (GCCE), pp. 219-223, DOI:10.1109/GCCE.2013.6664804

[9] Xu, F.; Jiao, X.; Sasaki, M.; Wang, Y. Energy management optimization in consideration of battery deterioration for commuter plug-in hybrid electric vehicle. // 55th Annual Conference of the Society of Instrument and Control Engineers of Japan (SICE) 2016, pp. 218-222.

[10] Hu, X.; Moura, S. J.; Murgovski, N.; Egardt, B.; Cao, D. Integrated Optimization of Battery Sizing, Charging, and Power Management in Plug-In Hybrid Electric Vehicles. // IEEE Transactions on Control Systems Technology, 24, 3(2016), pp. 1036-1043.

[11] Xuebing, H.; Minggao, O.; Languang, L. A comparative study of commercial lithium ion battery cycle life in electrical vehicle: Aging mechanism identification. // Journal of Power Sources, 251, (2014), pp. 38-54
[12] https://www.mathworks.com/help/physmod/sps/powersys/ref/battery.html
[13] Tremblay, O.; Dessaint, L.-A. Experimental Validation of a Battery Dynamic Model for EV Applications. // World Electric Vehicle Journal, 3, (2009), pp. 289-298.
[14] Tremblay, O.; Dessaint, L.-A.; Dekkiche A. I. A Generic Battery Model for the Dynamic Simulation of Hybrid Electric Vehicles. // IEEE Vehicle Power and Propulsion Conference, (2007), pp 284-289
[15] Barlow, T. J.; Latham, S.; McCrae, I. S.; Boulter, P. G. A reference book of driving cycles for use in the measurement of road vehicle emissions. // Published Project Report PPR354, Department for Transport, Cleaner Fuels &Vehicles, 2009.
[16] Husain, I. Electric and Hybrid Electric Vehicles, CRC Press, 2003.
[17] Hederić, Ž.; Hadžiselimović, M.; Štumberger, B. Modeling of a Serial Hybrid Powertrain for Busses in the City of Osijek, Croatia. // Proceedings EnergyCon 2014 - IEEE International Energy Conference / pp. 1537-1543.
[18] Hadžiselimović, M.; Blažnik, M.; Štumberger, B. Magnetically Nonlinear Dynamic Model of a Series Wound DC Motor. // Przeglad Elektrotechniczny, Vol: 87 Issue: 12B, 2011, pp 60-64

Authors' contacts:

Ivan BABOSELAC, Master student
Josip Juraj Strossmayer University of Osijek, Faculty of Electrical Engineering, Computer Science and Information Technology Osijek, Kneza Trpimira 2b, 31000 Osijek, Croatia

Željko HEDERIĆ, PhD, Associate Professor
Josip Juraj Strossmayer University of Osijek, Faculty of Electrical Engineering, Computer Science and Information Technology Osijek, Kneza Trpimira 2b, 31000 Osijek, Croatia
zhederic@etfos.hr

Tin BENŠIĆ, PhD student
Josip Juraj Strossmayer University of Osijek, Faculty of Electrical Engineering, Computer Science and Information Technology Osijek, Kneza Trpimira 2b, 31000 Osijek, Croatia
tin.bensic@ferit.hr

ISSN 1846-6168 (Print), ISSN 1848-5588 (Online)
ID: TG-20170223061859

Original scientific article

DEFLECTION AND BENDING MOMENTS AMPLITUDE DISTRIBUTION AT THE FORCED OSCILLATIONS OF THE EULER-BERNOULLI BEAM

Yurii KRUTII, Nikolay SURYANINOV

Abstract: The paper considers forced oscillations of a simply supported Euler-Bernoulli beam with inner inelastic resistance. Maximum values of non-dimensional amplitudes of bending moments and deflections which are invariants with respect to dimensional parameters of beam are calculated. For beams with any dimensional parameters calculation of the maximum amplitudes corresponding to the set frequency of forced vibrations, reduces to multiplication by appropriate dimensional factor already calculated invariant dimensionless values. In a specific example, a comparative analysis of accurate amplitude values for dynamic bending moments and deflections is calculated according to the author's method, with the same calculation in the ANSYS program complex. Values of the amplitudes in the vicinity of the resonance frequencies are clarified.

Keywords: amplitude of the bending moments and deflections, Euler-Bernoulli beam, transverse vibrations, frequency of forced oscillations, resonance.

1 INTRODUCTION

One of the major problems in the theory of oscillations of elastic systems is the study of the influence of external and internal resistances to oscillation processes. The calculations on the free oscillations consist in definition of own frequencies and forms of oscillations, as well as calculations on forced vibrations away from the resonance zones. The resistance forces are often neglected. This is due to the fact that when such calculations accounting the forces of resistance do not significantly influence the final result. Another thing is calculation of oscillation near resonance. This calculation requires the consideration of the resistance forces, since their effect is appearing in the greatest measure.

Effect of external and internal resistance to oscillations is different and depends on many factors: the oscillatory characteristics of the system, the material of which the elements of the system are made, parameters of environment. However, in this case, internal resistance of inelastic material is of particular importance.

2 BACKGROUND AND ANALYSIS OF RESEARCH

Presence of internal friction in the material was firstly found by Coulomb in experiments with a torsion balance. The study of internal friction involved W. Thomson. It was established experimentally that the resilient material does not strictly follow Hooke's law even if the elastic deformations within the limits of elasticity. This explains the internal energy loss fluctuations.

Many scientists talk about the importance of internal friction in the material studies conducted in the beginning of the 20th century. Experiments of Guye on the internal losses in the material during torsional vibration of metal wires showed a completely insignificant role of air friction as compared with losses in the metal. Rowett, exploring damping vibrations in machines, found that the share of domestic energy dissipation in the material accounts for at least two-thirds of all losses during vibration.

In the dynamic structural analysis, the hypothesis of Kelvin-Voigt, which is based on the idea of the viscosity of solids, is widespread when taking into account the internal resistance of inelastic material [1, 2]. The internal friction proportional to the velocity was used by the founders of the applied theory of vibrations A.N. Krylov [3] and S.P. Timoshenko [4].

However, as it is well known [2], the Kelvin-Voigt's hypothesis in its pure form has a number of drawbacks. The main point is the fact that the hypothesis leads to a conclusion about the frequency-independent internal friction in the material, which contradicts the experimental data. This disadvantage is eliminated by taking the corrected Kelvin-Voigt hypothesis, according to which the damping is taken into account in proportion to the strain rate, divided by the oscillation frequency [2].

Among the fundamental studies on this issue, particularly noteworthy are the works of A.N. Krylov [3], S.P. Tymoshenko [4], J.G. Panovko [5] and E.S. Sorokin [6].

Current studies are characterized by the extensive use of computer methods of mechanics. Works related to considering variable mass for different kinds of friction are published by V.P. Olshansky and S.V. Olshansky [7, 8]. The work of N.N. Berendeev is devoted to the problem of the influence of the internal friction on the system of forced oscillations [9].

3 MAIN CHAPTER

3.1 The main symbols and formulas

Consider the forced harmonic oscillations of a hinged beam internal forces taking into account the inelastic resistance. The general scheme of the oscillation is shown in Fig. 1. Fig. 2 shows a diagram of forces acting on the oscillations of the beam element.

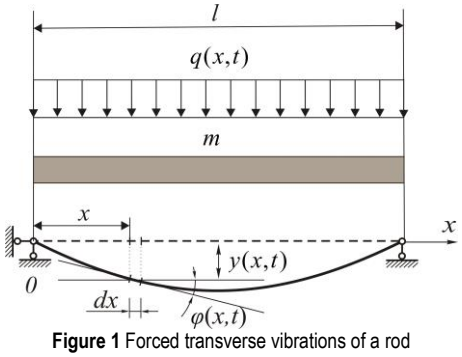

Figure 1 Forced transverse vibrations of a rod

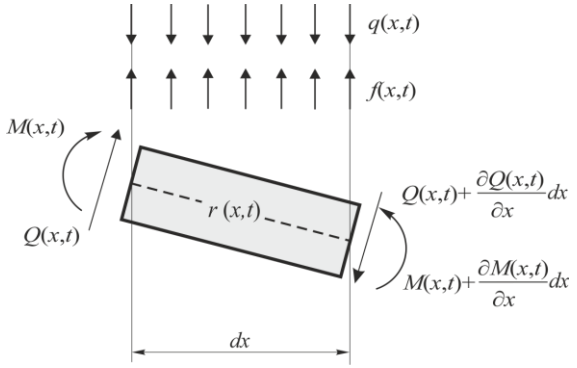

Figure 2 Driving forces acting on the rod element

The following designations are accepted: $q(x,t)=q\sin\theta t-$ external dynamic load, where $q-$ constant amplitude, $\theta-$ the frequency of the disturbing force; $m-$ the intensity of the distributed mass (mass per unit length) of the rod; $y(x,t)-$ lateral movement of the point with the coordinate axis of the rod at the time (dynamic bending); $\varphi(x,t)-$ dynamic rotation angle; $M(x,t)-$ dynamic bending moment; $Q(x,t)-$ dynamic shear force; $r(x,t)-$ the intensity of the internal forces of resistance; $f(x,t)=-m\dfrac{\partial^2 y}{\partial t^2}-$ the intensity of the inertial forces that arise in the course of the oscillation (the power of D'Alembert).

Assuming, according to the corrected hypothesis of Kelvin-Voigt [1, 2],

$$r(x,t)=\frac{\gamma}{\theta}EI\frac{\partial^5 y}{\partial t\partial x^4},$$

the equation of forced oscillations of the beam can be written as [1, 2]

$$EI\left(1+\frac{\gamma}{\theta}\frac{\partial y}{\partial t}\right)\frac{\partial^4 y}{\partial x^4}+m\frac{\partial^2 y}{\partial t^2}=q\sin\theta t, \qquad (1)$$

where $\gamma-$ inelastic resistance coefficient (dimensionless constant for a given material); $EI-$ the bending stiffness of the beam. To this we add the equation as defined boundary conditions:

$$y(0,t)=0;\ M(0,t)=0;\ y(l,t)=0;\ M(l,t)=0. \qquad (2)$$

In the absence of the scientific literature of the exact solution of the Eq.(1), for the study of forced oscillations of the beam based on the internal resistance to the present, as a rule, we used approximate methods. An exception may be the publication of M. Abu-Hilal [10], where the definition of the dynamic deflection of the beam is based on the method of Green's functions.

In [11] an exact solution of the Eq. (1) and fully defined dynamic parameters of the beam is found. In particular, formulas for the deflection and bending moments

$$y(x,t)=y_1(x)\sin\theta t+y_2(x)\cos\theta t \qquad (3)$$

$$M(x,t)=M_1(x)(\sin\theta t+\gamma\cos\theta t)+ +M_2(x)(\cos\theta t-\gamma\sin\theta t), \qquad (4)$$

where $y_k(x),\ M_k(x)\ (k=1,2)-$ the so-called constituent functions of their parameters. These functions with boundary conditions (2) at a point $x=0$, defined by the formula [11]:

$$\begin{aligned} y_k(x)=&\\ =(-1)^{k+1}&\left(\varphi_1(0)lX_{2,k}(x)-\frac{Q_1(0)l^3}{EI}X_{4,k}(x)\right)+\\ +\varphi_2(0)&lX_{2,3-k}(x)-\frac{Q_2(0)l^3}{EI}X_{4,3-k}(x)+\\ +(-1)^{k+1}&\frac{ql^4}{(1+\gamma^2)EI}(X_{5,k}(x)+(-1)^k\gamma X_{5,3-k}(x)); \end{aligned} \qquad (5)$$

$$\begin{aligned} M_k(x)=&\\ =(-1)^k&\left(\frac{\varphi_1(0)EI}{l}X^*_{4,k}(x)-Q_1(0)lX_{2,k}(x)\right)-\\ -\frac{\varphi_2(0)EI}{l}&X^*_{4,3-k}(x)+Q_2(0)lX_{2,3-k}(x)+\\ +(-1)^k&\frac{ql^2}{1+\gamma^2}(X_{3,k}(x)+(-1)^k\gamma X_{3,3-k}(x)), \end{aligned} \qquad (6)$$

where

$$X_{n,1}(x)=\frac{1}{(n-1)!}\left(\frac{x}{l}\right)^{n-1}+\sum_{k=1}^{\infty}\frac{L^{2k}\cos k\delta}{(4k+n-1)!}\left(\frac{x}{l}\right)^{4k+n-1}, \qquad (7)$$

$$X_{n,2}(x)=\sum_{k=1}^{\infty}\frac{L^{2k}\sin k\delta}{(4k+n-1)!}\left(\frac{x}{l}\right)^{4k+n-1}\ (n=2,3,4,5), \qquad (8)$$

$$X^*_{4,1}(x)=\sum_{k=0}^{\infty}\frac{L^{2k+2}\cos(k+1)\delta}{(4k+3)!}\left(\frac{x}{l}\right)^{4k+3}, \quad (9)$$

$$X^*_{4,2}(x)=\sum_{k=0}^{\infty}\frac{L^{2k+2}\sin(k+1)\delta}{(4k+3)!}\left(\frac{x}{l}\right)^{4k+3}; \quad (10)$$

$$L=\frac{\theta}{\sqrt[4]{1+\gamma^2}}l^2\sqrt{\frac{m}{EI}},\ \delta=\operatorname{atan}\gamma\ \left(0\le\delta<\frac{\pi}{2}\right). \quad (11)$$

It is important to note that the parameters L, δ and all functions (7)–(10) are dimensionless.

Constituent functions (5), (6) represented in a complex form [11]:

$$y_1(x)+iy_2(x)=(\varphi_1(0)+i\varphi_2(0))lX_2(x)-$$
$$-(Q_1(0)+iQ_2(0))\frac{l^3}{EI}X_4(x)+\frac{q}{(1+i\gamma)}\frac{l^4}{EI}X_5(x); \quad (12)$$

$$M_1(x)+iM_2(x)=$$
$$=-(\varphi_1(0)+i\varphi_2(0))\frac{EI}{l}K^2X_4(x)+ \quad (13)$$
$$+(Q_1(0)+iQ_2(0))lX_2(x)-\frac{q}{(1+i\gamma)}l^2X_3(x),$$

where

$$X_n(x)=X_{n,1}(x)-iX_{n,2}(x)\ (n=2,3,4,5),$$
$$K^2X_4(x)=X^*_{4,1}(x)-iX^*_{4,2}(x).$$

3.2 The dimensionless amplitude of dynamic deflections and bending moments

Unidentified initial parameters $\varphi_1(0)$, $\varphi_2(0)$, $Q_1(0)$, $Q_2(0)$ are determined from the boundary conditions (2) at the point $x=l$. These boundary conditions on the basis of formulas (3), (4) are equivalent to

$$y_1(l)=0,\ y_2(l)=0,\ M_1(l)=0,\ M_2(l)=0,$$

and their implementation, by the formulas (12), (13), leads to a system of equations:

$$X_2(l)(\varphi_1(0)+i\varphi_2(0))-$$
$$-\frac{l^2}{EI}X_4(l)(Q_1(0)+iQ_2(0))=-\frac{ql^3}{(1+i\gamma)EI}X_5(l);$$
$$-\frac{EI}{l}K^2X_4(l)(\varphi_1(0)+i\varphi_2(0))+$$
$$+lX_2(l)(Q_1(0)+iQ_2(0))=\frac{ql^2}{1+i\gamma}X_3(l).$$

Hence we find the complex initial settings:

$$\varphi_1(0)+i\varphi_2(0)=$$
$$=\frac{ql^3}{(1+i\gamma)EI}\frac{X_3(l)X_4(l)-X_2(l)X_5(l)}{X_2^2(l)-K^2X_4^2(l)}; \quad (14)$$

$$Q_1(0)+iQ_2(0)=$$
$$=\frac{ql}{1+i\gamma}\frac{X_2(l)X_3(l)-K^2X_4(l)X_5(l)}{X_2^2(l)-K^2X_4^2(l)}. \quad (15)$$

To determine the required initial parameters $\varphi_1(0)$, $\varphi_2(0)$, $Q_1(0)$, $Q_2(0)$ allocate the real and imaginary terms in the right-hand sides of the formulas (14), (15). The result

$$\varphi_k(0)=\frac{ql^3}{EI(1+\gamma^2)}H_k,\ \ Q_k(0)=\frac{ql}{1+\gamma^2}S_k\ \ (k=1,2),$$

where H_k, S_k – dimensionless constants, calculated according to the formulas:

$$H_1=\frac{a_1c_1+a_2c_2+\gamma(a_2c_1-a_1c_2)}{c_1^2+c_2^2};$$
$$H_2=\frac{a_2c_1-a_1c_2-\gamma(a_1c_1+a_2c_2)}{c_1^2+c_2^2};$$
$$S_1=\frac{b_1c_1+b_2c_2+\gamma(b_2c_1-b_1c_2)}{c_1^2+c_2^2};$$
$$S_2=\frac{b_2c_1-b_1c_2-\gamma(b_1c_1+b_2c_2)}{c_1^2+c_2^2};$$
$$a_1=X_{4,1}(l)X_{3,1}(l)-X_{4,2}(l)X_{3,2}(l)-$$
$$-X_{2,1}(l)X_{5,1}(l)+X_{2,2}(l)X_{5,2}(l);$$
$$a_2=X_{2,1}(l)X_{5,2}(l)+X_{2,2}(l)X_{5,1}(l)-$$
$$-X_{4,1}(l)X_{3,2}(l)-X_{4,2}(l)X_{3,1}(l);$$
$$b_1=X_{2,1}(l)X_{3,1}(l)-X_{2,2}(l)X_{3,2}(l)-$$
$$-X^*_{4,1}(l)X_{5,1}(l)+X^*_{4,2}(l)X_{5,2}(l);$$
$$b_2=X^*_{4,1}(l)X_{5,2}(l)+X^*_{4,2}(l)X_{5,1}(l)-$$
$$-X_{2,1}(l)X_{3,2}(l)-X_{2,2}(l)X_{3,1}(l);$$
$$c_1=X^2_{2,1}(l)-X^2_{2,2}(l)-X^*_{4,1}(l)X_{4,1}(l)+X^*_{4,2}(l)X_{4,2}(l);$$
$$c_2=X^*_{4,1}(l)X_{4,2}(l)+X^*_{4,2}(l)X_{4,1}(l)-2X_{2,1}(l)X_{2,2}(l).$$

Substituting the values of the initial parameters in the formula (5), (6) we have:

$$y_k(x)=\frac{ql^4}{(1+\gamma^2)EI}y^*_k(x); \quad (16)$$

$$M_k(x)=\frac{ql^2}{1+\gamma^2}M^*_k(x)\ \ (k=1,2), \quad (17)$$

where $y_k^*(x)$, $M_k^*(x)$ – dimensionless functions, which have the form

$$y_k^*(x) =$$
$$= (-1)^{k+1}(H_1 X_{2,k}(x) - S_1 X_{4,k}(x)) + H_2 X_{2,3-k}(x) -$$
$$-S_2 X_{4,3-k}(x) + (-1)^{k+1}(X_{5,k}(x) + (-1)^k \gamma X_{5,3-k}(x)),$$
$$M_k^*(x) =$$
$$= (-1)^k (H_1 X_{4,k}^*(x) - S_1 X_{2,k}(x)) - H_2 X_{4,3-k}^*(x) +$$
$$+S_2 X_{2,3-k}(x) + (-1)^k (X_{3,k}(x) + (-1)^k \gamma X_{3,3-k}(x)).$$

To study the vibrations, the formula, which clearly highlighted the amplitude function, will be more convenient. Rearranging equation (3), (4) to a desired form, taking into consideration the representations (16), (17) we finally obtain:

$$y(x,t) = \mathrm{Am}\, y(x,t)\sin(\theta t + \chi_y(x));$$
$$\mathrm{Am}\, y(x,t) = \frac{ql^4}{(1+\gamma^2)EI} y(x);$$
$$y(x) = \sqrt{(y_1^*(x))^2 + (y_2^*(x))^2},\ \chi_y(x) = \mathrm{atan}\frac{y_2^*(x)}{y_1^*(x)};$$
$$M(x,t) = \mathrm{Am}\, M(x,t)\sin(\theta t + \chi_M(x));$$
$$\mathrm{Am}\, M(x,t) = \frac{ql^2}{1+\gamma^2} M(x);$$
$$M(x) = \sqrt{(M_1^*(x) - \gamma M_2^*(x))^2 + (M_2^*(x) + \gamma M_1^*(x))^2};$$
$$\chi_M(x) = \mathrm{arctg}\frac{M_2^*(x) + \gamma M_1^*(x)}{M_1^*(x) - \gamma M_2^*(x)}.$$

As can be seen, the formula for the amplitude contains dimensionless factors $y(x)$ and $M(x)$, that is independent of the load. This factors up to size ratio $\frac{ql^4}{(1+\gamma^2)EI}$ and $\frac{ql^2}{1+\gamma^2}$ it defines the main forms for the dynamic deflection and dynamic bending moment. The functions $y(x)$ and $M(x)$ can also be interpreted as a dimensionless amplitude.

The maximum value of the amplitude will obviously be achieved in the middle of the beam, i.e.

$$\max \mathrm{Am}\, y(x,t) = \frac{ql^4}{(1+\gamma^2)EI} y\left(\frac{l}{2}\right), \quad (18)$$

$$\max \mathrm{Am}\, M(x,t) = \frac{ql^2}{1+\gamma^2} M\left(\frac{l}{2}\right). \quad (19)$$

Thus, to determine the maximum amplitude, it is necessary to calculate the corresponding value of the dimensionless amplitude in the middle of the beam. This will represent a special interest in the calculation of the resonance zones, when the frequency θ of forced oscillations will be located in the vicinity of the frequency of free vibrations of the beam.

As is known [1], for the frequency of free oscillations of the beam, excluding the resistances, there is the formula

$$\omega_j = \frac{K_j}{l^2}\sqrt{\frac{EI}{m}}\ (j = 1,2,3,...), \quad (20)$$

where K_j – dimensionless coefficients of free oscillations. In the case of simply supported beam $K_j = (j\pi)^2$.

As the frequency of forced oscillations set the following values:

in the interval $0 < \theta \le \omega_1$ we believe

$$\theta = k\frac{\omega_1}{10}\ (k = 1,2,3,...,10);$$

in the interval $\omega_1 < \theta \le \omega_2$ we believe

$$\theta = \omega_1 + k\frac{\omega_2 - \omega_1}{10}\ (k = 1,2,...,10);$$

in the interval $\omega_2 < \theta \le \omega_3$ we believe

$$\theta = \omega_2 + k\frac{\omega_3 - \omega_2}{10}\ (k = 1,2,3,...,10);$$

in the interval $\omega_3 < \theta < \omega_4$ we believe

$$\theta = \omega_3 + k\frac{\omega_4 - \omega_3}{10}\ (k = 1,2,3).$$

Substituting here instead of frequency ω_1, ω_2, ω_3, ω_4 their values (16), we obtain the representation

$$\theta = \frac{K^*}{l^2}\sqrt{\frac{EI}{m}}, \quad (21)$$

where K^* – dimensionless ratio of forced oscillations for which we have

$$K^* = \begin{cases} 0,1k\pi^2, \text{ when } \theta = k\frac{\omega_1}{10}; \\ (1+0,3k)\pi^2, \text{ when } \theta = \omega_1 + k\frac{\omega_2 - \omega_1}{10}; \\ (4+0,5k)\pi^2, \text{ when } \theta = \omega_2 + k\frac{\omega_3 - \omega_2}{10} \\ (k = 1,2,3,...,10); \\ (9+0,7k)\pi^2, \text{ when } \theta = \omega_3 + k\frac{\omega_4 - \omega_3}{10} \\ (k = 1,2,3). \end{cases}$$

When this parameter L, determined by the first of the formulas (11), taking into account (21), we obtain $L = \frac{K^*}{\sqrt[4]{1+\gamma^2}}$.

Tab. 1 shows the results of calculations of the dimensionless deflection and bending moment amplitudes in the middle of the beam, corresponding to different values of coefficient of forced oscillation K^*. Especially note that these values are invariant relative to dimensional values l, EI, m, q and depend only on beams ends restraints. In fact, they describe the very essence of the phenomenon.

Table 1 Maximum values of dimensionless amplitudes

K^*	For deflection	For bending moment
	$y(l/2)$	$M(l/2)$
$0.1\pi^2$	0.013204	0.127292
$0.2\pi^2$	0.013614	0.131360
$0.3\pi^2$	0.014358	0.138729
$0.4\pi^2$	0.015546	0.150496
$0.5\pi^2$	0.017393	0.168793
$0.6\pi^2$	0.020338	0.197974
$0.7\pi^2$	0.025397	0.248102
$0.8\pi^2$	0.035476	0.347992
$0.9\pi^2$	0.062745	0.618348
π^2	0.148025	1.466401
$1.3\pi^2$	0.018987	0.191677
$1.6\pi^2$	0.008483	0.087690
$1.9\pi^2$	0.005097	0.054210
$2.2\pi^2$	0.003483	0.038293
$2.5\pi^2$	0.002564	0.029264
$2.8\pi^2$	0.001982	0.023597
$3.1\pi^2$	0.001587	0.019803
$3.4\pi^2$	0.001306	0.017153
$3.7\pi^2$	0.001099	0.015250
$4\pi^2$	0.000941	0.013865
$4.5\pi^2$	0.000752	0.012349
$5\pi^2$	0.000622	0.011532
$5.5\pi^2$	0.000532	0.011248
$6\pi^2$	0.000468	0.011453
$6.5\pi^2$	0.000426	0.012213
$7\pi^2$	0.000402	0.013748
$7.5\pi^2$	0.000401	0.016610
$8\pi^2$	0.000434	0.022275
$8.5\pi^2$	0.000539	0.035211
$9\pi^2$	0.000629	0.054233
$9.7\pi^2$	0.000185	0.025754
$10.4\pi^2$	0.000051	0.013671
$11.1\pi^2$	0.000017	0.009066

Fig. 3, 4 are graphs of the maximum amplitude of the dimensionless deflection and bending moment on the coefficient of beam forced vibrations. As can be seen, the highest values of the amplitudes are achieved when the value of the coefficient of oscillations is π^2, which corresponds to the frequency of free oscillations ω_1.

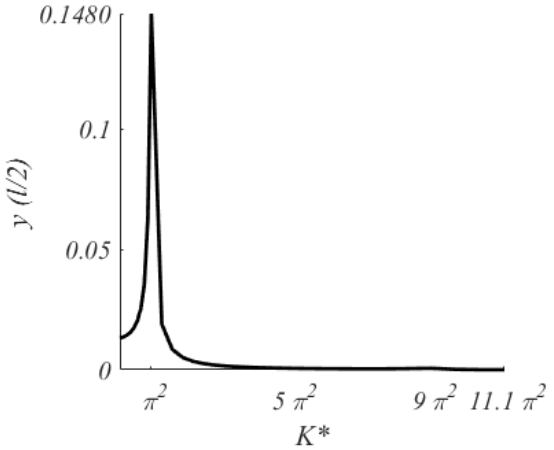

Figure 3 Dependence of the dimensionless deflection amplitude of the oscillation rate

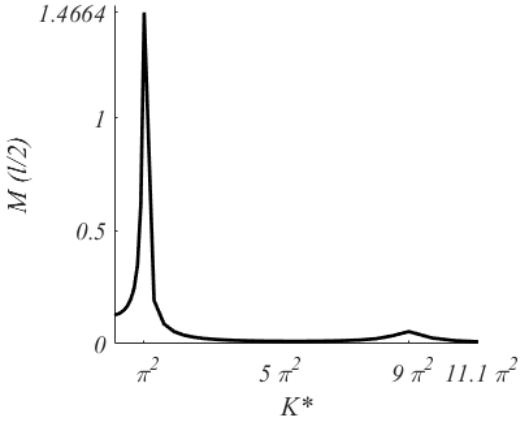

Figure 4 Dependence of the dimensionless bending moment amplitude of the oscillation rate

Thus, according to the formulas (21), (18), (19) the calculation of the maximum amplitudes of the dynamic deflection and bending moments of the beam caused by external dynamic load $q(x,t) = q\sin\theta t$ reduces to multiplication dimensionless value K^*, $y\left(\frac{l}{2}\right)$, $M\left(\frac{l}{2}\right)$, contained in Table 1, on the corresponding dimensional multipliers $\frac{1}{l^2}\sqrt{\frac{EI}{m}}$, $\frac{ql^4}{(1+\gamma^2)EI}$, $\frac{ql^2}{1+\gamma^2}$.

3.3 Example

Let us find the distribution of the amplitudes of the dynamic deflection and bending moments at the hinge beam for given values of higher frequency of forced oscillations. Inelastic material resistance factor is $\gamma = 0.089$. The force of inertia that occurs during the equipment operation is assumed to be q = 20 kN/m, mass per unit length of the beam m = 2.5 kNs^2/m^2, bending stiffness EI = 79615.11 kNm^2.

With such design data, the first four frequencies of oscillation beams excluding resistance according to (20) are equal:

$\omega_1 = 48.9243\ s^{-1}$; $\omega_2 = 195.6974\ s^{-1}$; $\omega_3 = 440.3191\ s^{-1}$; $\omega_4 = 782.7895\ s^{-1}$.

To calculate the required amplitude of dynamic deflections and bending moments corresponding to a given frequency θ, according to the proposed method, we multiply the values that appear in the first, second and third columns of Tab. 1, respectively, on the dimensional ratios

$$\frac{1}{l^2}\sqrt{\frac{EI}{m}} = 4.9571\ s^{-1},\ \frac{ql^4}{(1+\gamma^2)EI} = 0.3230\ \text{m},$$
$$\frac{ql^2}{1+\gamma^2} = 714.3417\ \text{kNm}.$$

Results are shown in Tabs. 2 and 3. For comparison, the results of calculations for a given beam finite element method are obtained using ANSYS [12] software package.

Table 2 Maximum values of dimensioned amplitudes

Frequencies θ, s^{-1}	For deflection, m	
	The author's method	ANSYS
4.8924	0.004265	0.004312
9.7849	0.004398	0.004402
14.6773	0.004638	0.004683
19.5697	0.005022	0.005074
24.4622	0.005618	0.005691
29.3546	0.006569	0.006611
34.2470	0.008204	0.008316
39.1395	0.011459	0.011700
44.0319	0.020267	0.020211
ω_1 = 48.9243	0.047813	0.041122
63.6016	0.006133	0.005918
78.2789	0.002740	0.002212
92.9562	0.001646	0.001533
107.6336	0.001125	0.001094
122.3109	0.000828	0.000800
136.9882	0.000640	0.000637
151.6655	0.000513	0.000510
166.3428	0.000422	0.000412
181.0201	0.000355	0.000349
ω_2 = 195.6974	0.000304	0.000293
220.1595	0.000243	0.000213
244.6217	0.000201	0.000180
269.0839	0.000172	0.000143
293.5461	0.000151	0.000139
318.0082	0.000137	0.000111
342.4704	0.000130	0.000100
366.9326	0.000129	0.000099
391.3947	0.000140	0.000100
415.8569	0.000174	0.000114
ω_3 = 440.3191	0.000203	0.000112
474.5661	0.000060	0.000058
508.8132	0.000017	0.000013
543.0602	0.000005	0.000005

Table 3 Maximum values of dimensioned bending moments amplitudes

Frequencies θ, s^{-1}	For bending moment, kNm	
	The author's method	ANSYS
4.8924	90.9303	90.9393
9.7849	93.8362	93.8732
14.6773	99.0996	99.1469
19.5697	107.5053	107.9006
24.4622	120.5757	120. 9934
29.3546	141.4211	142.1433
34.2470	177.2297	180.0014
39.1395	248.5850	256.4465
44.0319	441.7116	480.9984
ω_1 = 48.9243	1047.5114	1210.1123
63.6016	136.9229	134.4555
78.2789	62.6410	60.9702
92.9562	38.7246	38.3356
107.6336	27.3544	26.7447
122.3109	20.9048	20.8733
136.9882	16.8566	16.8341
151.6655	14.1464	14.0050
166.3428	12.2530	12.0405
181.0201	10.8938	10.9666
ω_2 = 195.6974	9.9044	9.8888
220.1595	8.8213	9.0403
244.6217	8.2375	8.7641
269.0839	8.0346	8.7445
293.5461	8.1815	11.2345
318.0082	8.7243	13.1477
342.4704	9.8206	19.2345
366.9326	11.8649	28.4332
391.3947	15.9119	45.3221
415.8569	25.1526	91.3576
ω_3 = 440.3191	38.7406	111.3787
474.5661	18.3970	76.3744
508.8132	9.7656	41.3222
543.0602	6.4760	26.8564

4 CONCLUSIONS

The maximum values of the amplitudes of the dimensionless dynamic deflections and bending moments are calculated. Analysis of the results shows that the sharp increase in the amplitude values of deflections and dynamic bending moments occur in the resonance regions corresponding to the first natural frequency of oscillation. At higher frequencies this effect is practically absent. At frequencies of the external load, close to the third natural frequency, there is quite a significant difference in the results obtained by the author's and the finite element method. Values obtained by the author, should be regarded as accurate, since they are obtained by the exact solution of the original differential equation by the method of direct integration.

5 REFERENCES

[1] Babakov I. M. Teoriya kolebanii / I. M. Babakov. – M.: Nauka, 1976. – 592 p.
[2] Vasilenko M. V. Teoriya kolyvan' i stiykosti ruhu / M. V. Vasilenko, O. M. Alekseychuk. – K.: Vyscha shkola, 2004. – 525 p.
[3] Krylov A. N. Sobranie trudov. Tom 10: Vibratsii sudov. / A.N. Krylov. – M.: Izd-vo AN USSR, 1948. – 402 p.

[4] Timoshenko S. P. Kolebaniya v inzhenernom dele. M.: Nauka, 1967. – 444 p.
[5] Panovko Y. G. Vnutrennee trenie pri kolebaniyakh uprugikh sistem. / Y.G. Panovko. – M.: Fiznatgiz, 1960. – 193 p.
[6] Sorokin E. S. K teorii vnutrennego treniya pri kolebaniyakh uprugikh sistem. – M.: Gosstroyizdat, 1960. – 131 p.
[7] Olshanskiy V. P. Nestacionarnie kolebaniya mekhanicheskoy sistemi lineyno-peremennoy massy s kombinirovannim treniem / V.P. Olshanskiy, S.V. Olshanskiy // Visnyk Natsionalnogo tehnichnogo universitetu "Kharkivskiy politehnichniy institute". – 2013. – №4 (1041). – P. 324–333.
[8] Olshanskiy V. P. Nestacionarnie kolebaniya oscillatora peremennoy massi s uchetom viazkogo treniya / V. P. Olshanskiy, S. V. Olshanskiy // Vibratsii v tekhnitsi ta tekhologiyakh. – 2014. – Vyp. № 3 (75). – P. 18–27.
[9] Berendeev N. N. Issledovaniye vliyaniya vnutrennego treniya i sposoba vozbuzhdeniya na vynuzhdennie kolebaniya sistemy / Elektronnoe uchebno-metodicheskoye posobie. – Nizhniy Novgorod: Nizhegorodskiy universitet, 2012. – 50 p.
[10] Abu-Hilal M. Forced vibration of Euler–Bernoulli beams by means of dynamic Green functions. // Journal of Sound and Vibration. 267, (2003), pp. 191–207.
[11] Krutiy Yu. S. Forced harmonic oscillations of the Euler–Bernoulli beam with resistance forces: Odeskyi Politechichnyi Universytet. Pratsi. Machine building. process metallurgy. materials science / Yu. S. Krutiy // Pratsi OPU. 3(47)(2015), pp. 9–16.
[12] Daschenko A. F. ANSYS v zadachakh inzhenernoi mekhaniki / A. F. Daschenko, D. V. Lazareva, N. G. Surianinov / Izd. 2-e, pererab. i dop. Pod red. N. G. Surianinova. – Odesa. – Palmira, 2011. – 505 p.

Authors' contacts:

Yurii Krutii,
Odesa State Academy of Civil Engineering and Architecture
Didrikhsona str. 4, 65029 Odesa, Ukraine
yurii.krutii@gmail.com

Nikolay Suryaninov
Odesa State Academy of Civil Engineering and Architecture
Didrikhsona str. 4, 65029 Odesa, Ukraine
sng@ogasa.org.ua

ISSN 1846-6168 (Print), ISSN 1848-5588 (Online)
ID: TG-20170404102749

Original scientific paper

NUMERICAL SIMULATION STUDY OF PARALLEL HYDRAULIC HYBRID SYSTEM FOR A DELIVERY VAN

Dino BRNČIĆ, Goran GREGOV

Abstract: In this paper an analysis of the hydraulic hybrid system with parallel architecture is carried out. Based on the different delivery van driving regimes a calculation of the van hydraulic hybrid system is conducted and standard hydraulic components are chosen. After that a numerical model of the parallel hydraulic hybrid system is developed using the Matlab/Simulink software. Using a developed numerical model, simulations for breaking and starting modes of the vehicle are performed. Simulation results have proven the real behaviour of the developed numerical model.

Keywords: Delivery van, Parallel hydraulic hybrid system, Numerical simulation,

1 INTRODUCTION

The idea of a hybrid vehicle is the result of the need to increase the efficiency of a conventional vehicle. This creates a vehicle with primary and secondary systems. The primary system is used to drive the vehicle and this is always the internal combustion engine (IC engine). The task of the secondary system is to produce, store and reuse energy which would be irrevocably lost in the environment. Losses in conventional vehicles such as losses in the IC engine, power transmission, as well as losses due to air resistance and rolling are inevitable. However, the energy that is lost during braking can be stored and reused, thus increasing the overall efficiency of the vehicle. This principle of the braking energy utilisation is called regenerative braking [1].

Depending on the design of the secondary system, hybrids are divided into electrical, hydraulic and mechanical hybrids. Hybrid electric vehicles are the most known hybrid vehicles because of the application of the electric hybrid technology in passenger cars. The main components of the hybrid electric vehicle are the generator, electric motor and electric battery. The biggest advantage of the hybrid electric vehicle is the ability to store a lot of energy in the compact and weightless electric battery. The main disadvantage of the hybrid electric vehicle is the low amount of stored energy density in the electric battery; therefore, the hybrid electric vehicle has to use an extra gearbox. Consequently, the hybrid electric technology is used in weightless passenger cars, while it is not used in commercial vehicles, buses, trucks and other heavy vehicles. In the aforementioned vehicles hydraulic hybrid technology is usually used [2].

The main components of hydraulic hybrid systems are the hydraulic pump, hydraulic motor and hydraulic accumulator, which are equivalent to the generator, electric motor and electric battery in electric hybrids. The main advantage of hydraulic hybrids compared to electric hybrids is the greater amount of stored energy density which is up to five times higher [3]. Another advantage of the hydraulic hybrid is great efficiency in cases of frequent braking and the starting of vehicles, e.g. garbage trucks and delivery vans. Taking into account the mentioned advantages of the hydraulic hybrid system, in this paper we will analyse the hydraulic hybrid system with parallel architecture for a delivery van.

2 PARALLEL HYDRAULIC HYBRID SYSTEM

The development of hybrid vehicles began in 1898 when Ferdinand Porsche introduced the first hybrid electric vehicle "Locher-Porsche Mixte Hybrida". This vehicle used an IC engine and two electric motors on the front wheels. When Henry Ford introduced an assembly line in car manufacturing, which resulted in his cheap car "Model T", hybrid vehicles no longer produced. After the first and second oil crisis, the hybrid vehicle became interesting again. In 1997, the modern hybrid electric car was presented by Toyota and Audi with their models “Prius” and “Duo”, respectively [4].

The development of the hydraulic hybrid began in the1980s. Hydraulic hybrid technology was originally developed by Volvo Flygmotor. Volvo developed a hydraulic hybrid system which was installed on buses in Stockholm. The reduction of the fuel consumption was between 16% and 25%. The first parallel hydraulic hybrid was "Cumolu Brake Drive" of the Parker Hannifin Corporation. In 1991, the Parker Hannifin Corporation also developed the first serial hydraulic hybrid. Nowadays many companies and university teams work on the hydraulic hybrid systems development such as Eaton, Parker, Bosch-Rexroth, Artemis, and others.

The basic division of the hydraulic hybrid is into serial and parallel hybrids. Typical serial hybrids are mounted on vehicles that already have a hydrostatic transmission, such as trucks or vehicles, whose driving mode is made up of a lot of stopping and starting. The serial hydraulic hybrid vehicle (Fig. 1) is composed of a hydraulic pump which is power operated by an IC engine, hydraulic motor which

drives vehicle wheel and low and high pressure accumulators.

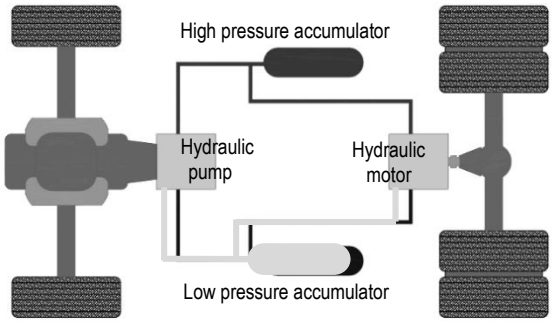

Figure 1 Serial hydraulic hybrid vehicle

The lack of a serial hybrid is the inability to achieve high-speeds, making it ideal for use on heavy vehicles, but not on vehicles in intercity traffic. For such a vehicle it is more convenient to use a parallel hydraulic hybrid system, because it allows the storage of energy during braking, but when it needs to achieve higher speeds, it uses the primary system. The parallel hydraulic hybrid vehicle is composed of a hydraulic pump which can work as a hydraulic motor, low and high pressure accumulators and a gearbox that is used for power take-off from the drive shaft (Fig. 2).

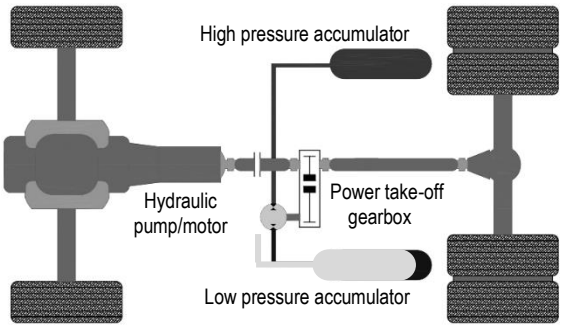

Figure 2 Parallel hydraulic hybrid vehicle

When the vehicle starts to brake, the hydraulic pump connected to the drive wheels via the drive shaft and the gearbox establishes the flow of the working fluid from the low to high pressure accumulator. The fluid that enters into the hydraulic accumulator must overcome the gas pressure, which is currently acting in the high pressure accumulator. The compressed gas creates resistance to the flow of the fluid in the accumulator, which creates the effect of braking on the wheels and slows down the vehicle. Thus, the kinetic energy of the vehicle is converted into energy of compressed gas in the accumulator.

When the vehicle begins to accelerate, the working fluid flows from the high to low pressure accumulator. Now the pump is acting as a hydraulic motor. When the vehicle consumes all the stored energy, the drive from the secondary system switches to the primary system, i.e. IC engine. At higher speeds (over 60 km/h) a vehicle can also store energy in the accumulator in short-term braking, although it does not stop. Accumulated energy, can later be used to accelerate the vehicle (e.g. when shifting gears) to help the IC engine, which also reduces fuel consumption.

3 CALCULATION OF A PARALLEL HYDRAULIC HYBRID SYSTEM FOR A DELIVERY VAN

Calculation of the parallel hydraulic hybrid system is carried out for the delivery van "Volkswagen Crafter TDI400" [5]. The vehicle has a 120 kW diesel engine, 6-speed manual gearbox, and a rear wheel drive. The maximum value of the payload plus vehicle weight is 3,500 kg. To design a parallel hydraulic hybrid system, the gearbox, drive shaft and differential gearbox have to be unchangeable, and new parts have to be added, such as the hydraulic pump/motor, low and high pressure accumulators, power take-off gearbox, and a control unit. Therefore, it is necessary to carry out a calculation of the main hydraulic part of the hybrid system, hydraulic pump/motor, high pressure accumulator, and low pressure accumulator.

Calculation has been carried out for two regimes of driving which are defined by the inclination of the road, vehicle driving speed and percentage of vehicle payload, as shown in Tab. 1.

Table 1 Driving regimes of delivery van

Driving regime	1	2
Inclination of road (%)	25	0
Driving speed (km/h)	12.7	120
Vehicle payload (%)	100	0

The first step in the calculation is to estimate all resistances that occur when the delivery van is driving: rolling friction force, air resistance force, resistance acceleration force, and inclination force. The sum of these forces results with a drag force F_{Vd}, which the vehicle must overcome. By knowing the value of the drag force and dimensions of the wheel (235/65R16), we are able to calculate the maximum torque on the vehicle wheels T_{Vmax}. By knowing the wheel dimensions and the vehicle driving speed, we can also calculate the rotational speed of the wheels n_V. The obtained results for the defined driving regimes are shown in Tab. 2.

Table 2 Calculated results for two driving regimes

Driving regime	F_{Vd} (N)	T_{Vmax} (N·m)	n_V (s^{-1})
1	13 934.9	7803.5	1.01
2	2583.5	1444.6	9.49

The torque on the hydraulic pump/motor shaft T_{shf} is the maximum torque on vehicle wheels divided by the sum of the vehicle differential gearbox ratio i_d = 3,923 and the power take-off gearbox ratio i_{pto} = 2. The chosen value of the take-off gearbox ratio is based on value of gearboxes ratio of similar hybrid vehicles.

Assuming the pressure drop Δp = 400 bar and the hydro-mechanical efficiency η_{hm} = 0.98, it follows that the displacement of the hydraulic pump/motor V_1 = 159.4 cm^3. According to the obtained value for displacement, the axial piston hydraulic pump/motor Bosch Rexroth A6VM has been chosen with characteristics shown in Tab. 3.

The calculation of the high pressure accumulator is based on the ability to absorb sufficient kinetic energy during the regenerative braking. It is assumed that the high pressure accumulator will be fully charged during the vehicle braking from v_2 = 70 km/h to v_1 = 10 km/h. When the vehicle decelerates to 10 km/h, the main braking system stops the vehicle. By knowing the regime of braking and the mass of vehicle, it follows that the maximum kinetic energy which can be absorbed during the braking E_B = 648 kJ.

Table 3 Characteristic of Bosch Rexroth A6VM hydraulic pump/motor

Max. displacement	V_{max}	171.8	cm^3
Max. speed	n_{max}	5750	min^{-1}
Max. flow	Q_{max}	533	l/min
Max. pressure	Δp	450	bar
Max. torque	T_{max}	1230	N·m

However, due to losses in the hydraulic system, 60 % of the whole kinetic energy can be stored in the high pressure accumulator [3], therefore E_B = 389 kJ. The high pressure accumulator with a nominal volume V_0 = 50 l and the minimum operating pressure of p_1 = 200 bar has been chosen as a preliminary. Parameter p_0 is the pre-charge pressure which is 10 % lower than the minimum operating pressure p_1. The maximum operating pressure was previously chosen and amounts to p_2 = 400 bar.

The process in the accumulator has been observed as a fast adiabatic process without heat transfer between a thermodynamic system and its surrounding. This can be explained with a value less than four minutes for charge and discharge of the accumulator. The maximum volume of working fluid, which can be charged in the high pressure accumulator, was calculated using the Eq. (1), whereby V_{oil} = 26 l.

$$V_{oil} = V_0 \left(\frac{p_0}{p_1} \right)^{\frac{1}{\kappa}} \left[1 - \left(\frac{p_0}{p_2} \right)^{\frac{1}{\kappa}} \right] \tag{1}$$

The maximum stored energy in the high pressure accumulator was calculated using the Eq. (2), whereby E_A = 392 kJ.

$$E_A = p_2 (V_0 - V_{oil}) - p_0 V_0 \tag{2}$$

The number of high pressure accumulators were calculated in such a way that the maximum kinetic energy attained during the vehicle braking E_B divided by the maximum stored energy in the high pressure accumulator E_A, which results in 0.99 accumulators. Therefore Bosch Rexroth HAB 50-414 bladder type accumulator with the nominal volume of 50 l [6] was chosen. The low pressure accumulator was not calculated because it was chosen according to the minimum operating pressure of the high pressure accumulator. The Bosch Rexroth HAB 50-207 bladder type accumulator was selected.

4 MATHEMATICAL MODELLING OF A PARALLEL HYDRAULIC HYBRID VEHICLE

The mathematical model is the fundamental model for describing the behavior of a physical system. It can be defined, for example, as a set of differential equations which describe the connection between the physical values in the observing system.

The mathematical model of the parallel hydraulic hybrid system has been analyzed as a mathematical model of the hydraulic pump/motor and the high pressure accumulator. The mathematical model of the hydraulic pump and hydraulic motor is described with the torque balance Eq. (3) for the hydraulic pump and the Eq. (4) for the hydraulic motor.

$$J^P \frac{\mathrm{d}^2 \varphi^P}{\mathrm{d}t} + T_f^{HP} \left(\frac{\mathrm{d}\rho^P}{\mathrm{d}t} \right) = T_{shf}^P - \eta_{vol}^P T_{th}^P \tag{3}$$

$$J^M \frac{\mathrm{d}^2 \varphi^M}{\mathrm{d}t} + T_f^{HM} \left(\frac{\mathrm{d}\varphi^M}{\mathrm{d}t} \right) = T_{shf}^M + \frac{1}{\eta_{hm}^M} T_{th}^M \tag{4}$$

J is the moment of inertia of the pump/motor, T_{shf} is the torque of the pump/motor shaft, T_f is the frictional torque of the pump/motor, T_{th} is the theoretical torque of the pump/motor, η_{vol} is the volumetric efficiency of the pump/motor and φ is the rotational angle of the pump/motor shaft [7]. The method for modelling the frictional torque of the pump/motor is to model friction as a function of velocity, which is referred to as the Stribeck curve. The three characteristic parts of this equation are the viscous friction T_v, Coulomb friction T_{c0} and static friction with the parameters T_{s0} and c_s, known as the Stribeck velocity (Eq. (5)).

$$T_f \left(\frac{\mathrm{d}\varphi}{\mathrm{d}t} \right) = T_v \frac{\mathrm{d}\varphi}{\mathrm{d}t} + \mathrm{sign} \left(\frac{\mathrm{d}\varphi}{\mathrm{d}t} \right) \left[T_{c0} + T_{s0}\, exp \left(- \frac{\left| \frac{\mathrm{d}\varphi}{\mathrm{d}t} \right|}{c_s} \right) \right] \tag{5}$$

The mathematical model of the high pressure accumulator is defined with the pressure, temperature and volume of the working fluid in the accumulator. Mathematical equations, which describe the mentioned parameters, are the ideal gas law and the real gas law. The ideal gas law is a good approximation of the behavior of many gases under many conditions. Consequently, the ideal gas law has been used for the mathematical model of the high pressure accumulator. Moreover, the process in the accumulator has been observed as a fast adiabatic process. This can be explained with a value less than four minutes for charge and discharge of the accumulator. The pressure and temperature alterations in the high pressure accumulator are described by using the following Eqs. (6) and (7), where θ_0 is the temperature of the surrounding.

$$\frac{\mathrm{d}p}{\mathrm{d}t} = p_0 \left(\frac{V_0}{\frac{\mathrm{d}V}{\mathrm{d}t}} \right)^{\kappa} \tag{6}$$

$$\frac{\mathrm{d}\theta}{\mathrm{d}t} = \theta_0 \left(\frac{p_0}{\frac{\mathrm{d}p}{\mathrm{d}t}} \right)^{\frac{1-\kappa}{\kappa}} \tag{7}$$

If the real gas law is used for the mathematical model, generally the Beattie-Brigdman equation or the Benedict-Webb-Rubin equation can be applied [8]. The disadvantages of using the mentioned equations for the mathematical model of the accumulator are their complexity and needs for the experimental measurement on the real hydraulic accumulator for determining all parameters.

Knowing the pressure dynamic of the high pressure accumulator the state of charge (*SOC*) of the accumulator can be defined. The state of charge of the high pressure accumulator is defined as the ratio of the current amount and the maximum amount of accumulator energy. If the amount of accumulator energy is described by the pressure of gas in accumulator, Eq. (8) can be used [9].

$$SOC = \frac{p_2 - \frac{\mathrm{d}p}{\mathrm{d}t}}{p_2 - p_0} \tag{8}$$

The state of charge is important for the hydraulic hybrid vehicle system control. This value defines when the high pressure accumulator is able to give energy to the hybrid vehicle and when it is necessary to start charging the high pressure accumulator during vehicle breaking.

5 NUMERICAL MODELLING OF A PARALLEL HYDRAULIC HYBRID VEHICLE

Based on the mathematical model, the numerical model can be developed using certain software. For numerical modelling, two principles can be used, the first is to use a very general description to represent a system (white-box model) and the second shows the use of a particular characterization for certain classes of systems (black-box model). A natural way to develop a numerical model is white-box modelling. It is based on the previous mathematical model, i.e. differential equations, algebraic equations, logical relationships and similar types of equations [10]. White-box modelling has been applied for numerical modelling of the parallel hydraulic hybrid system, using the Matlab/Simulink software. Two numerical models were carried out: the numerical model for the vehicle braking mode, and the numerical model for the vehicle starting mode.

The numerical model of the parallel hydraulic hybrid system for the vehicle breaking mode is composed of the numerical model of the hydraulic pump and the numerical model of the high pressure accumulator. The numerical model of the accumulator is based on the previously described mathematical model. On the other hand, the numerical model of the hydraulic pump did not use the mentioned differential equation, because the rotational speed of the pump is well known, however, the standard equation for the calculation of pump flow and torque was used [11]. Therefore the input value in the numerical model is the rotational speed of the hydraulic pump, i.e. rotational speed of the vehicle wheels.

The numerical model of the parallel hydraulic hybrid system for vehicle starting mode is shown in Fig. 3. Also this model is composed of the numerical model of the hydraulic motor and the numerical model of the high pressure accumulator. The numerical model of the hydraulic motor and the accumulator are based on the previously described mathematical model. The Coulomb friction and static friction were neglected in the numerical model of the hydraulic motor, only the viscosity friction was taken into account. The value of the viscosity friction torque was chosen from similar research [10].

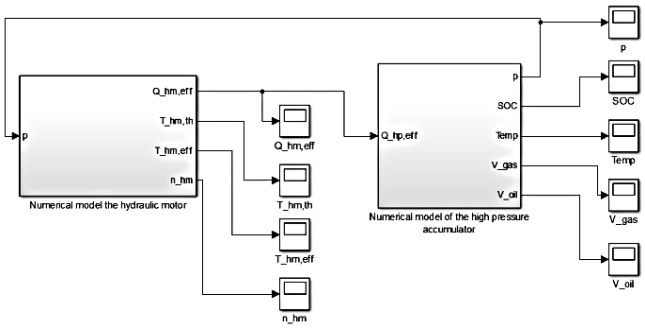

Figure 3 The numerical model of the parallel hydraulic hybrid system for vehicle starting mode

6 SIMULATION OF DEVELOPED NUMERICAL MODEL OF PARALLEL HYDRAULIC HYBRID SYSTEM

Simulations were conducted for the developed numerical model of the parallel hydraulic hybrid system. The aim of simulation results is to prove the accuracy of the developed numerical model. Simulations were carried out for the numerical model of the vehicle braking mode and the vehicle starting mode. Ten seconds of simulation duration were chosen for all simulations.

The simulation results which will be observed from the numerical models are pressure, *SOC*, volume and temperature of the working fluid and gas into the high pressure accumulator. Also, the torque and rotational speed of the hydraulic motor will be observed.

6.1 Simulation of a parallel hybrid system for a vehicle braking mode

The rotational speed of the hydraulic pump was calculated as linear decrease of the rotational speed from 44 s^{-1} to 6 s^{-1} during ten seconds, based on the previous assumption that the high pressure accumulator will be fully

charged during the vehicle braking from 70 km/h to 10 km/h. Values of the pump rotational speed are the input into the numerical model of the hydraulic pump. The output result from the numerical model of the pump is the pump flow which decreases from 432 l/min to 60 l/min as a result of the pump rotational speed decrease, as shown in Fig. 4. The decrease of the vehicle speed during the breaking mode is a result of the fluid that enters into the hydraulic accumulator and must overcome gas pressure in the high pressure accumulator. The compressed gas creates resistance to the flow of the fluid in the accumulator, which creates increases of pressure of the working fluid and a decrease of the pump rotational speed.

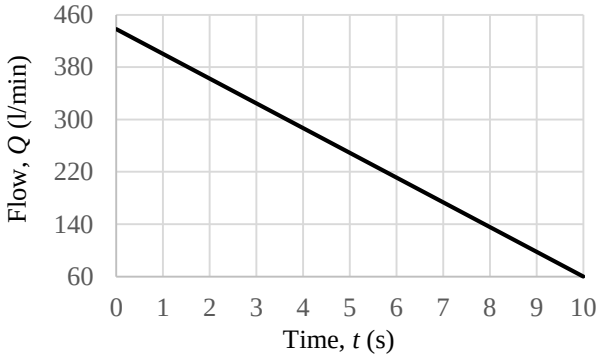

Figure 4 Simulation results of flow from hydraulic pump during vehicle braking mode

The input value in the numerical model of the high pressure accumulator is the output value from the numerical model of the pump, i.e. simulation results of the hydraulic pump flow. The simulation results of the pressure of working fluid in the high pressure accumulator (Fig. 5) show that at the beginning of the simulation the pressure is equal to the pre-charged pressure in the accumulator p_0 = 180 bar.

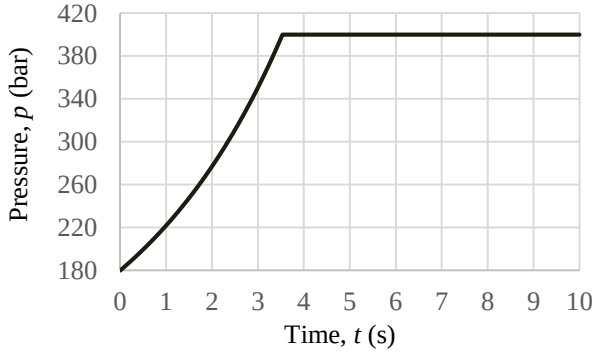

Figure 5 Simulation results of pressure of working fluid in the high pressure accumulator during vehicle braking mode

During the vehicle breaking, the hydraulic pump achieves a flow of the working fluid from the low to high pressure accumulator, which results in the charging of the high pressure accumulator and the increase of the pressure of the working fluid. After 3.5 seconds the maximum pressure of the selected accumulator p_2 = 400 bar is achieved. It can be concluded that the results indicate the real behavior of the developed numerical model. Also, it can be concluded that the chosen adiabatic process was properly chosen because the time of accumulator charge is less than four minutes.

When we compare the obtained results of the pressure with the previous assumption that the high pressure accumulator will be fully charged during the vehicle braking from 70 km/h to 10 km/h during 10 seconds, we can conclude that for the fully charged accumulator 3.5 seconds are necessary; therefore, during the first 3.5 seconds the vehicle is braking by charging the high pressure accumulator and after that the vehicle is braking with main braking system.

The state of charge of the high pressure accumulator is the function of pressure in an accumulator, which is described by the Eq. (8). Therefore, the simulation result (Fig. 6) shows identical behavior as a result of pressure in the high pressure accumulator. At the beginning of the simulation the accumulator is empty, *SOC* = 0, and after 3.5 seconds the accumulator is fully charged, *SOC* = 1.

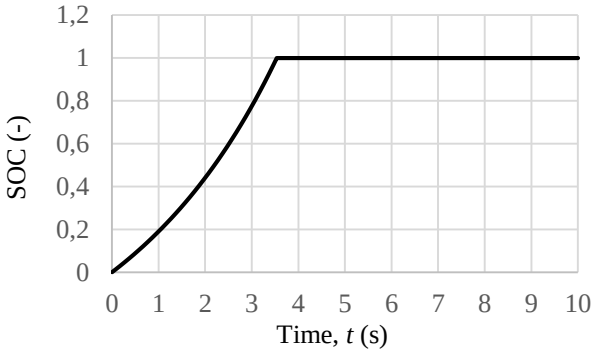

Figure 6 Simulation results of *SOC* of high pressure accumulator during vehicle braking mode

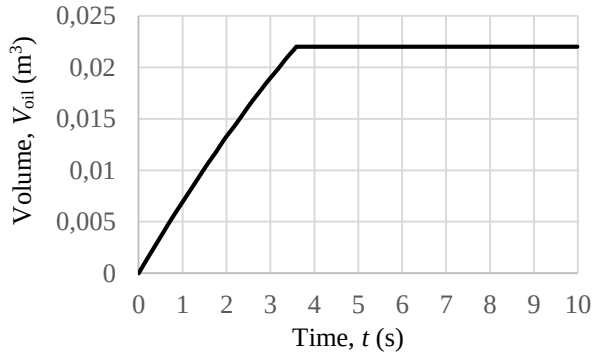

Figure 7 Simulation results of volume of working fluid in the high pressure accumulator during vehicle braking mode

The simulation results of volume of the working fluid in the high pressure accumulator (Fig. 7) show that at the beginning of the simulation the accumulator is empty, V_{oil}= 0. During vehicle braking the volume of the working fluid is increased and after 3.5 seconds V_{oil}=0.022 m^3 (22 l). It can be concluded that during the vehicle braking mode the accumulator is charged about 85% of the maximum value of the accumulator volume (26 l), because after 3.5 seconds of

the simulation the pressure in accumulator achieves the maximum value of the pressure of the hydraulic system (400 bar). In that moment, the hydraulic hybrid systems switch to the main braking system.

The simulation results of the volume of gas in the high pressure accumulator (Fig. 8) show that at the beginning of the simulation the gas has maximum volume, V_{gas}= 0.05 m^3 (50 l). During vehicle braking the volume decreases and after 3.5 seconds the value V_{gas} = 0.028 m^3 (28 l) is achieved. It can be concluded that the compression of gas is realized, and the value of compressed volume of gas is equal to the value of the charged volume of the working fluid.

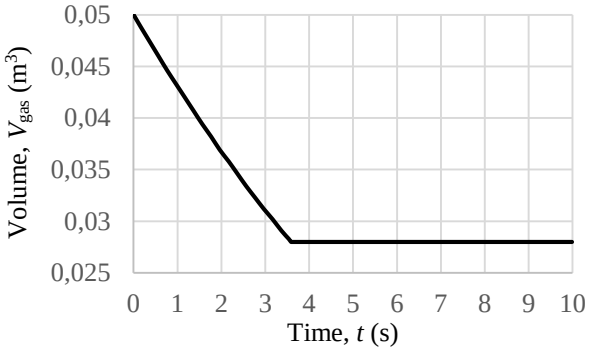

Figure 8 Simulation results of volume of gas in the high pressure accumulator during vehicle braking mode

The simulation results of the temperature in the high pressure accumulator (Fig. 9) show that at the beginning of the simulation the temperature is equal to the environment temperature θ_0 = 293 K. During vehicle braking the temperature increases and after 3.5 seconds the value θ = 369 K is achieved, which is lower than the maximum allowed temperature of the selected accumulator, θ_{max} = 380 K. Once more, it can be concluded that the chosen adiabatic process was properly chosen.

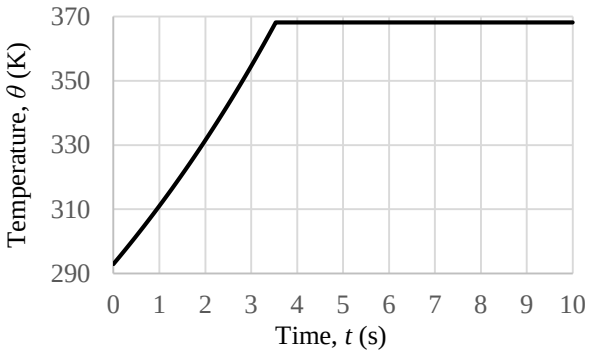

Figure 9 Simulation results of temperature in the high pressure accumulator during vehicle braking mode

The simulation results of the developed numerical model of a parallel hybrid system for a vehicle braking mode have proven the accurateness of the developed model. Also, the results have proven correctness of the previous calculation and selection of hydraulic components.

Furthermore, the simulation results have shown that after 3.5 seconds the maximum pressure (p_2 = 400 bar) of the hydraulic system was achieved and the accumulator was charged about 85%. That simulation result values prove that if the observed hydraulic hybrid system is mounted in the real delivery van, the sufficient amount of energy will be stored in short time. In this way the advantage of using the numerical simulation is also proven, which enables the observation of the dynamic of hydraulic hybrid vehicle in the time domain.

6.2 Simulation of a parallel hybrid system for a vehicle starting mode

When the vehicle begins to accelerate, the working fluid flows from the high to low pressure accumulator. The simulation results of the pressure of the working fluid in the high pressure accumulator (Fig. 10) show that at the beginning of the simulation the accumulator is fully charged and the pressure has maximum value, p_2 = 400 bar. During vehicle starting mode the pressure increases, which is the result of accumulator discharging, and after four seconds the value 330 bar is achieved.

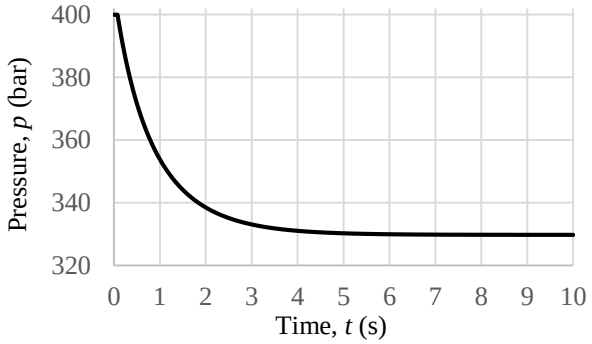

Figure 10 Simulation results of pressure of the working fluid in the high pressure accumulator during vehicle starting mode

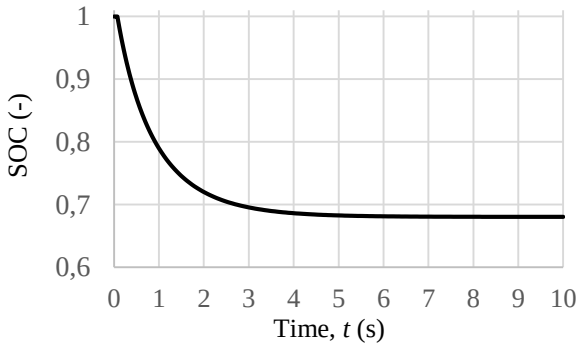

Figure 11 Simulation results of SOC of the high pressure accumulator during vehicle starting mode

Same as the result in the previous simulation, the results of the *SOC* of the high pressure accumulator (Fig. 11) show identical behavior as a result of the pressure in the high pressure accumulator. At the beginning of the simulation the accumulator is fully charged *SOC* = 1 and after four seconds the result of the *SOC* is 0.68. It can be concluded

that the high pressure accumulator was not fully discharged because of dynamic of the hydraulic motor effects to the high pressure accumulator, which will be described in following text.

The simulation results of the volume of the working fluid in the high pressure accumulator (Fig. 12) show that at the beginning of the simulation the volume V_{oil} = 0.022 m^3 (22 l). This value of volume was achieved after the vehicle braking (Fig. 7). During vehicle starting the volume of the working fluid is decreasing and after four seconds V_{oil} = 0.0176 m^3 (17.6 l) is achieved. It can be concluded that during the vehicle starting mode the accumulator discharges 4.4 liters of working fluid.

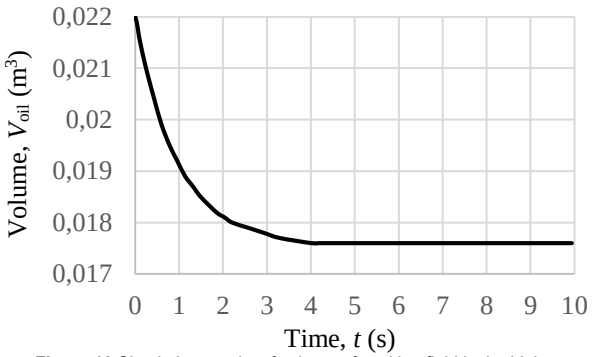

Figure 12 Simulation results of volume of working fluid in the high pressure accumulator during vehicle starting mode

The simulation results of the volume of gas in the high pressure accumulator (Fig. 13) show that at the beginning of the simulation the gas has the volume V_{gas} = 0.028 m^3. This value of the volume of gas is achieved after the vehicle braking (Fig 8.). During vehicle starting the volume increases and after four seconds the value V_{gas} = 0.0324 m^3 is achieved. It can be concluded that the expansion of the gas is realized, and the value of the expansion volume of gas is equal to the value of the discharged volume of working fluid.

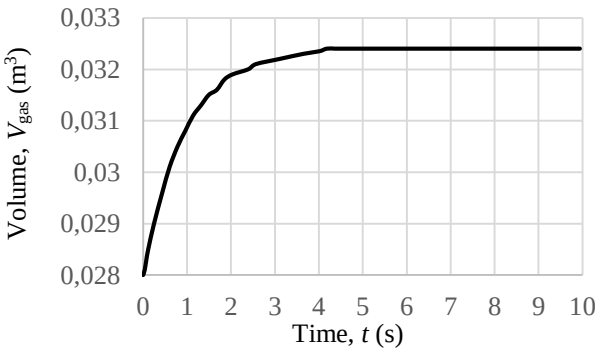

Figure 13 Simulation results of volume of gas in the high pressure accumulator during vehicle starting mode

During the starting mode, the pump acts as a hydraulic motor. The hydraulic motor has to be able to overcome the maximum torque which is needed to start the vehicle. The most unfavorable situation is when the vehicle is driving on an inclined road with the maximum payload where it is necessary to overcome the load torque of 920 Nm. The mentioned value of torque was used for the simulation of the vehicle starting mode during the whole simulation, although in real vehicles the value of load torque decreases after starting the vehicles. The simulation results of the torque of the hydraulic motor shaft (Fig. 14) show that during the first four seconds the hydraulic motor is able to overcome the torque necessary for starting the vehicle. Moreover, the simulation results show that after four seconds the value of the torque of the hydraulic motor is equal to the value of the maximum load torque, which is the result of the mathematical model of the hydraulic motor. Therefore, the hydraulic motor is not able to overcome the load torque of 920 N·m and the hydraulic motor stops rotating.

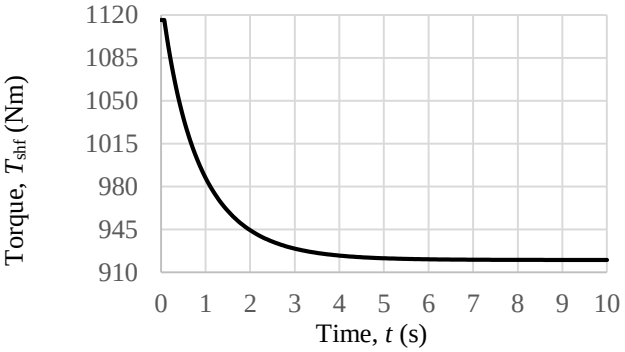

Figure 14. Simulation results of torque of hydraulic motor shaft during vehicle starting mode

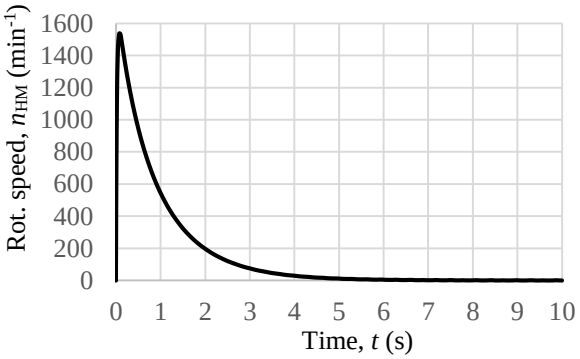

Figure 15 Simulation results of hydraulic motor rotational speed during vehicle starting mode

The simulation results of the rotational speed of the hydraulic motor (Fig. 15) show that at the beginning of the simulation the rotational speed increases to n_{HM} = 1540 min^{-1} and then decreases as a result of decreasing the pressure in the high pressure accumulator. After four seconds the rotational speed of the hydraulic motor n_{HM} = 0 is achieved. This is a result of decreasing the pressure in the high pressure accumulator, which after four seconds is not able to achieve the sufficient torque to overcome the load torque of 920 N·m and the hydraulic motor stops rotating. When the hydraulic motor has stopped rotating, the flow through the hydraulic motor also stops; therefore, the high pressure accumulator stops discharging. Consequently, after four seconds of the simulation, the pressure and volume of

the working fluid and gas in the high pressure accumulator have stopped changing.

From the simulation results it can be observed that after two seconds the rotational speed decreases under the minimum value of the hydraulic motor rotational speed 476 min^{-1}, which is defined by the driving regime. Therefore, when the hydraulic motor rotational speed decreases to the minimum value the hydraulic hybrid systems switch to the primary IC engine.

The simulation results of the developed numerical model of a parallel hybrid system for a vehicle starting mode have also proven the accurateness of the developed model and correctness of the previous calculation and selection of hydraulic components.

Moreover, the simulation results have proved that the stored energy in high pressure accumulator during the vehicle braking is sufficient for starting the vehicle in the most unfavorable situation when the vehicle is driving on an inclined road with the maximum payload. In this way, important energy saving is achieved because the delivery van required a lot of energy for starting.

7 CONCLUSIONS

The main objective of this research was to develop a numerical model of the parallel hydraulic hybrid system for the delivery van. The reason for that is that the numerical model can observe the dynamic of hydraulic hybrid vehicle in time domain. Based on the different driving regimes, a calculation of the van hydraulic hybrid system was conducted and standard hydraulic components were chosen. The numerical model of the parallel hydraulic hybrid system was developed using the Matlab/Simulink software. Two numerical models were carried out: the numerical model for the vehicle braking mode and the numerical model for the vehicle starting mode.

Simulation results of the developed numerical model for the vehicle braking mode have shown that during the vehicle braking, the pressure in the high pressure accumulator achieved the maximum value and the accumulator was charged about 85%. Simulation results of the developed numerical model for the vehicle starting mode have shown that the hydraulic motor is able to overcome the torque necessary for starting the vehicle, i.e. the stored energy in the high pressure accumulator is sufficient for starting the vehicle.

Simulation results have proven that the designed hydraulic hybrid system is able to produce, store and reuse energy for all driving regime for the chosen delivery van, and energy saving was demonstrated.

8 REFERENCES

[1] Brnčić, D.: Project of Hydraulic Hybrid System for Commercial vehicle, Diploma thesis, University of Rijeka, Faculty of Engineering, Croatia, (in Croatian), 2016

[2] Bertović, D., Gregov, G., Siminiati, D.: Modelling and Simulation of a Serial Hydraulic Hybrid Drive Train for a Forklift Truck, Advanced Engineering: International Journal, Vol. 8 (2014), 5-12.

[3] Rydberg, K.E.: Energy Efficient Hydraulic Hybrid Drives, The 11th Scandinavian International Conference on Fluid Power, SICFP'09, Linköping, Sweden, 2009.

[4] Ibrahim, M. S. A.: Investigation of Hydraulic Transmissions for Passenger Cars, Doctoral thesis, University of Aachen, Germany, 2011.

[5] http://en.volkswagen.com/en.ht

[6] (Acessed:03.04.2017.)

[7] http://www.boschrexroth.com/en/xc/ (Acessed:03.04.2017.)

[8] Jelali, M., Kroll, A.: Hydraulic Servo-systems, Modelling, Identification and Control, Springer, London, 2003.

[9] Larsen, J. M.: Validation Study of Real Gas Models, Doctoral thesis, Aalborg University, Denmark, 2010.

[10] Hoekstra, D.: Conceptual Design of Energy Exchange Systems for Hybrid Vehicle, Master thesis, Eindhoven University of Technology, Netherlands, 2005.

[11] Gregov, G.: Contribution to Research Modelling of the Hydrostatic Transmission Applied to the Forest Vehicle, Doctoral thesis, University of Rijeka, Faculty of Engineering, Croatia (in Croatian), 2012.

[12] Dietmar, F., Findeisen, F.: Oil hydraulic, Springer-Verland, Berlin, 1994.

[13] Xianwu, Z.: Improving the Energy Density of Hydraulic Hybrid Vehicle (HHVs) and Evaluating Plug-in HHV, Doctoral thesis, University of Toledo, 2009.

Authors` contacts:

Dino BRNČIĆ, Mag. ing. mech
University of Rijeka
Faculty of Engineering
Vukovarska 58, HR-51000 Rijeka
Croatia

Goran GREGOV, Ph.D, Assistant Professor
University of Rijeka
Faculty of Engineering
Vukovarska 58, HR-51000 Rijeka
Croatia
+385 51 651 528
gregovg@riteh.hr

ISSN 1846-6168 (Print), ISSN 1848-5588 (Online)
ID: TG-20170501101521

Original scientific paper

SUSTAINABLE PRODUCT DEVELOPMENT: PROVISION OF INFORMATION IN EARLY AUTOMOTIVE ENGINEERING PHASES

Helmut BRUNNER, Patrick ROSSBACHER, Mario HIRZ

Abstract: Sustainable product development is an important influencing factor in automotive engineering, whereby a comprehensive evaluation of its efforts and benefits is very complex. In addition, lots of information is not available in advance of mass production. This leads to the question, how results from impact assessment can be transferred to the beginning of the development process, where important decisions about product and production characteristics are made. The present paper discusses approaches for life cycle estimation and decision support in the concept phase of automotive engineering, especially focusing on the design engineer's requirements. It includes an overview of current development processes and discusses by use of examples different approaches to integrate relevant information concerning sustainable product development in development processes.

Keywords: sustainable product development; technology management; automotive industry; early product development phases

1 INTRODUCTION

Today, automotive development has to face numerous exciting challenges. The major reasons for that are a rising globalization, steadily increasing customer demands worldwide, as well as the fast advances in technological terms, e.g. alternative propulsion systems, new materials and innovations in the field of electronics and automation. During the past decades, automotive development has been characterized significantly by a growing share of intelligent components, increasing technical complexity of vehicles and vehicles modules, as well as steadily increasing model ranges. The manifold model types require the development of different body styles, different propulsion systems as well as different comfort functions and interior configurations. Simultaneously, the rising globalization yields to a stronger competition amongst the OEMs[1], and that results in the demand of accelerating the development, in order to introduce innovative products to the global market as fast as possible. On the other hand, the production period and number of produced units per car model decrease [1]. The increasing complexity of product technology and variety challenge both the entire product development and the production processes. In addition, decrease of product life cycles duration also demands shorter product development times [2]. Furthermore, a stronger focus on future environmental challenges and sustainability is required. In the last two decades, the energy consumption and hazardous emissions during the use phase of a car have been in the main focus of automotive engineering, and will be in future. But besides that, the phase of production and end of life gains in importance, which can be seen by a steadily increasing number of legislation directives and guidelines concerning the use, recovery and re-use of materials in the vehicle. To meet these development trends, the present paper discusses an integration of novel sustainable materials and technologies in state of the art vehicle development processes, especially focusing on early development stages.

In Chapter 2, the relevant development phases are explained. Chapter 3 deals with life cycle-relevant considerations in the development process. In Chapter 4, approaches for the provision of life cycle-relevant information in early development phases are discussed. Chapter 5 closes with a short summary.

2 THE AUTOMOTIVE DEVELOPMENT PROCESS

A modern vehicle consists of several thousand parts. Besides bringing the passenger from A to B, a broad range of further functions are being integrated into the car, ensuring e.g. safety, environmental standards or comfort for the passenger. To create such a complex machine and to consider previously described boundary conditions, a flexible development and production process is required, as can be seen in Fig. 1.

The automotive development process principally consists of five main process phases: the definition phase, the concept phase, the pre-development, the series development, and early stages of the production phase. Within the initial definition phase, the requirements on the concept are collected. This includes all boundary conditions targeting legislative, consumer- or company- related aspects. It also covers the consideration of possible production facilities, basic geometric dimensions and functional requirements. The subsequently performed phase that has main impact on product characteristics and further development is explained in the following section.

[1] OEM: original equipment manufacturer

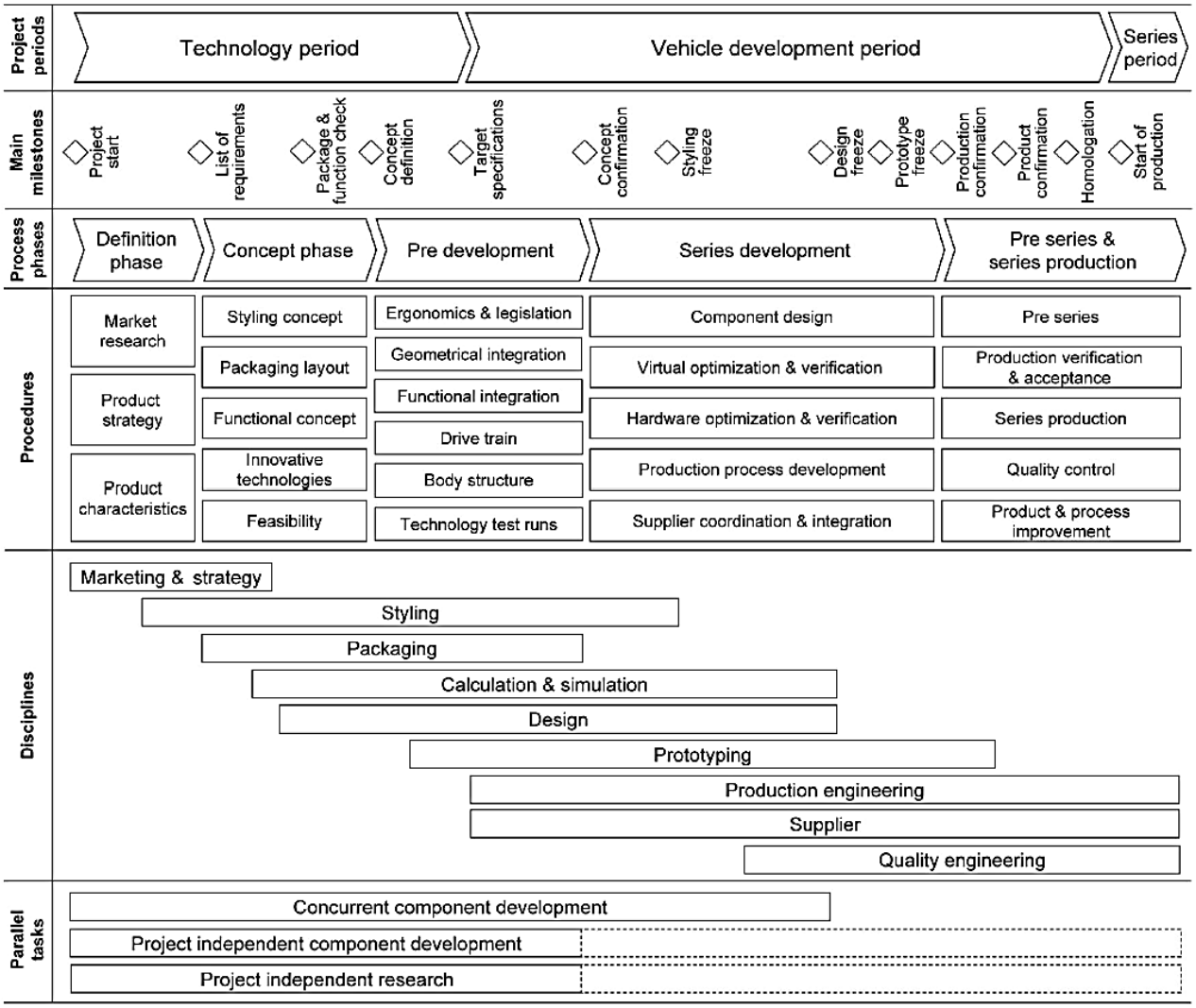

Figure 1 Principal stages in a typical state-of-the-art full-vehicle development process [3]

2.1 Concept phase

The definition phase is followed by the initial concept phase. Within this process step, first visions and ideas of the vehicle come to life; this ranges from the analysis of potential innovative technologies, first 3D drafts of spatial requirements (see Fig. 2), and an initial consideration of vehicle functions.

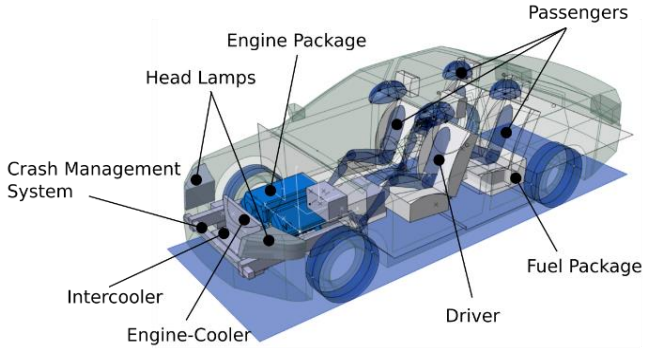

Figure 2 Preliminary 3D vehicle package as a result of the concept phase [13]

The result of the initial concept phase is a basic selection of possible suitable concept variants in the context of the defined technological and economical boundary conditions. Mostly, design principles are based on previous developments and experiences of engineers. After the initial concept phase has been passed successfully, the detail concept phase begins. In this phase, the preliminary concept ideas are refined, leading to further deeper analysis, targeting detailed 3D-CAD design models, more detailed package investigations, consideration of different styling concepts and the simulation of vehicle functions. The final step in the concept phase represents the concept decision, which is responsible for a proper selection of the detail concept. This means, if several concepts have been developed, at this point, the concept that is selected best suites to fulfill the stated requirements at the beginning of the process. As a result, dimensions of the basic vehicle architecture are defined, as shown in Fig. 3.

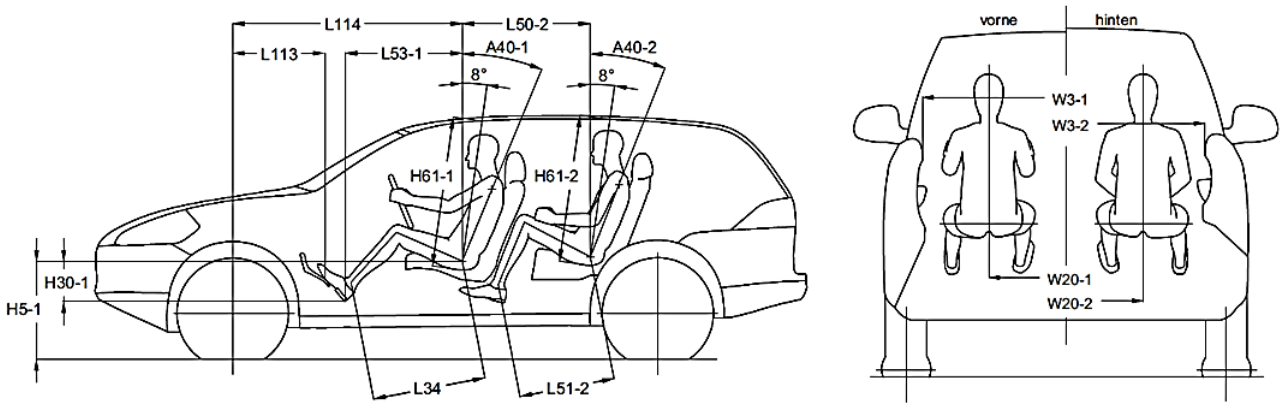

Figure 3 Defined basic vehicle dimensions in the concept phase (extract) [4]

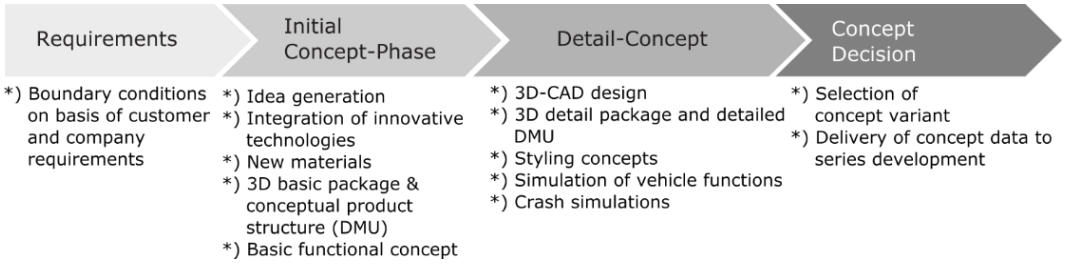

Figure 4 Steps of the early phase of development processes in automotive industry

As a conclusion, the main decisions for the development of a new vehicle or technology are made within this described four-step development process in the early stage of vehicle development (Fig. 4).

3 LIFE CYCLE CONSIDERATIONS IN THE AUTOMOTIVE DEVELOPMENT PROCESS

In this paper, the term *life cycle considerations* addresses the consideration of mainly ecologic and economic, and social impacts along the entire life cycle of a car (Fig. 5).

Figure 5 Schematic life cycle of a car

Focusing on automotive development processes, the life cycle starts with the requirements definition phase during vehicle conception. Currently, regarding life cycle considerations, sustainable automotive product development mainly focuses on existing directives to ensure compliance with material prohibitions and environmental regulations in vehicle production and end of life. One example of legal conditions is the ELV-directive of the European Union, which addresses the end-of-life treatment of vehicles [5]. Another focus of legislative lies in the reduction of greenhouse gas emissions and pollutants during operation. Therefore, the legal conditions are described in [6]. Considering the in-use phase of a car, most important fields of research in the area of energy demand and emissions reduction are

- mass reduction by lightweight construction (using high-strength alloys, light metal, fiber-reinforced plastics, multi-material construction),
- increasing the efficiency of the conventional internal combustion engines, hybridization and development of alternative drive systems, e.g. electrification of the powertrain [2].

Considering the production phase of a car, OEM's research and development strategies more and more focus on the reduction of environmental impacts, such as energy and resource demand or pollution emissions, as numerous environmental declarations from the automotive industry can be referred. One example can be seen in [7].

The next level of sustainable production is defined by the integration of sustainable materials in the car. A relatively simple example is the use of recycled materials (e.g. steel or plastics) and renewable materials (e.g. hemp, flax or wood) for parts in the vehicle interior. The simplicity of this step can be found in two reasons. On the one hand, technical requirements (e.g. stiffness) are lower in relation to structure-parts like doors or the car body. On the other hand, the integration of these parts does not necessarily intersect with defined requirements from the concept phase, as long as technical and geometric requirements are still fulfilled. As an example, the replacement of a standard hat rack by another, made of renewable materials and with the same geometry, does not need to be decided in the concept phase, but can be done in the later series development process step (Fig. 1).

The use of innovative sustainable materials in components that need to fulfil higher technical requirements

may influence the defined properties from the concept phase.

2.2 Impacts of life cycle considerations on the concept phase

Early stages in product development are of particular importance for cost reduction and improvements regarding sustainability, since the influence and saving potentials are the highest in this phase of the development [8]. In the early phases of the automotive conceptual development process, many decisions are made, which define the properties of the new vehicle, module, or at least a component to be developed. With the integration of life cycle considerations in this early concept phase of automotive development, a high influence on the definition of properties and the development of vehicle technologies can be expected. As an example, Fig. 6 shows a comparison of dissimilar automotive car bodies with different materials.

Figure 6 Comparison of automotive body types with different materials. 1: standard steel body (Volkswagen Golf [9]), 2: aluminum space frame technology with carbon fiber components (Audi R8 e-tron [10]), 3: prototype of a wood frame vehicle body (Nios [11])

Obviously, due to different physical and technical properties, different materials lead to different bodywork structures, challenging design, construction, simulation and verification. Exemplary, Fig. 7 illustrates the influence of the defined geometry of a longitudinal beam on the closed chain dimension in a schematic front end of a car.

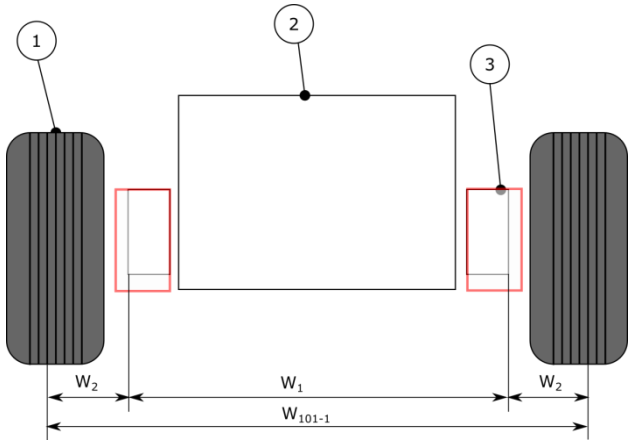

Figure 7 Schematic front end of a car. 1: tire, 2: engine, 3: longitudinal beams. W_1: distance between longitudinal beams, W_2: wheel contact distance to longitudinal beam, $W_{101\text{-}1}$: track width

The track width $W_{101\text{-}1}$ is an important dimension in the vehicle, that influences packaging, comfort and the vehicle driving dynamics behavior. $W_{101\text{-}1}$ is influenced by the outer dimensions of the tire, which (among others) affects the wheel contact distance to the longitudinal beam, W_2. The distance W_2 depends on chassis dimensions and the suspension system. As a simplification, it is considered as constant in this example. With changing dimensions of the longitudinal beam (3, transferring from the grey box to the red box), the wheel may change its position, which influences the track width $W_{101\text{-}1}$. Geometrical changes may occur with the use of alternative materials in the car body, due to different physical and technical properties. As those basic geometries are defined in the concept phase, this influence needs to be considered in the same phase. Especially alternative materials show different mechanical, structural and durability-related behavior, which requires more space for the components. Exemplary, aluminum space frame design is characterized by larger cross sections and different connection technologies than traditional bodywork made of steel. Carbon fiber or even composite made of sustainable material, e.g. wood based fibers and composites require more packaging space and new design solutions to tap their potential. These aspects have to be considered in the early layout phases of new cars. The goal is to find new solutions that provide advantageous characteristics in terms of life cycle related considerations, but that are also able to fulfil the long list of technological factors, e.g. load, stiffness, durability, eigenfrequency behavior, corrosion, predictability and costs.

Today, life cycle considerations, e.g. targeting the selection of proper materials for the required parts and components, typically start after the conceptual development, parallel and in conjunction with the delivery and supplier selection process. The term "supplier" includes all economic units which supply industrial intermediate products or provide corresponding services in the course of an inter-company work within the value chain. Suppliers are often structured according to the cooperation form with the OEMs. Typical classifications are research and development (R&D) suppliers, production suppliers, or development and production suppliers. Another classification addresses the positions of a supplier in the

value chain (Tier 0.5, Tier 1, Tier 2, etc.) [12]. In case of full-vehicle development, suppliers are increasingly deeply involved throughout the entire process chain, and even in the concept phase. In this way, supplier industry has a considerable effect on sustainable evaluation and life cycle assessment. In case of the exemplary mentioned bodywork design process, suppliers are integrated into packaging development and evaluation, functional layout and, of course production engineering of the delivered modules and components. In this way, suppliers play an important role as innovators, e.g. in the selection process of alternative technologies.

As previously illustrated, the physical vehicle base architecture is already defined in the initial concept phase. Changes, which are made in later process steps that have impact on the vehicle architecture, lead to increased costs and extend development time. This means, that the basic architectural spatial topology should remain untouched when finishing the concept phase. By this, especially components with a high spatial consumption require their life cycle considerations made in early stages of the development, because a modification is not possible anymore at later process phases.

As a conclusion, focusing on the design engineer's requirements in the concept phase, a need of information support can be detected, addressing possible changes and influences with the integration of innovative materials and sustainable technologies. Therefore, the following section introduces an approach to providing relevant information.

4 APPROACH TO PROVIDING RELEVANT INFORMATION IN THE EARLY CONCEPT PHASE

The approach targets a comprehensive consideration of influencing aspects for conceptual car design and layout. As a basis, influences in the basic concept of new technologies are identified and evaluated. Information about materials and technologies are sampled and clustered under consideration of their planned application. Focusing on the engineer's requirements, technical specifications need to be addressed, including influences on the production phase. Besides that, life cycle-relevant key indicators (e.g. cumulative energy demand or resulting CO_2 equivalent emissions for materials production) are calculated and brought into the decision processes. Especially in case of new (sustainable) technologies or material, a possible application has to be planned carefully. This includes risk analysis, cost calculation, and technology integration. Examples are information regarding stiffness and safety-relevant specifications (e.g. splinter behavior in the case of crash), or NVH[2]-behavior.

In state-of-the-art vehicle development, much of this information is provided by former similar developments and/or experiences. With the integration of novel technologies, the missing experience can only be compensated by a collection of relevant information from different R&D departments and the provision of a comprehensive database. With this database, the influence of material specifications on the component design needs to be evaluated, since the concept designer rather needs information concerning the basic geometry than technical specifications. This task is elaborated by pre-development departments, where developments and tests of technologies are carried out.

Component design and development is often carried out by or with subcontractors and suppliers. Since this process usually starts after the concept phase (see Fig. 1), information about the production process of parts from suppliers is not available during the concept phase. To meet this challenge, there is a need for closer collaboration between the engineers and the suppliers during the concept phase.

5 CONCLUSION

During the last decades, automotive development has been characterized significantly by a growing share of intelligent components, increasing technical complexity of vehicles and vehicle modules and steadily increasing model ranges. Furthermore, there is a need to focus even more on future challenges regarding sustainability. Besides the reduction of impacts from the use-phase of a car, the phase of production and end of life gains in importance. This trend is driven by a steadily increasing number of legislative boundary conditions and directives concerning the use, recovery and re-use of materials in the vehicle, but also by an increasing awareness of the customer. To meet those trends, the present paper has discussed an integration of novel sustainable materials and technologies in state of the art-vehicle development processes, and provided an approach that supports the implementation and evaluation during early development stages.

The main decisions in the development of a new vehicle or technology are made within a described four-step development process in the early stage of vehicle development. Focusing on the design engineer's requirements in the concept phase, a need for information support can be detected, addressing possible changes and influencing aspects that stem from the integration of innovative materials and sustainable technologies. An approach to answer this need includes the provision of material data, together with the evaluation of influencing factors on vehicle packaging and geometry, as well as a closer collaboration with supplier industry in vehicle conception.

6 REFERENCES

[1] Eigner, M.; Stelzer, R. Product Lifecycle Management: Ein Leitfaden für Product Development und Life Cycle Management, Springer-Verlag, Berlin-Heidelberg, 2009. DOI: 10.1007/b93672

[2] Brunner, H.; Hirz, M.; Wurzer, A. Considering Influences of Sustainable Production in Early Automotive Engineering Phases, Proceedings of MOTSP 2016, Porec, 2016.

[2] Noise, vibration, harshness

[3] Hirz, M.; Gfrerrer, T.; Lang, J.; Dietrich, W. Integrated Computer-Aided Design in Automotive Development - Development processes, Geometric Fundamentals, Methods of CAD, Knowledge Based Data Management, Springer Heidelberg New York Dordrecht London, 2013.
[4] Braess, H.-H.; Seiffert, U. Vieweg Handbuch Kraftfahrzeugtechnik, Vieweg+Teubner, Wiesbaden, 2011.
[5] Directive 2000/53/EC of the European Parliament and of the Council of 18th September 2000 on end-of-life vehicles, L 269-43, 34-42.
[6] UNECE R101, Regulation Nr. 101 of the United Nations Economic Commission for Europe (UN/ECE), 2007.
[7] Volkswagen AG: Umwelterklärung 2012 Standort Salzgitter, Wolfsburg, 2012.
[8] Mascle, Chr.; Zhao, H. P. Integrating Environmental Consciousness in Product/Process Development based on Life-Cycle Thinking, International Journal of Production Economics, 112(2008).
[9] Homepage of the Volkswagen AG: www.volkswagenag.com, 2017-01-30.
[10] Audi Media center, Audi R8 e-tron: www.audi-mediacenter.com/en/photos/detail/audi-r8-lms-20154, 2017-01-30
[11] Homepage of Hydrokultur: cad.burg-halle.de/hydro.html, 2017-01-30
[12] Wallentowitz, H.; Freialdenhoven, A.; Olschewski, I. Strategien in der Automobilindustrie: Technologietrends und Marktentwicklungen, Vieweg+Teubner, Wiesbaden, 2009.
[13] Rossbacher, P.; Hirz, M. Flexible parameterization strategies in automotive 3D vehicle layout, Journal of Computer-Aided Design and Applications, 2017.

Authors' contacts:

Helmut BRUNNER
Graz University of Technology, Institute of Automotive Engineering,
Inffeldgasse 11/II, 8010 Graz, Austria
E-mail: helmut.brunner@tugraz.at

Patrick ROSSBACHER
Graz University of Technology, Institute of Automotive Engineering,
Inffeldgasse 11/II, 8010 Graz, Austria

Mario HIRZ
Graz University of Technology, Institute of Automotive Engineering,
Inffeldgasse 11/II, 8010 Graz, Austria
E-mail: mario.hirz@tugraz.at

ISSN 1846-6168 (Print), ISSN 1848-5588 (Online)
ID: TG-20170124193850

Preliminary communication

THE IMPACT OF WORKPLACE SUPPLY ON PRODUCTIVITY IN FUNCTIONALLY ORGANIZED LAYOUTS

Grega KOSTANJŠEK, Brigita GAJŠEK

Abstract: In practice, way of supply of workplaces often affects production process realization. This is particularly true in the majority of small and medium enterprises in non-automotive sector, where production is functionally organized. Literature review confirms that production processes and their logistics support are organizationally and operationally connected to each other and in most cases even inseparable, performed by the same employees. The latter restricts efforts to determine the impact of supply on overall equipment effectiveness (OEE) and on productivity in a broader sense. Assessed impact of supply on OEE indicator forms an excellent starting point for decision making and planning of investments in production and inbound logistics. Practice shows that investments in production machines prevail over investments in inbound logistics. Why to invest in logistics is constantly recurring question between production managers, especially in nonautomotive sector. Operation and flow process charts are upgraded and used in combination with the equation for OEE indicator to determine the impact of supply (logistics) on Availability and on productivity in a broader sense.

Keywords: OEE; functional layout; productivity; inbound logistics; workplace; supply

1 INTRODUCTION

Productivity is a term that constantly hovers between employees and management, especially in automotive industry [3], where experts and researchers are not focused only on the production lines but also on logistics. Logistics can be seen as a key competitive factor in the automotive industry due to the rising number of model variants and options [1]. With the increasing importance of logistics [2], the evaluation of logistics effectiveness and efficiency is gaining increased attention. While the most advanced automobile industry develops and implements logistics performance management (LPM) [1], many other production companies are even unable to distinguish between logistics and technological operations. Nowadays, picking and sequencing of parts are not everywhere a core logistics activity, although from the perspective of the automotive industry this would be highly expected.

From the perspective of managers, at first sight, the easiest ways toward increased output are increasing overtime, increasing number of shifts [17], the introduction of machines with higher capacity, and the transition from manual to automated production. Less frequently, companies approach to productivity improvement progressively, with separation of logistics and technological operations on workstations with low value of Overall Equipment Effectiveness (OEE). Generally, it is difficult for companies to link supply of workstations (logistics) with productivity, especially since the same workers are performing alternately logistic and technological activities. It has been a known fact that the productivity of work system depends on the number of installed workplaces and logistics needed to produce a defined amount of units: the more wastes of time, such as walkways, idle times or non-value-adding handling operations a work system includes, the higher is the number of required employees and lower is the productivity [3,15].

Production companies are mostly familiar with OEE, which measures the gap between the actual performance and the potential performance of a manufacturing unit. OEE shows how well a company is utilizing its resources, which include equipment, labor and the ability to satisfy the customer. The OEE can be recognized as a tool that helps companies to determine the workstations with potential for improvements. An OEE score of 60 % is fairly typical for discrete manufacturers, but indicates there is substantial room for improvement [17].

Productivity focused managers can orient using several indicators. Three of them are OEE, Single Resource Productivity (SRP), and Total Resource Productivity (TRP). They all evaluate how effectively companies utilize production operations and the trend. However, OEE does not demarcate the logistics impact from technological one. For this purpose it is necessary to combine OEE with an additional methodology to explain indicator OEE on an analytical level. Distinction between two types of influences is important, because it indicates where to invest to improve productivity, in logistics or in technology.

In this paper we focus on the non-automotive sector, discrete manufacturing and SME type of company in order to develop a simple methodology that will help described companies make the first step towards defining the boundaries between logistics and technological activities and start with continuous improvements. Practice in automotive industry shows that it is necessary and possible to increase productivity. For this reason, a kind of process analysis was developed for a systematic approach to seeking time reserves in production processes organized on functional layout in SMEs. The fundamental contribution of the proposed procedure is firstly to determine the share of non-value added and logistics activities in production processes, and secondly to point on root causes for time inefficiency and connect them with the responsible persons/departments. In production companies, times and

types of necessary logistics activities are often not recorded in databases of business information systems. Generally, the formal technological procedures or routings define only preparatory closing times and piece times. Times of delays and transports between workstations are not planned. This situation is problematic in cases when someone is looking for areas with potential for improvement in terms of saving time. The latter is nowadays essential for business survival.

Improved analytical approach for distinguishing logistics and technological activities at any kind of workplaces serves us as base for defining the share of supply of workstation in OEE on a selected case in practice. Additionally, the relation between OEE and productivity will be discussed.

2 THEORETICAL FRAMEWORK

2.1 Productivity

The term productivity was probably first mentioned by French mathematician Quesnay in an article in 1766 [4]. In 1883, another Frenchman, Littre, defined productivity as "faculty to produce". In 1950, the Organisation for European Economic Cooperation (OEEC) issued a formal definition [16]: "Productivity is the quotient obtained by dividing output by one of the factors of production. In this way, it is possible to speak of the productivity of capital, investment, or raw materials, according to whether output is being considered in relation to capital, investment or raw materials, etc." In 1979, and later in 1984, American Productivity Center (APC) offered the first three (and in 1987 the fourth) basic definitions of productivity, particularly as relevant to companies [5]:

- Partial productivity is the ratio of output to one class of input. For example, output per person-hour (a labor productivity measure) is a partial productivity concept;
- Total factor productivity is the ratio of net output to the sum of associated labor and capital (factor) inputs. The net output here is sometimes called value-added output. In this ratio, we explicitly consider only the labor in capital input factors in the dominator;
- Total productivity is the ratio of total output to the sum of all input factors. This is a holistic measure which takes into consideration the joint and simultaneous impact of all the input resources on the output, such as manpower, materials, machines, capital, energy, etc.;
- Comprehensive total productivity index is the total productivity index multiplied by the intangible factor index. This is the most sophisticated measure that extends the total productivity measure to include any user-defined qualitative factors – as many as are relevant to a company – ranging from product quality and process quality to timeliness, market share, community attitude, etc.

Most of the indicators used by companies today are non-standard and cannot be distributed to any of above four basic productivity definitions, although companies are convinced that they are measuring productivity. Labor productivity is still often set in foreground. On the other hand, scientists try to determine total productivity and the broader, holistic productivity concept. Sumanth [4] stated some misconceptions about productivity. It is applicable to know the following truths, which are antonyms of mentioned misconceptions:

- production improvement does not necessarily mean productivity improvement;
- efficiency improvement does not guarantee productivity improvement;
- improvement in sales revenue does not necessarily ensure productivity improvement;
- quality improvement does not have to be at the expense of productivity.

Partial productivity, for example labor productivity expressed as output per man-hour, is a ratio of output to one type of input. Labor productivity originates from Taylor's scientific management. Work-study specialists and industrial engineers continue to place great emphasis on the output-per-man-hour measure to set up time standards, to prepare labor efficiency reports and to do labor planning and unit labor costing. Although Sumanth [4] suggests replacement of partial productivity with total productivity measure, this is unattainable in practice. However, precisely because of that it is important to be aware of partial productivity measure limitations [4]:

- if used alone, can be very misleading;
- do not have the ability to explain over-all cost increases;
- tend to shift the blame to the wrong areas of management control;
- profit control through partial productivity measures can be a hit-and-miss approach.

In practice, despite everything, the prevailing opinion is that low labor productivity threatens the survival of the company [13]. Productivity is often linked with "time and motion" [14]. The evidence of time and motion studies was used to put pressure on workers to perform faster. Not surprisingly, these studies had a bad press as far as workers were concerned. Similarly, the image of "time and motion" does not sit well with productivity specialists.

2.2 Manufacturing performance measurement system

The leading indicators of business performance cannot be found in financial data alone. Performance measurement is the process of quantifying action, where measurement is the process of quantification and action leads to performance. Companies achieve their goals by satisfying their customers with greater efficiency and effectiveness than their competitors [18]. The terms efficiency and effectiveness are used precisely in this context. Effectiveness refers to the extent to which customer requirements are met, while efficiency is a measure of how economically the firm's resources are utilized when providing a given level of customer satisfaction. This is an

important point because it not only identifies two fundamental dimensions of performance, but also highlights the fact that there can be internal as well as external reasons for pursuing specific courses of action [19]. Take, for example [20], one of the quality-related dimensions of performance – product reliability. In terms of effectiveness, achieving a higher level of product reliability might lead to greater customer satisfaction. In terms of efficiency, it might reduce the costs incurred by the business through decreased field failure and warranty claims. Hence the level of performance a company business attains is a function of the efficiency and effectiveness of the actions it undertakes, and thus:

- A performance measurement can be defined as the process of quantifying the efficiency and effectiveness of action;
- A performance measure can be defined as a metric used to quantify the efficiency and/or effectiveness of an action;
- A performance measurement system can be defined as the set of metrics used to quantify both the efficiency and the effectiveness of actions [21].

This article will focus on the issues associated with designing the process for quantifying the efficiency in general workplace.

According to [6], "Operations management literature considers throughput as a part of performance measurement." The throughput is output/machine hour or capacity utilized. TPM, a concept for corporate change, includes a way of defining OEE [7]. The definition of OEE includes downtime and other production losses, which reduces throughput. The definition of OEE does not take into account all factors that reduce the capacity utilization, e.g. planned downtime, lack of material input, lack of labor etc. OEE is just a useful component of a complete overall manufacturing performance measurement system, but it does not allow classification of observed inefficiency on technological and logistical causal areas.

The basis for implementation of any performance measurement system is trusted and quality data. In the TPM literature, collection of trusted data is something left to the inventiveness [6]. Usually several complementary systems are used, but neither of those data collection systems gives an appropriate and comprehensive picture of the losses and reasons for them. Companies can choose between manual and automatic data collection systems. Manual data collection systems are, in comparison with automatic data collection systems, cheaper, less complex, more detailed and failures can be carefully examined. Since there is no unified picture about lost productivity and reasons for it, there is also no general agreement on the magnitude of different types of losses, nor on the reasons for losses [26]. The reason for collecting data should not be to present neat figures, but to create a base for action and development of processes [27]. The set of measures should cover those aspects that indicate potential future improvements and the measure should in itself identify and generate continuous improvements, instead of working as passive control. The objective for future research of data collection should be finding a method that is not time-consuming, is at the same time precise and gives trusted data.

Performance measurement systems are often analyzed in scientific literature. Most studied companies seriously need to consider changing their performance measurements [28] because they use wrong measures or fail to use the right measures in correct ways. This was assessed as serious and therefore it seems important to identify the critical dimensions in a performance measurement system (what to measure) and the optimum characteristics of the measures (how to measure) [29]. New performance measurement systems should be dynamic and time should be important as a strategic performance measure.

Efficient flow of materials and short throughput times depend on effective manufacturing, comprising production and logistics actions; therefore we have to measure horizontal business processes instead of functional processes. This leads to flow-oriented measures. One way of switching to flow orientation is to measure times and throughput volume [30].

2.3 Process analysis based on ASME standard

The literature on tools for process analyses was reviewed with aim to find one for detecting inefficiency in production arising from logistics and separately technological activities. It should help to identify root causes for any kind of inefficiency. Frank and Lillian Gilbreth's Operation and Flow process charts have proved as good starting point and techniques of motion and process analysis, which unfortunately did not meet all our needs. They [31] defined process charts as "a device for visualizing a process as a means of improving it."

Later adopted ASME standard defines a flow process chart as a graphic representation of the sequence of all operations occurring during a process or procedure, and includes information considered desirable for analysis such as time required and distance moved. According to ASME standard, for analytical purposes and to aid in detecting and eliminating inefficiencies, it is convenient to classify the actions, which occur during a given process into five classes, known as operations (produces and accomplishes), transportation (moves), inspection (verifies), delays (interferes), and storages (keeps). Each class is represented with graphical symbol. These symbols serve as verbs, describing the actions, and provide observers with a powerful common language for describing work. They are an outstanding set of categories that are:

- mutually exclusive - each one represents a distinct type of action;
- universally applicable - they occur in all work areas (engineering, legal and other);
- comprehensive - they cover the work processes completely [19].

In the early 70s, Graham introduced additional three variations of the aforementioned operation symbol.

Symbols were later incorporated into a revised ASME Standard [32]. Two of them show "value-added" steps in information processing. Those are "origination" and "Add/Alter". "Origination" represents the creation of a record or a set of documents and "add/alter" an addition or change of information on an existing record or set of documents. The third symbol stands for "Handle" and represents make ready and put away, loading and unloading and all sorts of activities that do not involve information change.

The aim of the process chart has remained the same as in 1927. Several articles and multiple uses in practice have revealed the usefulness of Gilbreth's approach, sophisticated by Graham, for process analysis requirements. In practical part of this paper process charts were used for inefficiencies detection at production workplaces arising from logistics and to define causes for them.

2.4 Needs for customization and reuse of process charts

Implementation of manufacturing performance measurement system demands setting standards for performance measures. Setting those standards in general conflicts with continuous improvement [33] and the ability to be flexible. Carelessly set standards have effect of setting norms rather than motivating improvement. Continuous improvements and flexibility are important characteristics of SMEs in wood and metal processing sectors [34].

Logistics plays a vital role in economic systems and in everyday life. Given the significant cut of production and workforce costs, reducing logistics costs has also become an increasingly important task for managers. The latter are often hidden for identification, especially in production halls. In the face of competition, most sectors of European industry have made substantial efforts to upgrade their production infrastructures and integrate new forms of organization. One of further possibilities in reducing costs is in logistics industry as business supporting services provider. The global logistics industry is estimated at roughly 5.4 trillion euro or 13.8 % of the global GDP [22]. On average, logistics costs account for 10-15 % of the final cost of the finished product. Logistics therefore has great potential for cost reduction.

Costs of activities can be gradually reduced by eliminating activities that do not add value or by reducing their duration. Time management is extremely important also in production halls where logistics is mostly not recognized as function contributing to effectiveness. However, even in this field conditions are changing [23,24,25]. Trendy applications of lean thinking to productions companies require elimination of all types of unnecessary productivity losses that could in some cases largely fall on logistic activities. In order to eliminate wastes and improve lead-times it is certainly important to develop methodologies for searching non-value adding activities in production environments and wider.

Today companies are free to implement value stream mapping, Kaizen, any kind of performance measurement system, document their processes, and perform audits or certifications. However, not many SMEs can afford systems demanding a lot of administration, time and money. Today's companies are open to more simple solution that will help them to improve their processes faster and cheaper.

2.5 Overall Equipment Effectiveness

The equipment is a basic working tool in every production. Handling it in an inappropriate way is almost intolerable and performing preventive maintenance is a necessity. However, it happens that workers use machines and equipment until they break. Such unplanned defects decrease productivity in the absence of in-process inventory. Consequences are loss of revenue, missed deliveries, and waste of resources.

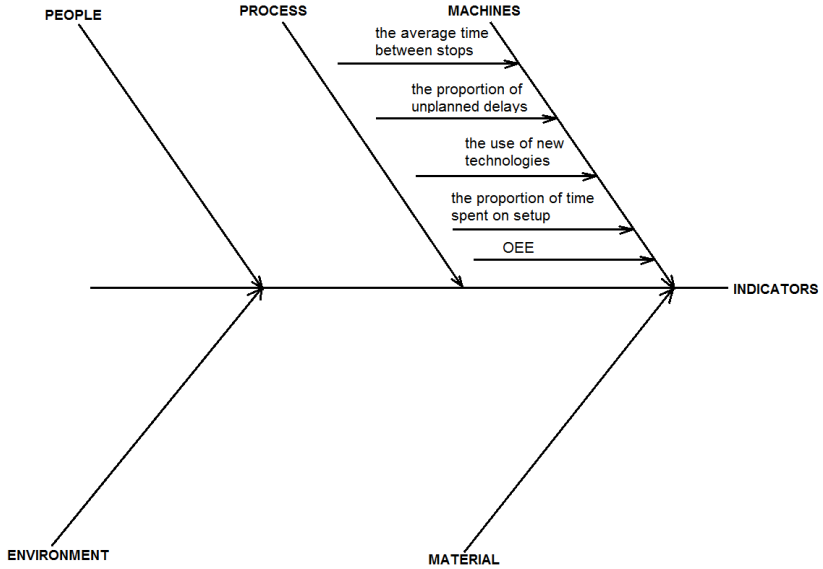

Figure 1 Indicator for "Machine" [27]

The production processes constantly repeat. Cyclicality allows the use of known methods and techniques for control and improvement. Historically, financial indicators were the most common way for operation valuation. However, over time this type of performance monitoring led average company to extremely poor performance. Companies have employed labor force, bought new machinery and equipment regardless of customer orders, rotate suppliers in order to achieve the lowest possible cost, while ignoring quality, the uncertainty of supplies and increased cost of large orders, etc.

In the last fifteen years due to the impact of total quality management implementations and Japanese manufacturers' competition on the market with short delivery times, companies slowly replace traditional cost and financial indicators with new or simply add additional ones. One of the biggest challenges in designing a system of indicators is to convince senior management and owners to satisfy with less than twenty indicators [35]. The indicators may be indexes, coefficients or shares.

Various indicators fall within different influential areas on Cause-effect diagram designed by Kaoru Ishikawa, Fig. 1. In many years of research, he discovered that causes for problems generally originate from five areas, namely process, machines, people, material, environment and measurements. OEE indicator very well covers the area "machines" on which we want to monitor the impact of supply [7].

OEE is a measurement method that is commonly used by companies on their way towards a Lean production where in specified it is a percentage number that is usually defined by multiplying the calculated availability rate, performance rate and quality rate [5]. It is a measure of equipment utilization in relation to its full potential. OEE and its individual factors give the company numbers to see where the equipment is losing time [6,5].

Availability (1) takes into account Down Time Loss. It is a percentage number that shows how often the machine is available when needed for production. It accumulates two wastes, breakdowns and setup/adjustments, which are downtimes measured at the equipment.

$$Availability = \frac{OT}{PPT} \tag{1}$$

OT – Operating Time
PPT – Planned Production Time

Performance (2) takes into account Speed Loss. It takes into account minor unplanned stops, for example idling and operation at a lower speed than the built-in.

$$Performace = \frac{ICT}{\frac{OT}{TP}} \tag{2}$$

ICT – Ideal Cycle Time
TP – Total Pieces

Quality (3) takes into account Quality Loss. The quality ratio includes losses due to ejection produced by the machine, as well as losses due to the occurrence of errors.

$$Quality = \frac{GP}{TP} \tag{3}$$

GP – Good Pieces

Improving OEE (4) should not be the only company's objective. OEE gives companies three values, which are all useful individually as situation changes from day to day. It also helps to visualize performance in simple terms.

$$OEE = Availability \cdot Performace \cdot Quality \tag{4}$$

The machines in discrete production usually have OEE rates between 45% and 65%. Companies' aim should be values from 85% to 95% [36].

3 METHODOLOGY

Inbound logistics activities are recognized as a potential for improvements to gain shorter lead times and increase productivity. Automotive industry is much ahead from other production sectors because of its specific, very work intensive environment. But competition is present in all production environments, not only in automotive one. We observed a segment of production companies that lags behind. Their employees perform alternately logistics and technological activities and achieve a low OEE indicator. Such companies need cheap, easy to use and effective methods to collect data for decision making on future improvements and investments.

Companies' needs for determining the share of non-value added and logistics activities in production processes were noticed in Slovenian wood and metal processing sectors, specifically in SME with production processes organized on functional layout. 20 selected companies mostly:

- dispose with limited financial resources to invest in development and implementation of new technologies;
- have lack of trained employees who are free to implement any kind of manufacturing performance measurement system;
- are not aware or are unwilling to admit the existence of reserves on side of logistics;
- have limited options for automation;
- did not install the mechanism of continuous improvement yet;
- are familiar with the principles of lean production, but practical implementation is weak.

Typical for functional layouts is the large amount of transportation and handling. Workstations that frequently interact with movement of material, semi products or people are located close together. Products are produced in batches and all machines performing similar type of operations are grouped at one location. Companies exploit this layout

when the production volume is not sufficient to justify a product layout. Its limitations are backtracking and long movements of materials/semi products, inability of mechanized material handling, prolonged process time, lower inventory turnover, frequent set-ups, longer throughput time and work-in-process ties up space and capital [5].

Functional layout largely influences on efficiency of logistics activities, although this is not always recognizable by managers. In such production facilities, in addition to machines, there are many chaotically distributed logistics units and means of transport. In the researched branch, 5S method is usually completely unknown to managers, Fig. 2.

Figure 2 Common situation in observed companies

Firstly we improve Gilbreth's approach, sophisticated by Graham, for process analysis requirements. The goal was to develop a tool for inefficiency detection in production processes adapted to the requirements of our time.

Methodology for process analysis was spontaneously developed at the Faculty of Logistics, University of Maribor, through the last six years. At the beginning we were using original ASME standard for flow process chart. The standard was used to present information on existing and proposed processes. Because the feedback information for partner's companies was possible to present in a simple form, the methodology became immediately applicable by students and employees in observed companies before any changes in their processes whatever actually were made, so that the special knowledge and suggestions of those in positions of minor importance, skills and knowledge were fully utilized.

The idea is that qualified person follows the material flow through the production plant and records the sequence of actions, determines the type of each activity, assignees the ASME symbols, measures the duration of each activity, and travels distances for all movements. This kind of research work requires short preparation on the observation and allows participation of methodologically unskilled persons but with invaluable work experience. The use of cameras resolves dilemma with occasional uncertainty concerning the classification of certain activities.

The methodology was used in 20 SMEs with functional layout and above mentioned characteristics. Weaknesses of the basic procedure were gathered, discussed and used for development of improved methodology.

In the second phase OEE indicator was analyzed. Case study method was used to determine the impact of supply on OEE indicator.

4 RESULTS

4.1 Renewal of time study technique

Motion and time study aim to eliminate unnecessary work and design most effective methods and procedures while providing methods of measuring work to determine a performance index for an individual or group of workers, department or entire plant [5]. A group of scientists lists four time study types. Those were stopwatch, work sampling, predetermined motion time system (PMTS) and Maynard's Operation Sequencing Technique Methodology (MOST). Today, of course, we note a number of variants, which were developed according to the specific needs of the user. In this paper we used process analysis bases on ASME standard.

Frank and Lillian Gilbreth originally developed Operation and Flow process charts as techniques of motion and process analysis. They defined process charts as "a device for visualizing a process as a means of improving it. Every detail of a process is more or less affected by every other detail; therefore, the entire process must be presented in such form that it can be visualized all at once before any changes are made in any of its subdivisions. In any subdivision of the process under examination, any changes made without due consideration of all the decisions and all the motions that precede and follow that subdivision will often be found unsuited to the ultimate plan of operation" [10]. That is only one of many techniques that identify the different types of activity that take place during the process and show the flow of materials or people or information through the process. According to ASME standard, for analytical purposes and to aid in detecting and eliminating inefficiencies, it is convenient to classify the actions, which occur during a given process, into five classifications. These are known as operations (produces and accomplishes), transportation (moves), inspection (verifies), delays (interferes), and storages (keeps) [11].

Quantity unit charted	Symbols	Description of event	Distance moved [m]	Unit oper. time	Unit transp. time	Unit inspect. time	Delay time	Storage time
1 palette	O ⇨ □ D ▽	Moved to delivery point	105		120 *s*			
1 box	O ⇨ □ D ▽	Moved to machine	1		20 *s*			
	O ⇨ □ D ▽	Box waits for operator					2 min	

Figure 3 Example of initial flow process chart fragment for "as is" process

Group of students followed different material flows through 20 production plants and recorded the sequence of activities, determined the type of each activity, assigned the ASME symbols, measured the duration of each activity and

travelled distance for all movements. They filled the data into the pre-prepared table (Fig. 3). This kind of work requires short preparation for the observation and allows participation of methodologically unskilled persons. After third cycle we started to use cameras and resolved the dilemma with occasional uncertainty concerning the classification of certain activities.

After methodology application in 20 companies, some weaknesses of the basic procedure were gathered. The most important finding was that logistics activities could not be easily separated from the production ones, excluding transportation and storage. Logistics activities, including transportation and storage, in manufacturing environments do not add value. Further finding was that delay can characterizes two types of activities with significantly different characteristics. The first type of delay activities comprises those activities that are necessary for the completion of the process and the second type of delay activities comprises those activities that are not associated with the process at all. We noticed that logistics activities in production environments do not add value for the customers who order products, but companies need to realize them for process completion. The situation is completely different in the case of logistics company selling logistics services, but this does not fall within described research. It is difficult to understand the practical value of technological and administrative activities equation under "operations" as proposes ASME standard. According to ASME an "operations" also occurred when information is given or received or when planning or calculating takes place.

To improve the approach we introduced four types of activities/times rather than just value-added and non-value-added activities/times. Those are:

- beneficial – activities/times that are directly related to a product that is the subject of the contract with company's customer (e.g. painting);
- non-beneficial - activities/time that are not directly related to a product that is the subject of the contract with company's customer (e.g. paperwork);
- necessary – activities/times that are strictly necessary for realization of customer's orders (e.g. painting and paperwork);
- unnecessary – fully redundant activities/times that are not related to the customer's order and the manufacturing process at all (e.g. coffee break, private conversation).

From the list above three meaningful pairs describing specific operation can be formed:

- beneficial - necessary (add value);
- non-beneficial - necessary (do not add value);
- non-beneficial - unnecessary (fully redundant).

Two changes of initial Gilbreth's methodology have been introduced. Firstly, the symbol for work with documentation, namely "diamond", was added. In production environments, any kind of work with documentation does not add value. Nowadays physical work with documents is becoming redundant, non-value-adding and need special attention. Secondly, in standard flow chart, initial types of time were replaced with proposed (beneficial/necessary, non-beneficial/necessary, non-beneficial/unnecessary) and a column with an additional symbol for work with documents was added (Fig. 4). In such a manner, pure technological activities were successfully separated from all other. Too many production companies still do not have any sense of how much time they spend for logistics and transport activities, downtimes or even for with the process entirely unrelated activities inside production halls. Constantly monitoring the situation is questionable for SMEs from the point of efficiency. It is advisable that companies at least occasionally monitor those processes that bring them the majority of revenues. After the renovation, the methodology was again tested and used in practice.

Quantity unit charted	Symbols	Description of event	Distance moved [m]	beneficial – necessary time	non-beneficial – necessary time	non-beneficial – unnecessary time
1 palette		Moved to delivery point	105		120 s	
1 palette		Confirmation of the movement from the warehouse			10 s	
1 box		Moved to machine	1		20 s	
		Operator checks missed calls				15 s

Figure 4 Improved flow process chart

The observation of specific process was always performed several times on different shifts (night, morning), at rush hours and non-rush hours. Each time, observers made flow process chart. Normally, five repetitions were performed, preferably using the camera, without prior notice.

To combine longer and/or non-value adding times with the causes for them, the resources that are necessary for each cycle of the observed process were preliminary listed and systematically arranged in groups like material, technology, documentation, work organization and so on. Existing characteristics of each group can be a potential source of inefficiency. These groups can afterwards label categories of the cause-effect diagram. Data on the repetition frequency of individual cause and on total process time were also collected. Cause-and-effect diagrams revealed key relationships among various variables. Defined root causes provided additional insight into process behavior. The use of 5W technique to trace causes back to root causes was also encouraged on side of observers.

Companies initially wanted to shorten their process times and did not know where or how to start. They looked for the professionals who would later also be hired to design a tailored system for processes improvement.

Average cycle time in observed processes lasted 29 minutes, of which we observed in average:

- 53 % of beneficial - necessary time,
- 36 % of non-beneficial - necessary time,
- 10% of non-beneficial - unnecessary time.

Production lead-time could be on average shortening by 10 % without any investment, usually with only minor organizational changes. 36 % of non-beneficial - necessary time on average was spent on:

- logistics and transportation (22%),
- administration work (8%),
- inspection (4%),
- necessary delays (2%).

By investing in logistics and transportation it would be possible to reduce the lead-time on average by maximum of 22 %. Delays were mostly caused by long search times (logistic units, tools, documents, vehicles), not defined work organization, duplications of tasks, absence of detailed scheduling, low and basic IT support, absence of IT support, lack of prevention in the field of quality assurance, not optimal layout, disadvantageous features of workshop.

4.2 Defining the impact of supply in OEE indicator

With process flow charts collected data was used for calculating OEE indicators.

Actual time needed for supplying the workplace with materials, tools, documents and alike is incorporated in Actual Production Time (ATP) in equation for Availability. If data is collected according to previously described methodology, APT can be calculated using the equation (5) where PPT represents Planned Production Time. It is calculated in a way that the maximum available time is reduced for planned breaks (lunch) and planned maintenance works on the machine.

$$APT = PPT - \sum_{i=0}^{n} NVARS_i - \sum_{k=0}^{n} NVARO_k - \sum_{j=0}^{n} NVANR_j \qquad (5)$$

Non-value adding required supply time (NVARS) represents the sum of all supply times/operations that are not directly related to the production of products and are the objects of the contract between company and its customers. Execution of these operations is strictly necessary for realization of customesrs' orders.

Non-value adding required non-supply time (NVARO) represents the sum of all non-supply times/operations that are not directly related to the production of products that are the subjects of the contract between company and its customers. Execution of these operations is strictly necessary for realization of client orders.

Non-value adding non-required time (NVANR) represents the sum of all times/operations that are not in any way related to the customer order and are fully redundant.

Hereinafter we want to explore how OEE indicator will change if we exclude NVARS.

4.3 Case study

We chose a modern and innovative European company with several decades of experiences on development, production and marketing of superior manufactured furniture. Their activities combine flexibility of the production process, cutting-edge CNC technology and years of experience, which enable them to produce perfect construction solutions. Therefore, the results of their work are high quality and aesthetically sophisticated products that make them one of the top manufacturers of interior design for recreational vehicles, boats, mobile homes and other special furniture. The company has about 320 employees coming mainly from the local environment. Investing in new technologies requires a highly trained staff. Therefore, educational structure of employees keeps growing every year. [12]

The observation and time study was carried out in the workplace 122 4SSS Weinig. Two operators work on this machine. The main operator works at the entrance and the assistant manipulates outputs. They use floor storage places and wooden EURO pallets for storage of materials and products. Main operator sets the machine on computer. The machine operates on average 3 days per week, for one shift per day. Operator's work hour costs 10.35 €. The purchase price of the machine was 193,337.47 €. Depreciation rate is 12.5%. Each hour of this machine costs 23.38 €. Ideal machine cycle is equal to 8 seconds/piece. Operator moves in a quite big radius around the machine. The observation lasted 1 hour 15 minutes and 22 seconds.

The collected data were presented in a form of process chart. Table contains the following data types:

- name of activity;
- cumulative process time;
- duration of each activity;
- value adding / non-value adding activity;
- type of loss (eight losses in the concept of lean);
- supply / non-supply time;
- number of workers who carried out the activity.

First, the indicator of OEE was calculated by equations 1 to 4. The calculated OEE value was 0.27 (6).

$$OEE = 0.33 \cdot 0.84 \cdot 0.97 = 0.27 \qquad (6)$$

We wanted to define the influence of supply on calculated value of OEE. For the calculation, we considered the equation with the expressed proportion of times spent for supply of the workplace (5). In recalculation, we set times spent for supply of the workplace on zero. Supply times were excluded from the calculation. In general, we can say that eliminated times relate to losses. Those losses appear because necessary things (tools, documents, information, materials, and semi products) are not located in the site of technological processing and in the form that would allow immediate use in technological processing. The calculated OEE value was 0.48 (7).

$$OEE_{teo} = 0.59 \cdot 0.84 \cdot 0.97 = 0.48 \qquad (7)$$

OEE indicator can occupy any value from 0 to 1 or from 0 to 100 %. Elimination of supply times in our case resulted in change of OEE value. The impact of supply reflects in the Availability. The impact of supply on the value of the Availability was in our case 26 or 26 % of the maximum value of the Availability.

Table 1 OEE on different work places

Company	Workplace	OEE	OEE_{teo}	Difference because of supply
A	1	0.27	0.48	0.21
A	2	0.46	0.62	0.16
A	3	0.40	0.57	0.17
B	1	0.57	0.78	0.21
B	2	0.66	0.86	0.20
B	3	0.44	0.76	0.32
C	1	0.50	0.64	0.14
C	2	0.45	0.60	0.15
Average		0.47	0.66	0.19

The survey was repeated at several workplaces with similar characteristics. We present OEE values before and after the elimination of supply times in Tab. 1. Average calculated value of OEE was 0.48. After elimination of supply times, this value has risen to 0.66. Influence of supply times on OEE was 0.19 on average, more specifically; availability of machines in focused category can be raised for approximately 19 % on average by improved logistics activities.

5 CONCLUSIONS

In practice, supply of workplaces often affects the production process realization. This is particularly true in the majority of SMEs, where production is functionally organized. Production processes and logistics services are connected to each other and in most cases even inseparable. We upgraded Operation and Flow process charts and used them in combination with the equation for OEE indicator to determine the impact of supply (logistics) on Availability and on productivity in a broader sense. In the calculation, we preserved machine Performance on original level, assuming that the greater machine Availability will reflect in greater quantity of produced pieces. The impact of supply on OEE calculation would form an excellent starting point for decision making and planning of investments in equipment and logistics. Practice shows that investments in machinery prevail over investments in logistics. Constantly recurring question between managers is why to invest in logistics. We upgrade Operation and Flow process charts and OEE, hierarchy of metrics, in order to help measure the impact of workplace supply.

Data for the calculation was acquired in a modern and innovative European company with several decades of experiences on development, production and marketing of superior manufactured furniture. We observed one workplace that is very typical for most wood processing companies with functionally organized production. If it was possible to completely remove the supply operations and employees could deal only with the technological operations, Availability would increase for maximum 26 %. By raising the Availability, it is not necessary to achieve the increase of Performance. Later depends on whether the workers will really produce more pieces of the product after the change.

The survey was repeated at several workplaces with similar characteristics. Average calculated value of OEE indicator was 0.48. After elimination of supply times, this value has risen to 0.66. Influence of supply times on OEE indicator was 0.19 on average, more specifically; availability of machines in focused category can be raised for approximately 19 % on average by improved logistics activities.

We will continue the research, mostly towards estimation of the assessed metric parameters impact on productivity improvements realized by their utilization. Additional examples from real production environment will be added.

We cannot claim that the improved value of OEE indicator will raise the total productivity of the company. Production improvements do not necessarily mean any kind of productivity improvement. Most probably only partial productivity will improve, for example a labor productivity measured as the ratio of output to one class of input (output per person-hour). In order to increase holistic comprehensive productivity, it is not enough merely to remove supply operation from the set of operator's tasks, which must be done on individual workplace. However, this can be a good starting point. These efforts must continue with comprehensive package of measures, which reflect in the increase of total productivity.

6 REFERENCES

[1] Dörnhöfer, M., Schröder, F., Günthner, W.A.: Logistics performance measurement system for the automotive industry, Logistics Research, 9(2016), 1-26. doi:10.1007/s12159-016-0138-7
[2] Gunasekaran, A., Patel, C., McGaughey, R.: A framework for supply chain performance measurement, International Journal of Production Economics, 87(3), 333–347.
[3] Sternatz, J.: The joint line balancing and material supply problem, International Journal of Production Economics, 159(2015), 304-318.
[4] Sumanth, D.J.: Productivity Engineering and Management, McGraw, New York, 1984.
[5] Puvanasvaran, A.P., Mei, C.Z., Alagendran V.A.: Overall Equipment Efficiency Improvement Using Time Study in an Aerospace Industry, Procedia Engineering, 68(2013), 271–277.
[6] Hogfeldt, D.: Plant efficiency: A value stream mapping and overall equipment effectiveness study, University of Technology, Lulea, 2005.
[7] Hohnjec, M.: Measurement and evaluation of process, Master's thesis, Faculty of Logistics, University of Maribor, Celje, 2008.
[8] User manual to Key 9: maintenance of machinery and equipment, Deloitte & Touche, 2000.
[9] Thakre, A. R., Jolhe, D. A., Gawande, A. C.: Minimization of engine assembly time by elimination of unproductive activities through 'MOST', Second international conference on emerging trends in engineering and technology (ICETET), 2005.

[10]Gilbreth, F. B., Gilbreth, L. M.: Process charts, The American Society of Mechanical Engineers, New York, 1921.
[11]Gajšek, B., Lerher, T., Rosi, B.: Approach to detecting promising areas for improvement in production processes, Proceedings of ICIL, Bol, June 2014, 206-215.
[12]Kostanjšek, G.: Measuring the influence of a workplace supply on productivity in companies within the manufacturing sector, Faculty of logistics, University of Maribor, Celje, 2014.
[13]Drucker, P.: Managerski izzivi v 21. stoletju, GV Založba, Ljubljana, 2001.
[14]What is productivity? [Scott-Grant], http://www.scott-grant.co.uk/pages/what_is_productivity.php, 2015-03-16.
[15]Ohno, T.: Toyota Production System: Beyond Large Scale Production, Productivity Press, Portland, 1988.
[16]OEEC: Terminology of Productivity, Andre-Pascal, Paris, 1950.
[17]Sowmya, K., Chetan, N.: A Review on Effective Utilization of Resources Using Overall Equipment Effectiveness by Reducing Six Big Losses, International Journal of Applied Engineering and Technology, 2(2016)1, 556-562.
[18]Kotler, P.: Marketing Management Analysis, Planning and Control, Prentice-Hall, Englewood Cliffs, NJ, 1984.
[19]Slack, N.: The Manufacturing Advantage: Achieving Competitive Manufacturing Operations, Mercury, London, 1991.
[20]Neely, A., Gregory, M., Platts, K.: Performance measurement system design: A literature review and research agenda, International Journal of Operations & Production Management, 15(1995): 80-116.
[21]Neely, A.D.: Performance measurement system design – third phase, Draft of the fourth section of the "Performance Measurement System Design Workbook", April (1994).
[22]COM, Communication from the Commission to the Council, the European parliament, the European Economic and Social Committee and the Committee of the regions: Freight Transport Logistics in Europe – the key to sustainable mobility, Brussels (2006).
[23]Kuhlang, P., Edtmayr, T., Suhn, W.: Methodical approach to increase productivity and reduce lead time in assembly and production-logistic processes, Journal of Manufacturing Science and Technology, 4(2011), 22-32.
[24]Luo, H., Wang, K., Kong, X.T.R., Lu, S., Qu, T.: Synchronized production and logistics via ubiquitous computing, Robotics and Computer-Integrated Manufacturing, 45(2017), 99-115.
[25]Bauer, W., Ganschar, O., Gerlach, S.: Development of a Method for Visualization and evaluation of production logistics in a multy-variant production, Procedia CIRP, 17(2014), 481-486.
[26]Ljungberg, Õ.: Measurement of overall equipment effectiveness as a basis for TPM activities, International Journal of Operations & Production Management, 18(1998)5, 495-507.
[27]Ishikawa, K.: Guide to Quality Control. Asian Productivity Organization, Tokyo, 1982.
[28]Schmenner, R.W., Vollmann, T.E.: Performance measures: gaps, false alarms and the 'usual suspects', International Journal of Operations and Production Management, 14(1994)12, 58-69.
[29]Jonsson, P., Lesshammar, M.: Evaluation and improvement of manufacturing performance measurement systems - the role of OEE, International Journal of Operations & Production Management, 19(1999)1, 55-78.
[30]Azzone, G., Masella, C., Bertele, U.: Design of performance measures for time-based companies, International Journal of Operations & Production Management, 11(1991)3, 77-85.
[31]Gilbreth, F.B., Gilbreth, L.M.: Process charts, The American Society of Mechanical Engineers, New York, 1921.
[32]Graham, B.B.: Rediscover Work Simplification, http://intranet.imet.gr/ Portals/0/Useful Documents/documents /03065.pdf (01.12.2014).
[33]Ghalayini, A.M., Noble, J.S.: The changing basis of performance measurement, International Journal of Operations & Production Management, 16(1996)8, 63-80.
[34]Fisher, J.: Use of non-financial performance measures, Journal of Cost Management, 6(1992), 31-8.
[35]Nakajima, S.: TPM Development Program, Productivity Press, Cambridge, MA, 1989.
[36]SCDigest editorial staff: Supply Chain Graphic of the Week: Logistics Costs as Percent of GDP by Country, 2013, URL: http://www.scdigest.com/assets/newsviews/13-06-20-2.php ?cid = 7168 (14.03.2014).

Authors' contacts:

Grega KOSTANJŠEK
3 Projekt d.o.o.
Kebetova ul. 18, 4000 Kranj, Slovenia

Assist. prof. dr. Brigita GAJŠEK
University of Maribor, Faculty of Logistics,
Mariborska 7, 3000 Celje, Slovenia
E-mail: brigita.gajsek@um.si

ISSN 1846-6168 (Print), ISSN 1848-5588 (Online)
ID: TG-20170202195813

Preliminary communication

LABORATORY SCALE BIOREMEDIATION OF CRUDE OIL IMPACTED SOIL USING ANIMAL WASTE COMPOST

Adebola A. ADEKUNLE, Iheoma M. ADEKUNLE, Adedayo A. BADEJO, Funmilayo M. ALAYAKI, Adekoya O. OLUSOLA

Abstract: This study investigated various ways by which the rate of biodegradation of hydrocarbons {ex-situ treatment} can be enhanced in an efficient, cost effective and environmentally friendly manner. To achieve this, bioremediation processes were applied to a crude oil impacted soil. Tests were conducted to evaluate the biodegradation effect of the oil on the soil e.g. effect on density, electrical conductivity, etc. The percentage of organic matter and carbon was evaluated in order to determine the organic carbon interaction with the contaminated soil sample. The effect of contamination on the geotechnical properties of the contaminated soil was also evaluated using compaction test. Two types of compost - sheep waste compost and crude oil (SCRO), and goat waste compost and crude oil (GCRO) - with an application rate of {0g, 350g and 550g} were applied in the treatment. The results showed that all bioremediation agents applied enhanced the natural bioremediation of the contaminated soil and the most preferred results were obtained when treatments were done using SCRO compost. This study revealed that the remediation process was influenced by application period, type of oil, and compost rate.

Keywords: Remediation, Contaminated soil, Soil sample and crude oil, Compost and Crude Oil.

1 INTRODUCTION

Royal Dutch Shell was granted an exploration license in 1956, after discovering the first commercial oil field at Oloibiri, a village in the Niger Delta, and commercial production began in 1958 (NNPC [1]). With a total of about six hundred and six (606) oil fields in the Niger Delta out of which three hundred and sixty (360) are on-shore and two hundred and forty-six (246) offshore (Nwilo and Badejo [2]), oil exploration and production activities have significant environmental consequences that occur.

The search for oil in Nigeria begun in 1937 (Awobajo, [3] Ifeadi, C.N and Nwankwo, J. [4]): with increasing production of crude oil and discovery of major oil reserves, more effort was added to exploit this resource. Operations include oil exploration, oil drilling, oil production, oil transportation, oil processing, and oil storage (Bossert and Bartha, [5], Odeyemi and Ogunseitan, [6]).

Oil spill is a release of petroleum hydrocarbon into the environment as a result of human activities. They are usually mostly caused by accidents involving oil tankers, barges, refineries, pipelines and oil storage facilities. These accidents can be caused by human mistakes or carelessness and sometimes by natural disaster such as earthquakes, deliberate acts by terrorists, militants or vandals. Another major cause of oil spill here is sabotage which involves bunkering by some unpatriotic Nigerians. They damage pipelines in the attempt to steal oil from them.

In twenty years (1976-1996), four thousand six hundred and forty-seven (4,647) incidents resulted in the spill of approximately two million three hundred and sixty-nine thousand four hundred and seventy (2,369,470) barrels of oil into the environment. Of this quantity, an estimated one million eight hundred and twenty thousand four hundred and ten and a half (1,820,410.5) barrels were lost to the environment as reported (Nwilo and Badejo, [2]).

The growth of oil industry alongside population increase with a lack of enforcement of environmental laws has led to substantial damage to Nigeria's environment especially in the Niger Delta area. Oil spillage in petroleum producing communities produces a two sided problem; sterile land and polluted water.

Oil spillage leads to contamination of the natural environment and these petroleum-derived substances especially contribute to the degradation of land around the contaminated area. Changes in some soil properties resulting from contamination of soil with petroleum-derived substances bring about soil changes. Also, oil contamination is known to alter the properties of soil. According to (Head, [7] and Adekunle [8]) oil contamination alters soil moisture condition and can lead to non-homogenous distribution of water in soil due to the hydrophobic nature of oil. Contamination modifies the engineering properties of soil, thereby restricting its further use either as a construction material or as a supporting medium. Due to the scarcity of land, it becomes imperative to reuse the land for infrastructure developmental activities. Remediation has been defined as the management of a contaminant at a site so as to prevent, reduce or mitigate damage to human health, or the environment, which can also lead to quick recovery of the affected lands (Doelman, [9] and Christofi et. al [10]). Physical, biological and chemical processes are employed for remediation. But for the purpose of this study, only biological process of remediation will be discussed.

For bioremediation to be successful, the bioremediation methods depend on having the right microbes in the right place with the right environmental factors for degradation to occur. The right microbes are bacteria or fungi, which have the physiological and metabolic capabilities to degrade the pollutants.

Bioremediation is not a new technology but it has been discovered that among several clean-up techniques available to remove petroleum hydrocarbons from the soil and

groundwater, bioremediation processes are gaining ground due to their simplicity, higher efficiency and cost-effectiveness when compared to other technologies. These processes rely on the natural ability of microorganisms to carry out the mineralization of organic chemicals, leading ultimately to the formation of CO_2, H_2O and biomass (Duarte da Cunha and Leite, [11] and Adekunle et al. [12]).

Petroleum hydrocarbons in oil polluted soils create a condition which makes nutrients such as nitrogen and oxygen - essential nutrients for plant growth, unavailable to plants with an increased level of toxic nutrients according to (Samina et al. [13] and Jorgensen, [14]). Hence, oil contamination of the soil makes arable land unsuitable for agriculture as well as for engineering purposes.

Therefore, this study is aimed at determining the feasibility of bioremediation technique using compost technology as a treatment option for a chronically crude – oil contaminated soil. This was done by:

- Assessing the impact of different compost material in cleaning up crude oil contaminated soil.
- Remediating the soil biologically so that the soil's bearing capacity and other properties would be sufficient to withstand a structure instead of using more expensive methods like pile foundation to support the structure.
- Conducting assessment test on remediated soil in term of checking soil pH, soil organic carbon and matter and electrical conductivity.

2 METHODOLOGY

Crude oil impacted soil sample used for this analysis was taken next to the Civil Engineering building, Federal University of Agriculture Abeokuta, Ogun State, Nigeria. The analysis of soil was carried out by the determination of the pH, soil organic carbon and organic matter, percentage moisture content and determination of heavy metals. These analyses were carried out after air drying of the procured sample.

2.1 Experimental Design

Soil samples, mixed as follows, were weighed and set up in plastic pots in the laboratory and labeled:

SCRO = Soil + Crude oil + Compost (in 3 plastic pots)
GCRO = Soil + Crude oil + Compost (in 3 plastic pots)
SCDO = Soil + Crude oil (in 3 plastic pots)

Where: SCRO - sheep waste compost and crude oil, GCRO - goat waste compost and crude oil, SCDO - soil sample and crude oil.

2.2 Remediation of contaminated soil samples

The remediation process began by the addition of the compost to each of the soil samples procured, mixing it thoroughly with a little amount of water to moisten the mixture in other to enhance biodegradation. Each pot was then covered with polythene bag and left for a week. At the end of one week, the pots were opened, temperatures were taken, and samples were equally taken at the four sides of the sample, mixed together for analysis. Then an additional 350g was added to the samples, mixed together, returned to the pots and covered again. After another 7 days, the samples were opened, the temperature was taken and portions were taken for analysis. This procedure continued for another two week with no further addition of compost.

3 RESULTS AND DISCUSSION

3.1 Effects of compost induced remediation on sample pH

The pH for each replicate of the soil sample was taken before and during the process of remediation with SCRO and GCRO compost. The results of the pH value over the remediation period ranged from 6.16 to 6.37 with a means value of 6.31 ± 0.1 before crude oil spill. Immediately after the crude oil spill, the soil pH varied from 5.67 to 6.59 with a mean value of 6.13 ± 0.39. The use of composted waste increased the soil pH from 6.5 to 8.73, a 34.3 % increase. The pH range before remediation was from 6.5 to 8.73 for the sample treated with SCRO compost and varied from 6.63 to 8.22 for sample treated with GCRO compost. The value generally increased for both treatments with that of SCRO and GCRO after the remediation period. Although there was fluctuation in the pH value during the remediation period, there is an increment in pH value and this indicates that the compost reduces the acid content of the contaminated soil, which shows the effectiveness of the method applied to remedy the soil.

Table 1 Mean pH values before and after remediation for each treatment over the remediation period of 0 to 28 days.

S/N	Sample code/Remediation period	pH Before remediation	pH After remediation
1	GCRO/day 7	6.5 ± 0.361	8.45 ± 0.132
2	GCRO/day 14	6.5 ± 0.361	8.73 ± 0.10
3	GCRO/day 21	6.5 ± 0.361	8.41 ± 0.133
4	GCRO/day 28	6.5 ± 0.361	8.51 ± 0.080
5	SCRO/day 7	6.63 ± 0.294	8.06 ± 0.032
6	SCRO/day 14	6.63 ± 0.294	8.20 ± 0.052
7	SCRO/day 21	6.63 ± 0.294	7.96 ± 0.055
8	SCRO/day 28	6.63 ± 0.294	8.22 ± 0.082
9	S+CDO/day 7	6.8 ± 0.1	7.62 ± 0.049
10	S+CDO/day 14	6.8 ± 0.1	7.45 ± 0.380
11	S+CDO/day 21	6.8 ± 0.1	7.49 ± 0.096
12	S+CDO/day 28	6.8 ± 0.1	7.23 ± 0.195

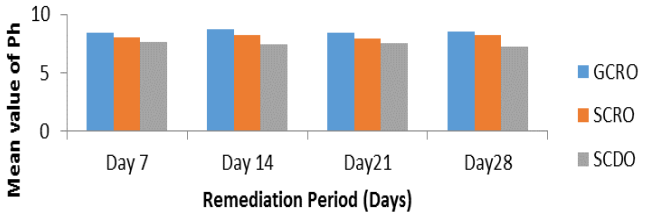

Figure 1 Mean pH Value in samples treated with SCRO and GCRO compost in relation to remediation period.

3.2 Effect of compost induced remediation on the content of zinc, copper and cadmium

The content of heavy metals like zinc (Zn), copper (Cu) and cadmium (Cd) was evaluated at the start and end of the remediation process. The samples treated with SCRO showed a significant reduction in the content of these heavy metals and the same is valid for those treated with GCRO compost. The results are as shown in Fig. 2 in the form of heavy metals over the remediation period. The range at the beginning of remediation was from 85.57 to 294.33 mg/l, 6.24 to 12.36 mg/l and 86.33 to 239 mg/l for zinc, copper and cadmium respectively for the samples treated with SCRO compost and it varied from 136.83 to 210.83 mg/l, 6.24 to 11.68 mg/l and 107.33 to 238.67 mg/l for Zn, Cu and Cd respectively for samples treated with GCRO compost. The value generally decreased for both treatments with that of SCRO having a mean value of 168.29 mg/l, 9.1 mg/l and 199.05 mg/l for Zn, Cu, and Cd respectively and a mean value of 211.95 mg/l, 11.42 mg/l and 174.6 mg/l for Zn, Cu, and Cd respectively for samples treated with GCRO.

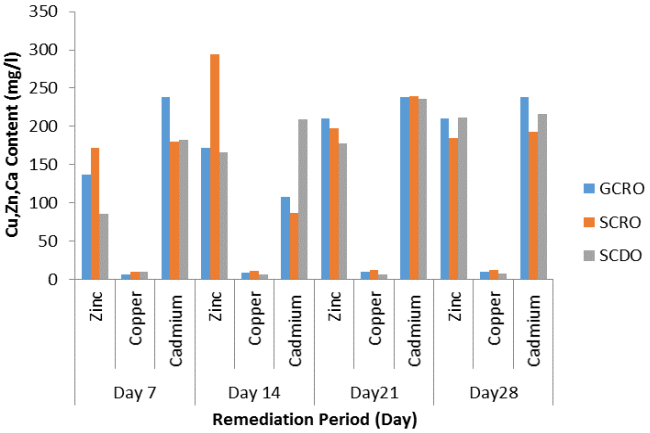

Figure 2 Heavy metals (Cu, Zn, and Ca) content over the remediation period

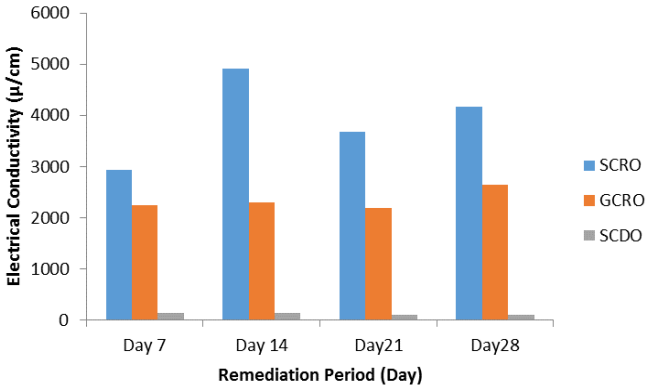

Figure 3 Percentage of electrical conductivity in treated samples in relation to remediation period

3.3 Effect of compost induced remediation on electrical conductivity

The Electrical Conductivity {EC} values for crude oil polluted soils are presented in the appendix. The values before crude oil spill ranged from 153.63 µs/cm to 5231.40 µs/cm, immediately after crude oil spill, the soil EC varied from 98.67 µs/cm to 4916.33 µs/cm.

3.4 Effect of compost induced remediation on sample organic carbon

The percentage of organic carbon of each replicate of the soil sample was calculated before and during the process of remediation with SCRO and GCRO compost. The results are plotted in Fig. 4 in the form of the percentage of organic carbon versus the remediation period. The range before remediation was from 2.7 % to 3.2 % for the samples treated with SCRO compost and varied from 0.52 % to 2.3 % for samples treated with GCRO compost. The value generally increased for both treatments with that of SCRO by 8.45 % and GCRO increase by 12.82 % after the remediation period. The increase in soil percentage organic carbon seen in this write up indicates that the compost increased the organic carbon content of the contaminated soil after treatment. The samples treated with SCRO compost have a lesser percentage increment but with a high efficiency of remediation. This is due to the consistency shown by the compost throughout the remediation process.

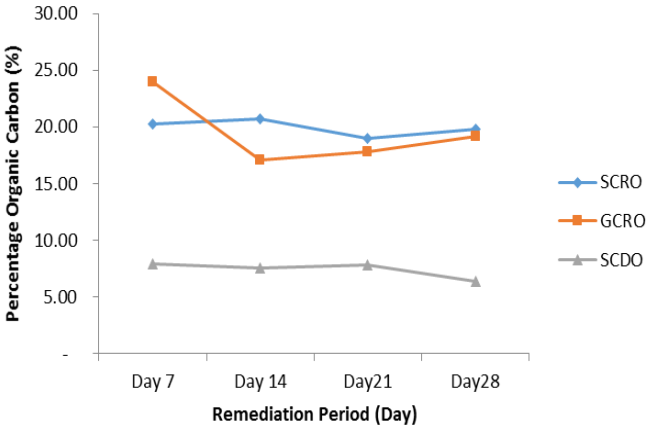

Figure 4 Percentage of organic carbon in treated samples in relation to remediation period.

3.5 Effect of compost induced remediation on sample organic matter

The percentage of organic matter of each replicate of the soil sample was calculated before and during the process of remediation with SCRO and GCRO compost. The results are plotted in Figure 5 in the form of the percentage of organic matter versus the remediation period. The value generally increased for both treatments with that of SCRO increased by 5.67 % and GCRO increased by 18.84 % after the remediation period. The increase in soil percentage organic matter as observed in this write up indicates that the

compost increased the organic matter present in the contaminated soil after treatment. The samples treated with SCRO compost have a lesser percentage increment but with a higher efficiency of remediation. This is due to the consistency shown by the compost throughout remediation process.

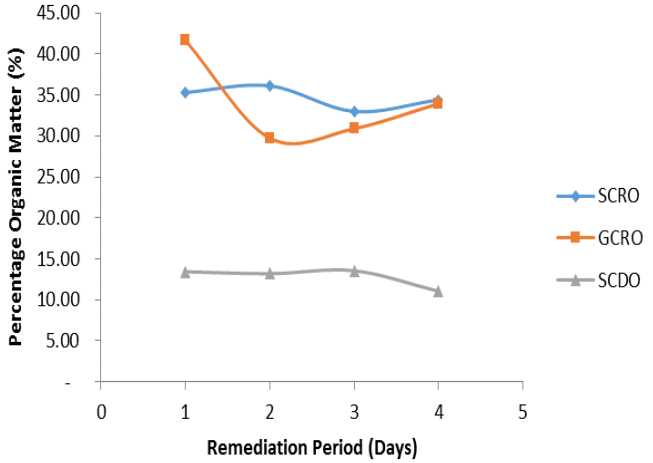

Figure 5 Percentage of organic matter in treated samples in relation to remediation period.

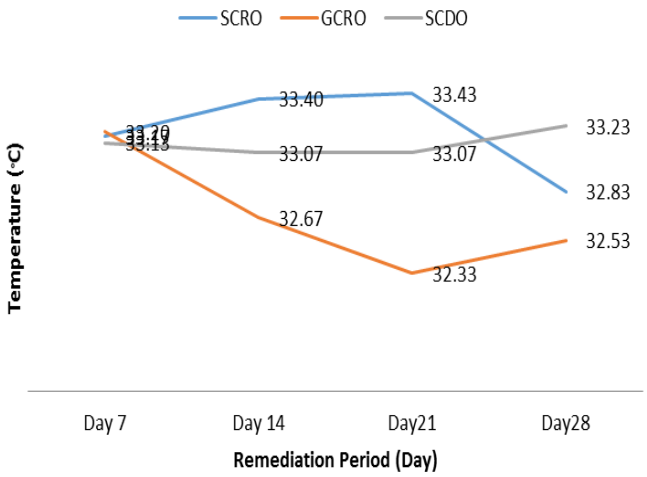

Figure 6 Temperature of treated samples as against the remediation period

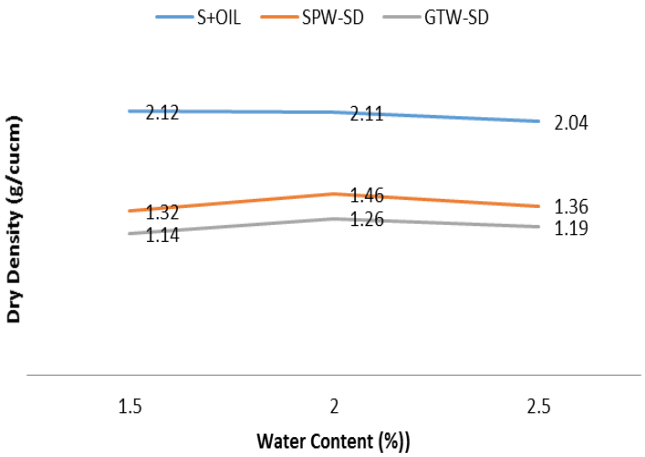

Figure 7 Dry density versus percentage of water content for untreated and treated samples.

3.6 Effect of compost induced remediation on sample compactive efforts

Standard Proctor Compaction Test (ASTM-D698) was carried out on the contaminated soils samples. The results are plotted in Fig. 7 in the form of dry density with increasing water content. They generally show a reduction in dry density with increasing water content before remediation process. After remediation, the samples treated with SCRO compost gave a maximum dry density of 1.46 g/cm^3 and a value of 1.26 g/cm^3 for samples treated with GCRO compost. After remediation, there is a reduction in the maximum dry density with increasing water content and this is depicted in the graph below.

4 CONCLUSION AND RECOMMENDATION

4.1 Conclusion

Bioremediation using compost technology to enhance the biodegradation of crude oil contaminated soil showed a satisfactory result. It positively modified soil quality in terms of pH, temperature, percentage organic carbon and matter, the content, electrical conductivity and the heavy metals analyzed. For the pH value, it increases for both treated with SCRO and GCRO. The increase shows that the acidic nature of the contaminated soil has been reduced to the barest minimum. Moreover, as for the heavy metals like zinc, copper and cadmium, it shows a considerable reduction in their contents. This is indicative of the efficiency of the bioremediation methods used and it shows that the content of heavy metals in the soil contaminated is reduced. With this, some of the plants can survive from it. The electrical conductivity of the remediated soil also reduces, which shows the effectiveness of the remediation process. The organic carbon and organic matter increase for the sample treated with both SCRO and GCRO. With this increment in the organic content of the crude oil contaminated soil, it will be rich enough for plant to survive. However, since we know that a soil which has a high organic content is not suitable for engineering

purposes, the soil has to be used for farming for a period of time and then later it will be useful for engineering purposes because the farming will reduce the level of organic carbon and matter concentration on the soil. The reduction in optimum moisture is indicative of excess oil in the soil before remediation process. This also indicates the efficiency of the bioremediation method used.

The application of composted organic waste is a good and efficient way of remediating crude oil contamination. It is also environmentally sound and not hazardous to the health.

4.2 Recommendation

Considering the efficiency of the method of bioremediation during the short period of application, it is recommended that further application of the compost technology in bioremediation of crude oil contaminated soil should be conducted for a long period of time so as to achieve increased degradation of total petroleum hydrocarbon and to increase the suitability of the soil for engineering application.

It is also recommended that further studies be conducted in the application of this method of bioremediation to other petroleum products so as to further probe the efficiency and effectiveness of the method in treating oil related spillage.

5 REFERENCES

[1] NNPC: Development of Nigeria's Oil Industry: http://nnpcgroup.com/NNPCBusiness/BusinessInformation/OilGasinNigeria/DevelopmentoftheIndustry.aspx (Accessed: 2016-08-16)

[2] Nwilo P. C., Badejo, O. T. (2005) Oil Spill Problems and Management in the Niger Delta. International oil spill conference proceedings: May 2005, Vol. 2005, No. 1, pp. 567-570.

[3] Awobajo, S. A (1981) An analysis of spill incidents in Nigeria (1976-1980). In: Proc. Seminar on Petroleum Industry and the Nigerian Environment, NNPC/FMOW and Housing PT, Warri.

[4] Ifeadi C. N., Nwankwo J. (1980) Oil Spill incidentsin Nigeria Petroleum Industry. A Critical Analysis Napetcor. 8:11-45.

[5] Bartha R. and Bossert, I. (1984) The treatment and disposal of petroleum waste. In: R. M. Atlas (Ed.) Petroleum Microbiology, Macmillan, New York, pp 553-577.

[6] Odeyemi O. and Ogunseitan O. A. (1985) Petroleum industry and its pollution potential in Nigeria, Oil and Petrochemical Pollution, 2(3), pp. 223-229.

[7] Head, I. M. (1998) Bioremediation: toward a credible technology. Microbiology, 144, pp. 599-608.

[8] Adekunle I. M. (2011) Bioremediation of soils contaminated with Nigerian petroleum products using composted municipal wastes. Bioremedmdiation Journal, 15:4, 230-241, DOI: 10.1080/10889868.2011.624137

[9] Doelman P. (1994) European Perspectives of field research on bioremediation. Special attention to the Netherlands. Invited paper for the 5 th International Congress of soil science, Acapulco, Mexico, P15.

[10] Christofi N., Joshua J. B., Kuyukina M. S. and Philp J. C. (1998) Biological treatment of crude oil contaminated soil in Russia. Geological society, London, Engineering Geology Special Publications, 14: 45-51.

[11] Duarte da Cunha C., Leite S. G. F. (2000). Gasoline biodegradation in different soil microcosms. Braz. J. Microbiol., 31, 45-49.

[12] Adekunle A. A., Adekunle, I. M. and Tobit O. Igba (2012) Impact of bioremediation formulation from Nigeria local resource materials on moisture contents for soils contaminated with petroleum products. International Journal of Engineering Research and Development, 2 (4): 40-45 http://www.ijerd.com/paper/vol2-issue4/F02044045.pdf.

[13] Samina B. E., Glaser J. A., Baveye P. V. (2001) The Utilization of Bioremediation to Reduce Soil Contamination: Problems and Solutions. Dordrecht: Kluwer Academic Publishers.

[14] Jorgensen K. S., Puutstinen J. and Suortt A.-M. (2000). Bioremediation of petroleum hydrocarbon-contaminated soil by composting in biopiles. Environmental Pollution, 107: 245-254.

Authors` contacts:

Adebola A. ADEKUNLE
Department of Civil Engineering, Federal University of Agriculture, Abeokuta, Ogun, Nigeria
Tel: +2348033010552
E-mail: adebolamay@gmail.com

Iheoma M. ADEKUNLE
Department of Chemistry, Federal University Otuoke, Bayelsa State, Nigeria

Adedayo A. BADEJO
Department of Civil Engineering, Federal University of Agriculture, Abeokuta, Ogun, Nigeria

Funmilayo M. ALAYAKI
Department of Civil Engineering, Federal University of Agriculture, Road, Abeokuta, Ogun, Nigeria

Adekoya O. OLUSOLA
Department of Civil Engineering, Federal University of Agriculture, Road, Abeokuta, Ogun, Nigeria

ISSN 1846-6168 (Print), ISSN 1848-5588 (Online)
ID: TG-20170509132026

Preliminary communication

EVALUATION OF LIMESTONE LAYER'S EFFECT FOR UWB MICROWAVE IMAGING OF BREAST MODELS USING NEURAL NETWORK

Ahmet AYDIN, Emine AVŞAR AYDIN

Abstract: X-ray mammography is widely used for detection of breast cancer. Besides its popularity, this method did not have the potential of discriminating a tumor covered with limestone from a pure limestone mass. This might cause misdetection of some tumors covered with limestone or unnecessary surgery for a pure limestone mass. In this study, Ultra-Wide Band (UWB) signals are used for the imaging. A feed-forward artificial neural network (FF-ANN) is used to classify the mass in the breast whether it is a tumor or not by using the transmission coefficients obtained from UWB signals. A spherical tumor covered with limestone and pure limestone masses were designed and placed into the fibro-glandular layer of breast model using CST Microwave Studio Software. The radius of the masses for both cases is changed from 1 mm to 10 mm with 1 mm steps. Horn antennas were chosen to send and receive Ultra-Wide Band (UWB) signals between 2 and 18 GHz frequency range. The obtained results show that the proposed method, on the contrary of the mammogram, has the potential of discriminating the tumor covered with limestone from the pure limestone, for the mass sizes of 7, 8 and 10 mm. Consequently, the UWB microwave imaging can be used to distinguish these cases from each other.

Keywords: breast cancer; feed forward artificial neural network ((FF-ANN); limestone; microwave imaging

1 INTRODUCTION

Breast cancer is one of the major causes of female death in the world and so breast cancer detection is one of the most intriguing fields of microwave imaging. An early diagnosis of tumor presence absolutely increases the survival rate in women and gives the opportunities of getting through the problem. Therefore, timely detection and early stage treatment are important factors. There are widespread detection methods such as X-ray mammography, Magnetic Resonance Imaging (MRI), and ultrasound [1-18]. Although X-ray mammography is currently the most popular screening tool, it also has its restrictions - one of them is the high misdetection ratio, and the other one is its insufficiency to discriminate between malignant and benign tumors. All existing screening tools including X-ray mammography are expensive, uncomfortable, and incapable in terms of detection and location of the tumor [1-12]. In addition to these, existing methods cannot detect the tumor if there is limestone layer, which is caused by the milk ducts, surrounding of the tumor. It is known that chemical and physical properties tissues, including their electron density and molecular dynamics, are important for imaging and diagnosis methods [15]. Consequently, limestone effect is analyzed to investigate the radiation from the skin regarding whether there is limestone or not surrounding of the tumor. These restrictions embolden to seek for the better alternative methods. Microwave Ultra-Wide Band (UWB) imaging, which is one of the alternative methods, is the most interesting method these days [5, 10, 16-18]. In this method, the system consists of one transmitting and one receiving antenna to send and record UWB signals through the breast tissue. Microwave imaging utilizes the difference in the dielectric properties of benign and malignant breast tissues. And the previous studies show that artificial neural networks can be trained based on this difference to automate diagnosis phase [19-22].

2 BREAST DESIGN AND DATA COLLECTION

There have been alternative breast design dimensions [16-18]. We have done a hemisphere shape design as showed in Fig. 1 and Tab. 1.

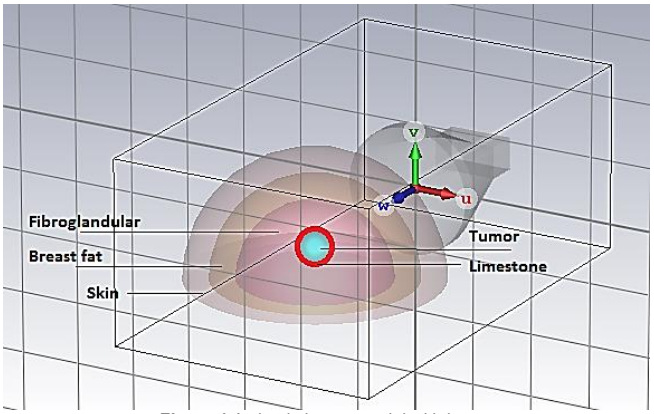

Figure 1 A simple breast model with layers

Table 1 Breast layer sizes

Model Layer	Diameter	Thickness
Skin	10 cm	2 mm
Breast fat	8 cm	2 mm
Fibro glandular	6 cm	2 mm

Table 2 Debye parameters of breast model layers at 6 GHz [23]

Tissue	ε_∞	ε_s	σ_s	τ (ps)
Skin	4.00	37.00	1.10	7.37
Breast fat	6.57	16.29	0.23	7.00
Fibro glandular	5.28	35.14	0.46	7.00
Tumor	3.99	54.00	0.70	7.23

The Debye parameters that have been used are shown in Tab. 2 [23] where, ε_∞, ε_s and τ, are exponent parameters, infinite permittivity constant, static permittivity constant, and time constant, respectively.

Tumor radius sizes have been chosen from 0.2 cm to about 1.5 cm in the literature [24-28]. However, 0.25 cm is the frequently used one. Besides, it is ideal for the minimum used tumor size. We created a spherical tumor with radius from 1mm (0.1 cm) to 10 mm (1 cm). Although dielectric properties of the healthy and fat tissues are generally constant, this case is not the same for the tumor. In other words, the dielectric property of the tumor changes with respect to the frequency. The main aim of this study is to discriminate a tumor covered with limestone from a pure limestone mass. Therefore, a spherical tumor model covered with limestone and pure spherical limestone model were designed. The used frequency range is from 2 GHz to 18 GHz in our simulation study. To obtain the data, we applied the following steps:

1) As shown in Fig. 2, lay down a pair of transmitter-receiver horn antennas at opposite sides of the breast model in the axis.
2) Put a spherical tumor model covered with limestone and pure spherical limestone model at any location *l* along the *y*-axis in the breast model.
3) Transmit signal using plane wave and receive the signal on the opposite side.
4) Transmission coefficients over the breast tissue with a spherical tumor model covered with limestone and pure spherical limestone model are obtained.
5) The above-mentioned steps are performed for 10 different radii.

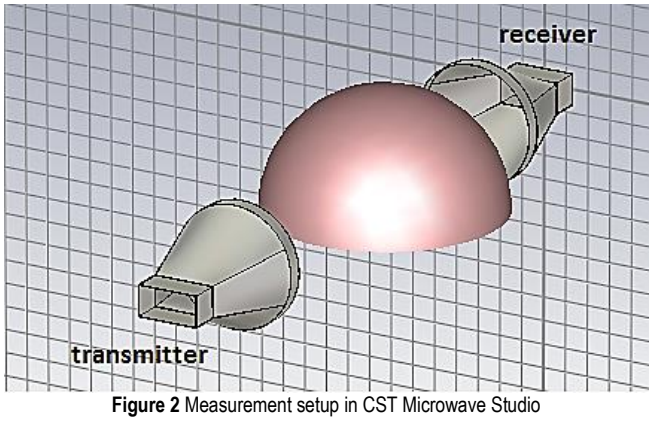

Figure 2 Measurement setup in CST Microwave Studio

Furthermore, the breast model was simulated to get the propagated signals through breast model with a spherical tumor model covered with limestone and pure spherical limestone model. The distance between transmitter and receiver antennas is only 25.9925 cm. Therefore, noise is remissible in this case.

Microwave imaging is performed by transmitting a sequence of electromagnetic waves through the female breast and measuring the scattered field on the breast. The electromagnetic signals fed to the transmitting antennas and captured by the receiving antennas are characterized by scattering parameters "S-parameters". Data acquisition process was conducted under simulation environment using CST Microwave Studio Software. The frequency was set from 2 GHz to 18 GHz. Fig. 2 shows the data collection process using Horn antennas at opposite sides of the breast model in the axis. This data process is repeated for 10 different radii of tumor.

3 TUMOR DETECTION USING ARTIFICIAL NEURAL NETWORK

One of the main problems of the mammogram is that the pure limestone and a tumor covered with limestone will produce same images on the X-ray film and this makes it impossible to distinguish these two cases from each other. However, the UWB imaging has the potential of discriminating these two cases from each other.

In this study, a feed-forward artificial neural network (FF-ANN) is trained to classify and predict the situation of the mass in the breast and decide whether it is a tumor covered with limestone or only a limestone without tumor. The input of the FF-ANN is the measurement frequency and the transmission coefficient parameters obtained at the receiver antenna, and the output is the classification result as a tumor or not. The transmission coefficients of the simulation result are given as complex numbers. The magnitude of these complex numbers is used for the FF-ANN. Although the simulation data is obtained for the frequencies between 2 ÷ 18 GHz, the data between 6.48 ÷ 11.50 GHz is more separable. Hence, the data between these frequencies, totally 315 different samples for each case, is used. The mean, range, standard deviation of the input data and the correlation between the data of the tumor covered with limestone and pure limestone are given in Table 3 for each mass size.

Table 3 Mean, range and standard deviation of the input data for each mass size

Mass Size (mm)	Mean	Range	Standard Deviation	Correlation
1	0.0271	0.0191	0.0056	0.9999
2	0.0270	0.0194	0.0056	0.9998
3	0.0271	0.0189	0.0055	1.0000
4	0.0271	0.0191	0.0056	0.9999
5	0.0270	0.0189	0.0055	0.9998
6	0.0271	0.0188	0.0055	0.9999
7	0.0274	0.0201	0.0055	0.9859
8	0.0263	0.0196	0.0054	0.9882
9	0.0296	0.0208	0.0060	0.9798
10	0.0293	0.0231	0.0064	0.9699

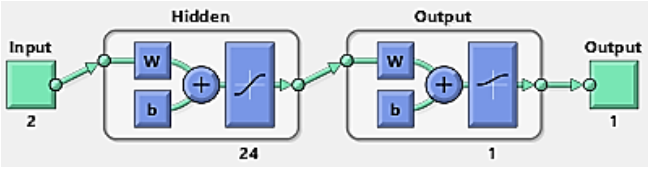

Figure 3 The ANN model schematic

For the number of the nodes in the hidden layer, all cases between 5 ÷ 25 nodes are tested and the best results are obtained with 24 nodes, Fig. 3. The learning function is selected as scaled conjugate gradient (trainscg) in MATLAB.

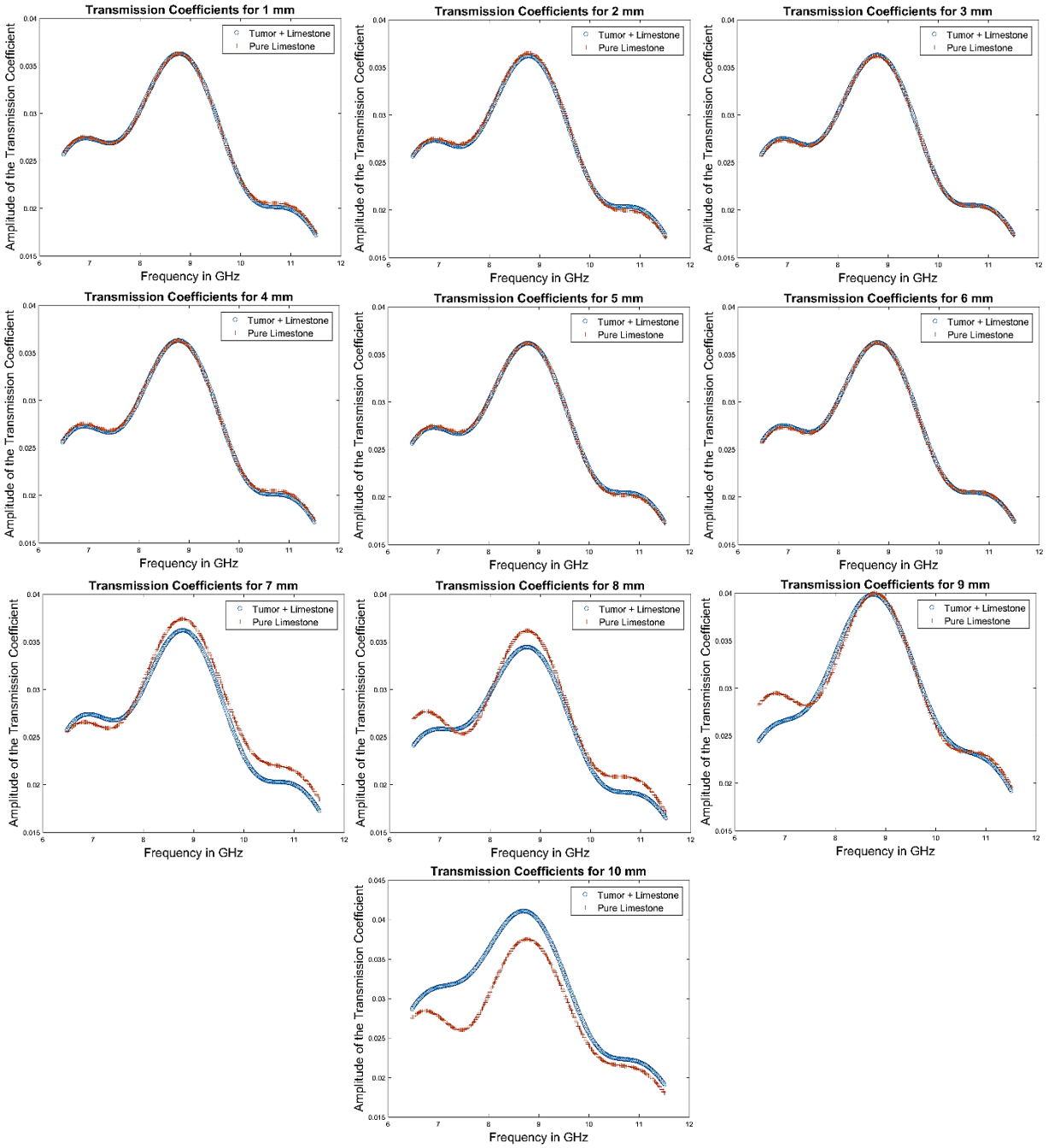

Figure 4 The transmission coefficients of tumor covered with limestone and pure limestone for mass sizes between 1 ÷ 10 mm

4 RESULTS AND DISCUSSIONS

10-fold cross validation is used to train and test the FF-ANN model. The data folds are created by randomly sampling the input data into 10 different groups. 9 groups are used for training and the last one for testing. These steps are repeated for all folds and the mean of the Correct Rate, Sensitivity and Specificity are calculated as total performance metric. The obtained results for different mass sizes are given in Tab. 4.

The prediction results, which are given in Tab. 4, show that the proposed method, on the contrary of the mammogram, has the potential of discriminating the tumor covered with limestone from the pure limestone, for the mass sizes of 7, 8 and 10 mm.

The reason why the method did not work well for the other mass sizes is that there is no usable difference between transmission coefficient parameters at any frequency in the given range, as it can be seen in Fig. 4 and Tab. 3.

Table 4 Mean Correct Rate, Sensitivity and Specificity for 10-fold cross validation of each mass size

Mass Size (mm)	Correct Rate	Sensitivity	Specificity
1	0.4889	0.4177	0.5680
2	0.4778	0.5022	0.4458
3	0.4841	0.4757	0.5263
4	0.4968	0.4845	0.5205
5	0.4905	0.4488	0.5565
6	0.4460	0.4857	0.4071
7	0.9111	0.8992	0.9249
8	0.8667	0.8167	0.9217
9	0.5524	0.5963	0.5303
10	0.9968	1.0000	0.9943

As a result of this study, if the examined mass size is 7,8 or 10 mm, the trained FF-ANN can be used for any input frequency and resultant transmission coefficient parameters between 6.48 ÷ 11.50 GHz to predict whether the mass is a tumor covered with limestone or pure limestone.

5 CONCLUSION

The results of the study show that UWB microwave imaging outperforms X-ray mammogram in cases of discriminating a tumor covered with limestone from a pure limestone mass. Although the UWB microwave imaging is a promising method for the mentioned problem, the performance of the method for the mass sizes smaller than 7 mm can be increased with different antenna designs. Therefore, better transmission coefficients, which make it possible to differentiate both cases from each other, might be obtained.

6 ACKNOWLEDGEMENT

This article is supported by the Scientific Research Unit of Adana Science and Technology University (Project number: 16119001).

7 REFERENCES

[1] Mahalakshmi, N.; Eyakumar, J. V.: Design and Develeopment of Single Layer Microstrip Patch Antenna for Breast Cancer Detection. // Bonfiring International Journal of Research in Communication Engineering, 2, 1(2012).

[2] Yu, J.; Yuan, M.; Liu, Q. H. A Wideband Half Oval Patch Antenna for Breast Imaging. // Progress in Electromagnetics Research, PIER 98, 2009, pp. 1-13.

[3] Saw, A.; Jone, A. A. Ultra Wide Band Radar Based Breast Cancer Detection Using Stacked Patch and Wide Slot Antenna. // International Journal of Electronics Signals and Systems, 3, (2013).

[4] Bohra, S.; Shaikh, T. UWB Microstrip Patch Antenna for Breast Cancer Detection, International Journal of Advanced Research in Electronics and Communication Engineering (IJARECE), 5, (2016).

[5] Adnan, S.; Abd-Alhameed, A.; Hraga, H. I.; Elfergani, I. T. E.; Noras, J. M.; Halliwell, R. Microstrip Antenna for Microwave Imaging Application. // Progress in Electromagnetics Research Symposium, Marrakesh, Morocco, 2011, pp. 20-23.

[6] Singh, S. K.; Singh, A. K. UWB Rectangular Ring Microstrip Antenna with Simple Capacitive Feed for Breast Cancer Detection. // Progress in Electromagnetics Research Symposium, Beijing, China, 2009, pp. 23-27.

[7] Choudhary, H.; Choudhary, R.; Vats, A.: Design and Analysis of Circular Patch Microstrip UWB Antenna for Breast Cancer Detection. // International Journal of Innovative Research in Science Engineering and Technology (IJIRSET), 4, (2015).

[8] Minz, L.; Simonov, N.; Ik Jeon, S.; Lee, J. M. Dual Layer UWB Dielectric Probe for Bistatic Breast Cancer Detection System, Proceedings of ISAP2012, Nagoya, Japan, 2012.

[9] Ragha, L. K.; Bhatia, M. S. Numerical Assessment of UWB Patch Antenna for Breast Tumor Detection. // ACEEE Int. J. on Electrical and Power Engineering, 1, 3(2010).

[10] Bah, M. H.; Hong, J. S.; Jamro, D. A. Ground Slotted Monopole Antenna Design for Microwave Breast Cancer Detection Based on Time Reversal MUSIC. // Progress in Electromagnetics Research C, 59, (2015), pp. 117-126.

[11] Kim, T. H.; Pack, J. K.: Measurement of Electrical Characteristics of Female Breast Tissues for the Development of the Breast Cancer Detector, 30, (2012), pp. 189-199.

[12] Adnan, S.; Abd-Alhameed, R. A.; See, C. H.; Hraga, H. I.; Elfergani, I. T. E.; Zhou, D.: A Compact UWB Antenna Design for Breast Cancer Detection. Progress in Electromagnetics Research Symposium Proceedings, China, 2010, pp. 887-890.

[13] Cheng, X.; Mao, J.; Bush, R.; Kopans, D. B.; Moore, R. H.; Chorlton, M.: Breast cancer detection by mapping hemoglobin concentration and oxygen saturation. // Applied Optics, 42, 31(2003).

[14] Ovechkln, A. M.; Yoon, G. Infrared Imaging for Screening Breast Cancer Metastasis Based on Abnormal Temperature Distribution. // Journal of the Optical Society of Korea, 9, 4(2005), pp. 157-161.

[15] Emwas, A. M.; Antakly, T.; Saoudi, A.; Al-Ghamdi, S.; Serrai, H. Magnetic Resonance Spectroscopy and Imaging in Breast Cancer Prognosis and Diagnosis. // Applications of NMR Spectroscopy, 3, (2015), pp. 4-35.

[16] Shao, W.; Zhou, B. UWB microwave imaging for breast tumor detection inhomogeneous tissue. // Proceedings of the 2005 IEEE Engineering in Medicine and Biology, 27th Annual Conference, Shanghai, China, 2005, pp. 1496-1499.

[17] Fear, E. C.; Stuchly, M. A. Microwave detection of breast cancer. // IEEE Transactions on Microwave Theory and Techniques, 48, (2000), pp. 1854-1863.

[18] Klemm, M.; Craddock, I.; Leendertz, J.; Preece, A.; Benjamin, R. Experimental and clinical results of breast cancer detection using UWB microwave radar. // Proceedings of IEEE Antennas and Propagation Society International Symposium, 2008, pp. 1-4.

[19] Abdel-Zaher, A. M.; Eldeib, A. M. Breast cancer classification using deep belief networks. // Expert Systems with Applications, 46, (2016), pp. 139-144.

[20] Caorsi, S.; Lenzi, C. A Breast Cancer Detection Approach Based on Radar Data Processing using Artificial Neural Network. // Research Journal of Advanced Engineering and Science, 1, 4(2016), pp. 213-222.

[21] Guan, J. S.; Lin, L. Y.; Ji, G. L.; Lin, C. M.; Le, T. L.; Rudas, I. J. Breast Tumor Computer-aided Diagnosis using Self-Validating Cerebellar Model Neural Networks. // Acta Polytechnica Hungarica, 13, 4(2016).

[22] Żejmo, M.; Kowal, M.; Korbicz, J.; Monczak, R. Classification of breast cancer cytological specimen using convolutional neural network. // In Journal of Physics: Conference Series, 783, (2017), 012060.

[23] Khuda, I.; Khatun, S.; Reza, K. J.; Rahman, Md. M.; Fakir, Md. M. Improved debye model for experimental approximation of human breast tissue properties at 6 GHz ultra-wideband centre frequency. // International Journal of Engineering and Technology (IJET), 5, 6(2013), pp. 4708-4717.

[24] Sill, J. M.; Fear, E. C.: Tissue sensing adaptive radar for breast cancer detection-experimental investigation of simple tumor models. // IEEE Transactions on Microwave Theory and Techniques, 53, (2005), pp. 3312-3319.

[25] Wang, M.; Yang, S.; Wu, S.; Luo, S. A RBFNN approach for DoA estimation of ultra-wideband antenna array. // Neurocomputing, 71, (2008), pp. 631-640.

[26] Lim, H. B.; Nhung, N. T.; Li, E.; Thang, N. D. Confocal microwave imaging for breast cancer detection: Delay-multiplyand-sum image reconstruction algorithm. // IEEE Transactions on Biomedical Engineering, 55, (2008), pp. 1697-1704.

[27] Fear, E. C.; Still, J.; Stuchly, M. A. Experimental feasibility study of confocal microwave imaging for breast tumor detection. // IEEE Transactions on Microwave Theory and Techniques, 51, (2003), pp. 887-897.

[28] Davis, S. K.; Tandradinata, H.; Hagness, S. C.; Veen B. D. Ultra-wideband microwave breast cancer detection: A detection-theoretic approach using the generalized likelihood ratio test. IEEE Transactions on Biomedical Engineering, 52, 7(2005), pp. 1237-1250.

Authors' contacts:

Ahmet AYDIN, Assistant Prof. Dr.
Çukurova University,
Department of Biomedical Engineering
Sarıçam-Adana/TURKEY
aaydin@cu.edu.tr

Emine AVŞAR AYDIN, Assistant Prof. Dr.
Adana Science and Technology University,
Department of Aeronautics Engineering
Adana/TURKEY
eaydin@adanabtu.edu.tr
rasvaenime@gmail.com

ISSN 1846-6168 (Print), ISSN 1848-5588 (Online)
ID: TG-20170209154052

Subject review

REVIEW OF LOW EMISSION ZONES IN EUROPE: CASE OF LONDON AND GERMAN CITIES

Matevž OBRECHT, Bojan ROSI, Tajda POTRČ

Abstract: Over 72% of population in Europe lives in cities nowadays, using a variety of different transportation vehicles for their intercity mobility. A high density of transportation vehicles in cities is a substantial problem in urban areas, since these vehicles are almost exclusively powered by fossil fuels. Fossil fuels have an impact on human health and emit harmful emissions to the environment when burned. Nevertheless, modern lifestyle is highly dependent on fossil fuels and therefore also highly vulnerable in the case of supply shortfalls. Nowadays, environmental problems and the impact of concentrated transport on human health, especially in cities, gained importance and lead to the detection and greater implementation of alternative technologies and advanced sustainable solutions in the field of environmental protection in cities. Since the EU is heavily dependent on imported fossil fuels and has very small oil reserves and a high share of urban population affected by transport pollutants, it is particularly important for the EU to reduce their impact as efficiently as possible and to implement new solutions for a more sustainable future. One such solution is represented with Green zones - areas where we try to minimize harmful transport related environmental and social impacts such as emissions, noise, smog, particle matter, etc. Therefore, this paper consists of an identification and examination of green zones in the selected EU member states (including UK) with special emphasis on German cities and London and analysis of their pros and cons.

Keywords: environmental impact; green cities; green zones; the EU

1 INTRODUCTION

More than one-half of the world's population now lives in urban areas, but they are blamed for producing as much as 80% of humanity's greenhouse gas emissions. Furthermore, increasing urbanization can negatively impact everything - from the availability of arable land and vital green spaces to potable water and sanitary waste disposal facilities.

Urbanization is one of the major problems in nowadays world. Population shifts from country to urban (city) areas to urban society with its growth that can very rarely be described as environmentally friendly or green [18]. It is predicted that by 2050 about 64% of the developing world and 86% of the developed world will be urbanized. As a result, the percentage of land with green spaces and environmentally friendly neighborhoods begin to decrease rapidly. Moreover, this is followed by factors such as overpopulation, overcrowding, housing problems, trash disposal problems, transport related problems, water supply and sewerage problems, and the problem of urban pollution [12].

A high density of transportation vehicles is also a substantial problem in urban areas, since these vehicles are almost exclusively powered by fossil fuels. Fossil fuels are a mixture of hydrocarbons that impact human health and emit to the environment harmful emissions when burned. In cities, conurbations and near busy roads, particulate emissions often account for clearly over 50% of air pollution. In an effort to protect human health, the EU has passed a European Directive which allows municipalities to establish environmental zones (also green zones) in city centers and conurbations [21]. European Union transport White Paper published in 2011 [5] also stresses the need to develop new transport systems which consume less energy and therefore produce less pollution. The goal of this White Paper is to achieve transport which is more sustainable, particularly in urban areas where environmental sustainability issues are more severe due to the high concentrations of activities and people [3]. Environmental zones, therefore, enable higher quality of living, less pollution, and smaller risk for human health [13]. Whether such zones are established and when they will become effective depends on the local conditions. It was studied that the most restrictive environmental zones are also most successful in decreasing pollution and increasing the quality of human health [13, 9].

Modern lifestyle is highly dependent on oil and therefore also highly vulnerable in the case of supply shortfalls. Rarity and transience of fossil fuels also lead to the detection and greater implementation of green technologies and advanced sustainable solutions in the field of environmental protection. Since the EU is heavily dependent on fossil fuels and has very small oil reserves, it is particularly important for the EU to reduce the use of fossil fuels as efficiently as possible and to implement innovative systems and solutions for a more sustainable future. One of these solutions is the introduction of green zones. These are the areas where we try to minimize green-house gas (GHG) emissions that result particularly from unsustainable transport [16].

Therefore, this paper is dedicated to pointing out the importance of growing environmentally friendly neighborhoods in cities, developing green zones, introducing emission free zones and stopping the greenhouse effect. The purpose of this work is to find out how green zones expansion helps to protect environmental and economic health of a community.

2 GREEN ZONES

If we try to define what a green zone is, we can get very different answers. The definition of a green zone can vary between different communities. However, the common

concept of a green zone is that it provides a local framework to protect the environmental and economic health of a community heavily affected by local pollution [2]. Problems related to urbanization mentioned before in the introduction help to picture green zone as a modern community or community area which is transformed from an economically depressed and highly polluted into sustainable, socially friendly, with new practices of green business, healthier environment, and capable economic future. Green zones can sometimes be defined also only as a green space (etc. a park or a green promenade). Growing appreciation of the role played by green spaces in regulating the local mesoclimate and in the removal of gaseous air pollutants derived from human activities has led many cities to become immersed in a frantic greening process, which has had a direct impact on the citizens' quality of life [1].
In 2010, the Environmental Protection Agency (EPA) confirmed the wide accepted concept of a green zone [2]:

1) Well developed regulation and its enforcement to punish responsible polluting industries;
2) A community voice in making land-use decisions;
3) Land use policies that prevent new pollution projects from locating them in these communities;
4) Focused private and public investment in local green development;
5) Support for businesses in the green zone that want to "green up" operations;
6) Greening these communities by creating more parks, community gardens and urban farms, and developing green businesses and jobs.

Even an entire city may be formed as a green zone. This concept of a green zone connects governmental institutions, society and business to work more effectively by creating communities in which all the stakeholders will have their profit. At the same time, the government could save money from inefficient investments. Nevertheless, the most important factor is that people enjoy living in a safe and healthy society with more new green jobs.

Green zones can be related to the so called "environmental justice", which means that an environment or a zone is healthy and safe, worth to live in, with access to arable land, clean water and air. People see amazing opportunities by themselves. Review of best practices revealed that since the 8th decade of the 19th century the better environment communities have been working on reducing and preventing local pollution in neighborhoods that endangers health and causes unhealthy life. That means that the concept of a green zone is entirely new.

Establishing green zones can have impact on the society where introduced and on municipality (or national) legislation and finances. On the one hand, public support can be gained with promotional events, calculations on emission reduction, and improved air quality. In Ljubljana, the green capital of the EU for 2016, it was stated that black carbon emissions had been reduced for over 70% [8]. On the other hand, financing the green zones can always be problematic in the beginning. However, external and related benefits must also be acknowledged. Wheeland [23] states that an investment of $ 1 million in green economy and clean technologies as well as sustainable development schemes generates 16.7 jobs while the same investment in e.g. fossil fuels generates only about 5.3 jobs. In addition to social efficiency, an investment in green zone will reduce health and environmental problems of a city.

One segment of a green or environmental zone is also a low emission zone (LEZ), where air pollution stemming from motor vehicle exhaust is minimized or completely prevented [9], and to which access of most polluting motor vehicles is restricted [3]. LEZs are becoming more and more globally extended, especially in environments where people are aware of negative impacts of personal vehicles on general health and quality of living as well as on the protection of buildings and general infrastructure. A LEZ essentially introduces a step change in the normal fleet turnover, resulting in lower emissions than those that would have occurred without the LEZ. Over time, the fleet emissions will become similar to those that would have occurred without the LEZ. For further benefits, it is necessary to periodically tighten the scheme's criteria [12].

3 METHODOLOGY

To achieve the objective, major tasks have been stated. In this paper, the selected best practices of green zones in the EU have been identified by reviewing special databases and best practices of green zones, emission free zones and traffic restricted zones throughout the EU. Different types of green zone schemes have been identified as well as their importance. Results have been analyzed and discussed. According to the impact, publicity, public acceptance of the selected green zones, time of establishment and data availability, this paper focuses especially on the green zone established in London, as a case of a mega-city green zone, and on green zones in Germany, as a case of a green zone scheme established on a country level.

Another goal was to explore the impacts of green zones on living environment and to identify and analyze core differences between the studied emission free zones in the selected EU member states and cities, where London is still defined as a city within the EU despite Brexit.

At the last stage of the study, by reviewing significant professional and scientific papers and specialized databases all best known green zones within the EU have been identified. These schemes have been analyzed and cross compared to examine what had already been done in existing green zone schemes and what their future plans and improvements are with regard to protecting the environment and create healthy communities. The relation between selected objects is followed by additional comments and proposals for the improvement.

4 LOW EMISSION ZONE IN SELECTED EU MEMBER STATES AND CITIES

4.1 Low emission zone in London

Among others, London has been identified many times as a financial and cultural capital of the world but its air quality is considered to be the worst amongst all the EU member states. London also failed to meet both the EU and the UK standards for air quality in urban areas.

That was one of the reasons why London implemented its first low emission zone in 2008 with a goal to reduce polluting emissions and their harm to society and architecture. Heavy diesel vehicles, buses and coaches were targeted as the most problematic polluters and were addressed in the first phase of the project. Therefore, minimum emission standards were requested for all vehicles operating and covering most of Greater London. Since implementation was phasal, data about its success are not yet sufficient. However, many improvements were identified in recent years, such as the turnover of fleet for problematic vehicle classes. In the second phase (starting in 2012), light commercial vehicles became subject of the low emission vehicle scheme and it also showed similar effect – turnover of a fleet. Despite the growth in freight vehicles operating in London, the number of pre-Euro 3 vehicles has been decreased and switched from rigid vehicles to light commercial vehicles. Environment air quality increased as particulate matter in London low emission zone decreased by 2.46 to 3.07 % [4].

By now, the low emission zone covers all local roads in Greater London as shown in Fig. 1. Dashed green line shows territory of Greater London which is covered as a low emission zone. Vehicles which do not meet minimum requirements and choose to enter the zone are required to pay a congestion price of £100 for large vans and £200 for heavy vehicles. Another special feature of London is that if the charge is not paid by midnight on the day the vehicle entered the zone, the adjusted penalty fine is five times higher. Central London colored in darker grey has additional £10 congestion charge as it is the most important and most densely populated part of the city with all of the most important institutions and buildings located there. Main roads and motorways which connect Greater London (black and grey lines) also belong to low emission zone scheme. Approximately 150,000 vehicles enter the London low emission zone daily. Out of that 95,000 vehicles are private. Some electric cars have filled up the streets, but their share is still marginal.

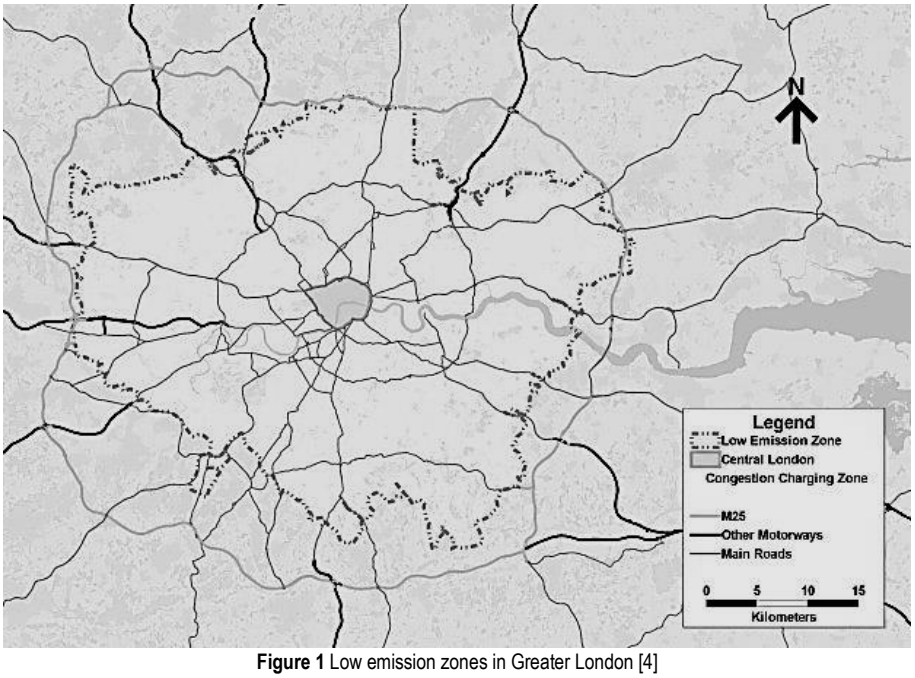

Figure 1 Low emission zones in Greater London [4]

Key achievements obtained with implementation of a low emission zone in London are:

1) Vehicle fleet change (people buying new produced cars with better environmental performance)
2) Downsizing - turnover from heavy to light vehicles;
3) Additional 20% drop in pre Euro 3 rigid vehicles in London (in comparison with areas outside LEZ);
4) Additional 10% drop in pre Euro 3 LCVs in London (in comparison with areas outside LEZ);
5) Air quality changes in the London's LEZ – slight improvement and lacking data measures on air quality.

By 2020, it is planned to turn the entire downtown area into an Ultra – LEZ in which only battery electric and low emission vehicles will be allowed to. The aim of zero emission by 2020 will also be set for all of the city's new taxis. Creating the world's first big-city ultra-low emission zone has the potential to be a changing moment in the quality of life in multimillion cities [15]. The massive use of

bicycles will bring benefits to air quality and encourage people to use new low emission technologies. A combination of restrictions, stimulation and opportunities gives more efficient results in society. One of the priorities that London should focus on when developing ultra-LEZ, is certainly to ensure appropriate infrastructure (e.g. sufficient amount of charging stations for electric vehicles).

4.2 Low emission zones in Germany

Germany established their first LEZs in January of 2008 in Berlin, Cologne and Hanover. Other cities also followed them in the following years. All vehicles entering LEZ no matter whether registered in Germany or abroad need to indicate an environmental badge to enter it. This badge is standardized for all the LEZs in Germany (Green zones n.d.). This stands for the implementation of German law based on the EU Directive 1996/62/EC and 1999/30/EC on ambient air quality and fine particles PM 2.5. In order to get an environmental badge your vehicle must be registered in and have a certain EURO standard.

Development of EURO standards for diesel and petrol technologies is already used in LEZ and in other countries and cities within the EU. Their development and restrictions are presented in Fig. 2 (Fig. 2a for diesel and Fig. 2b for gasoline technology). It is clearly visible that improvement of gasoline and diesel powered engines in accordance with EURO standards significantly reduces released emissions. The implementation of these standards is also widely accepted and mandatory for car manufacturers. For example, EURO 6 standard is mandatory for all newly produced cars from September 2015. Therefore, LEZ related to EURO standards can be easier to implement and control, since every vehicle EURO standard can be checked. Reduction of older, more environmentally disputable vehicles that cause higher pollution and emissions can be achieved with restrictions related on EURO standards as already implemented in many EU cities.

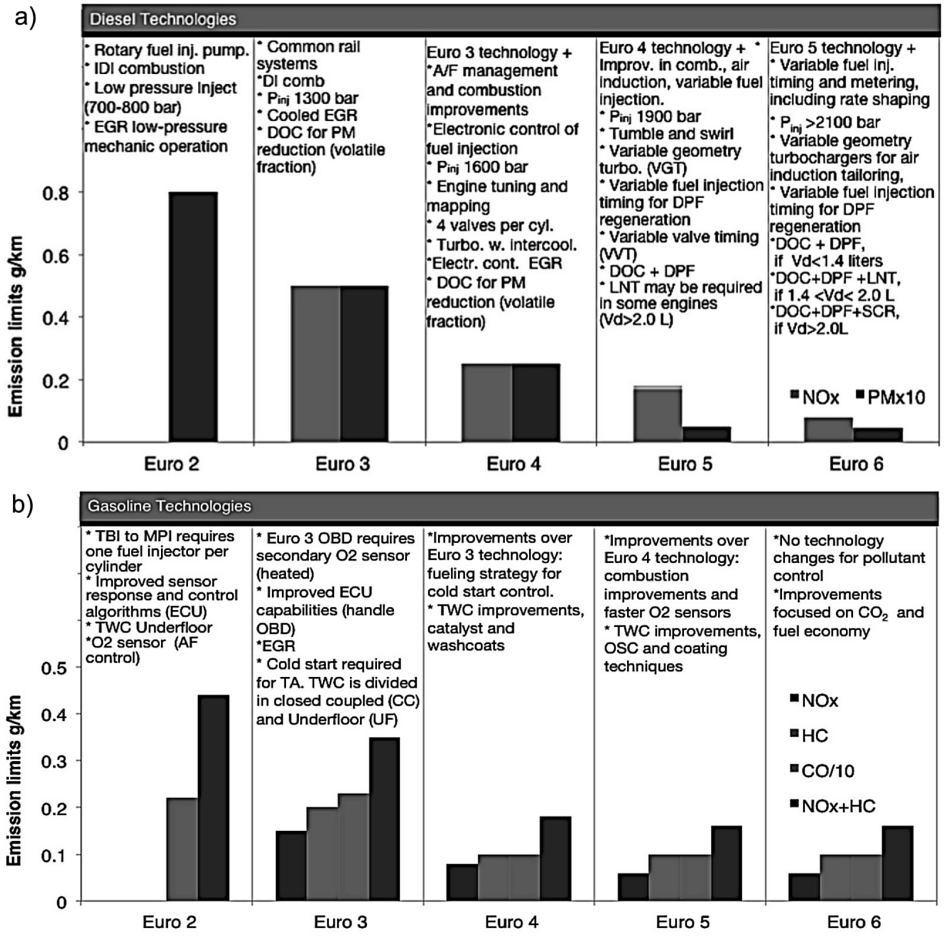

Figure 2 Development of EURO standards for diesel (2a) and gasoline (2b) technologies and their restrictions [20]

LEZ scheme in Germany also offers high quality information about all the Germany's LEZs, restrictions and regulations as well as presentation of prices of badges. This kind of information tool is important for faster implementation of LEZs and for their better acceptance in the public. Public therefore evaluates this service as user friendly.

Germany's LEZs are segmented in three groups and labelled with special signs on the roads (Green zones EU, 2010) as presented in Fig. 3 (upper right corner).

LEZs started to develop rapidly and efficiently after the failure in 2006, when Germany failed to meet up pollution standards for fine particulates of the EU [19], similarly as in the case of London. Currently, there are three stages of LEZ: Stage 1 LEZ only bans very high-emitting, non-sticker vehicles from entering the zone. Stage 2 LEZ bans non-sticker and red-sticker vehicles. Stage 3 LEZ only grants access to low-emitting vehicles with a green sticker. In all three stages of LEZs, certain exceptions apply, for example for vehicles on medical emergency calls, the police and fire brigades. Vehicle owners who enter LEZ illegally pay a fine of 80 EUR [13]. Since 2004, many car manufacturers in the EU have focused on revolutionizing the diesel engine by making it cleaner and significantly more fuel efficient so new diesel engines meet the highest emission standards as they have lower CO_2 emissions than gasoline powered vehicles [17].

In Fig. 3, different LEZs in Germany (in 2014) are presented. More than 70 German cities have one kind of a LEZ. Almost all of them are ranked in the environmentally friendly green class. Some crucial findings can be obtained when analyzing Fig. 3.

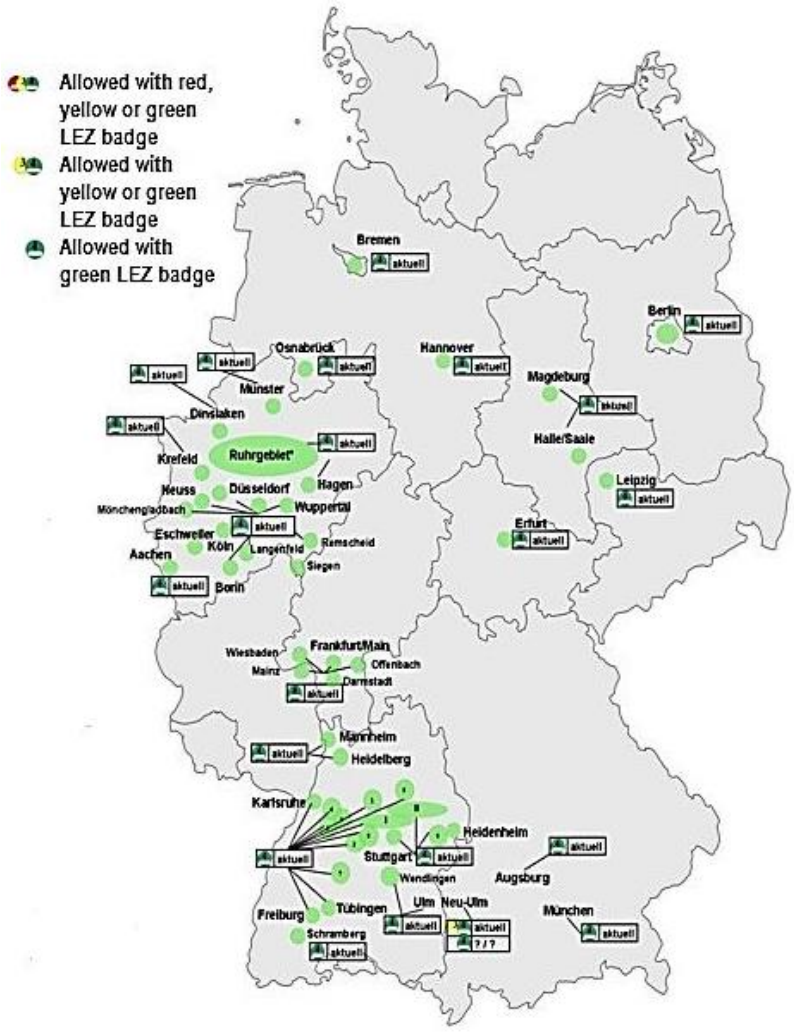

Figure 3 Low emission zones in Germany [22]

There are significant differences between states. North Rhine-Westphalia and Baden-Württemberg have significantly higher number of established LEZs. Geographically, most of Germany's LEZ are positioned in former West Germany, with exception of Bavaria, with relatively small number of established LEZs or even without them (i.e. Schleswig-Holstein).

The German example proves that LEZ means more than signs on the roads with begging and end and more than just badges and fines. The change from environmentally disputable vehicles powered by fossil fuels to low emission vehicles makes air cleaner. LEZ also promote combination of walking and cycling instead of driving internal combustion car. The main objective could be defined as to make cities more livable. Integrating green mobility within broader policy of green city development also encourages the use of public transport, which is more environmentally friendly, uses less space and causes less pollution per user than personal vehicle. If the public realized that moving on foot or by bicycles would dominate in future, quality of the journeys could also significantly improve. As a result, the air becomes cleaner and the noise level decreases to a

comfortable level. Government aim is not only to strictly match levels of the EU legislation but also to improve living environment for the society and to implement polluter pay principle (PPP) in practice.

Therefore, information about LEZs is available to everyone and is easy to understand. Funds collected with selling environmental badges and fines will further enhance and enable development of greener cities and development of LEZs (or also designated as green zones) in other cities and geographical areas. Progress can already be seen. Since many cities in Germany turned greener, vehicles that belong to the emission class 3 or lower are not permitted anymore and will therefore be substituted with newer and environmentally friendlier vehicles (environmentally friendlier in the use phase). There is still a dilemma whether this transition is environmentally friendly because old cars really do cause more environmental impacts in the use phase, but are already produced and do not need new materials and energy for their production like new ones. On the other hand, new cars cause less environmental impacts in the use phase but have higher environmental impact as an inevitable consequence of their production. Therefore, we can assume that in some cases life cycle assessment of all environmental impacts of a certain vehicle might actually favor the use of existing ones instead of new ones.

4.3 Comparison of green zones within the EU member states

Restrictions on urban areas transportation can be implemented through access limitations in the form of environmental zones, city tolls, congestion charging, etc. This measures spread rapidly in the recent years throughout the whole EU. Main objective is to establish "green zones" with reduced carbon, noise and light pollution.

However, the EU directives, national legislation and local regulations can differ widely. We have witnessed that local regulations can sometimes be very successful and should be taken into account also when preparing general EU directives on the field of sustainable urban transport planning. The European Commission [6] therefore expressed concerns with respect to an increasingly complex situation in Europe with traffic restrictions through environmental zones in the Green Paper 'Towards a new culture for urban mobility'. It has acknowledged the environmental objectives of these actions. In the Green Paper consultations many stakeholders called for guidance and for development of harmonized and unique rules for green zones within the EU. Standardization of green zones would be appreciated in order to enable a wide use of such measures without creating disproportionate barriers to mobility for citizens and goods especially when coming from another city or a EU member state with different regulation.

Better known green zones in the EU and their restrictions are presented in Tab. 1.

Table 1 Comparison of well-known green zones / low emission zones in the EU [10, 11, 12]

Vehicle Type	LEZ	Current Emissions standard (data for 2014)	Future Emissions standard
Lorries only	Netherlands	Euro 4	-
	Austria (Motorway A12)	Euro 2/3	-
	Austria (Steiermark & Graz)	Euro 3	-
	France/Italy (Mont Blanc Tunnel)	Euro 3	-
	Czech Republic (Prague)	Euro 2	-
	Hungary (Budapest)	Differential parking charges	-
Heavy duty vehicles	United Kingdom (London)	Euro 4 (PM)	-
	Denmark	Fit Filter if less than Euro 4	-
	Sweden	8 years old / Euro 3	
Vehicles with 4+ wheels	Germany	Euro 3-4 (PM) & Euro 1 Petrol	Euro 4 (PM) & Euro 1 Petrol
	Portugal (Lisbon)	Euro 1 or Euro 2	Planned: Euro 3 all (date not specified)
	Greece (Athens) Netherlands	Euro 1/Euro 4	Utrecht from 1/1/2015. Must be first registered after 1/1/2001
All vehicles	Italy	Euro 1-4 / no 2-stroke motorcycles	Euro 2-4 / no 2-stroke motorcycles
	Slovenia (Maribor)	Euro 0 and Euro 1	Continuing with LEZ if the test phase is successful
Local buses under agreements	United Kingdom (Norwich)	Euro 3 (NOx)	-
	United Kingdom (Oxford and Brighton)	Euro 5	-
Vans	United Kingdom (London)	Euro 3(PM)	
	Germany	Euro 2-4 (PM) & Euro 1 Petrol	Euro 3-4 (PM) & Euro 1 Petrol
	Italy	Euro 1-4 / no 2-stroke motorcycles	Euro 2-4 / no 2-stroke motorcycle
	Netherlands		Utrecht from 1/1/2015. Must be first registered after 1/1/2001

As presented in Tab. 1, different cities across the EU have established different green zones for different types of vehicles. Some of them already have developed long term strategy for further improvement of green zone standards. These future restrictions and standards will become more and more important and will have significant impact also on vehicle demand. It is predicted that green zones will also have positive effect on purchasing electric vehicles, hybrids and other vehicles powered by alternative environmentally friendlier fuels, since conventional vehicles will not be able to enter future green zones. However, it can be tricky that different green zones have different restrictions which are not customer friendly for people traveling between different cities. Therefore, the EU should consider standardized green zone policy framework and unique environmental tag for vehicles.

5 CONCLUSION

Green cities, neighborhoods and zones are being rapidly developed and implemented in many cities across Europe as well as in other continents. Since environmental awareness and energy prices are increasing, demand for green, efficient and rational transportation has increased in last decade. Green cities and green zones within them are becoming essential part of sustainable urban development with great potential for the future.

Further development of green zone research has also been identified. One idea is the monitoring of green zone development within the cities in the EU with regard to their environmental performance. This could represent a tool for improvements on lowering GHG emissions and other environmental impacts caused by unsustainable transport within the cities and would be useful as a model for the development of a larger number of standardized green zones inside the studied area. Tool or index could be primarily developed for the EU but could (with certain modifications) be generally applicable also to other geographical areas. Furthermore, such index would also allow monitoring of progress of a certain city on the field of environmental policy and their benchmarking. This could also be seen as a potential improvement for the monitoring of the efficiency of the EU environmental policies.

6 REFERENCES

[1] Carinanos, P.; Casares-Porcel, M. Urban green zones and related pollen allergy: A review. Some guidelines for designing spaces with low allergy impact. // Landscape and Urban Planning. 101, (2011), pp. 205-214.

[2] CBE. 2014. Green zones. Communities for a better environment. http://www.cbecal.org/issues/green-zones/ (3.2.2017).

[3] Cruz, C.; Montenon, A. Implementation and Impacts of Low Emission Zones on Freight Activities in Europe: Local Schemes versus National Schemes. // Transportation Research Procedia. 12, (2016). Pp. 544-556.

[4] Ellison, R. B., Greaves, S. P.; Hensher, D. A. Five years of London's low emission zone: Effects on vehicle fleet composition and air quality. // Transportation research part D. Transport and Environment. 23, (2013), pp. 25-33.

[5] European Commission (EC). 2011. WHITE PAPER: Roadmap to a Single European Transport Area – Towards a competitive and resource efficient transport system. http://eur-lex.europa.eu/legal-content/EN/TXT/PDF/?uri= CELEX:52011DC0144&from=EN.

[6] European Commission (EC). 2012. Clean transport, Urban transport - Green zones. http://ec.europa.eu/transport/ themes/urban/urban_mobility/urban_mobility_actions/green_zones_en.htm (10.1.2017).

[7] European Union. 2014. Owerview of LEZs. http://www.lowemissionzones.eu/overview-of-lezs, (22.1.2017).

[8] Ficko, T. Ljubljana - Green capital of Europe 2016. Oral presentation, 21.12.2016, Ljubljana city hall. (2016).

[9] Gehrsitz, M. The effect of low emission zones on air pollution and infant health. // Journal of Environmental Economics and Management. 83, (2017), pp. 121-144.

[10] Green zones. n.d. Information about German environmental zones**.** http://www.umwelt-plakette.de/englis_ informations. php (22.1.2017).

[11] Green zones EU. 2010. Environmental badge. http://www.environmental-badge.co.uk/en/environmental-badge.html (25.1.2017).

[12] Holman, C.; Harrison, R.; Querol, X. Review of the efficacy of low emission zones to improve urban air quality in European cities. // Atmospheric Environment. 111, (2015), pp. 161-169.

[13] Malina, C.; Scheffler, F. The impact of Low Emission Zones on particulate matter concentration and public health. // Transportation Research Part A: Policy and Practice. 77, (2015), pp. 372-385.

[14] MOM, Okoljska cona. http://www.maribor.si/ podrocje.aspx?id=1209 (25.1.2014), 2014 (in Slovenian language only).

[15] Motavalli. London to be an 'Ultra-Low Emission Zone' by 2020. // Forbes. 20.2.2013.

[16] Obrecht, M.; Knez, M. Development and Review of Green zones. / ICLST. Celje: Faculty of Logistics, 2014.

[17] Roland, M. Are diesel cleaner than gasoline engines. http://www.achatespower.com/diesel-engine-blog/2014/ 01/07/are-diesels-cleaner-than-gasoline-engines/ (8.1.2017).

[18] The Economist. Urban life: Open-air computers. The Economist. 27 October 2012. http://www.economist.com/ news/special-report/21564998-cities-are-turning-vast-data-factories-open-air-computers (2.10.2016).

[19] The German way. Driving in Germany: Green zones. http://www.german-way.com/travel-and-

tourism/driving-in-europe/driving/driving-in-germany-green-zones/ (22.1.2017).
[20] Transport policy. EU: Light-duty – Emissions. http://transportpolicy.net/index.php?title=EU:_Light-duty:_ Emissions (10.1.2017).
[21] TÜV. Emission stickers. http://www.tuev-sued.de/auto_ fahrzeuge/feinstaub-plakette/feinstaubplakette_ausland/ england (10.5.2017).
[22] Umweltbundesamt. Low emission zones in Germany – status. https://www.umwelt-plakette.de/de/home.html (25.1.2017).
[23] Wheeland, M. Green economy investments bring 300 percent more jobs. // Greenbiz. http://www.greenbiz.com/news/ 2009/06/18/green-economy-investments-bring-300-percent-more-jobs-reports-find (15.1.2017).

Authors' contacts:

Matevž OBRECHT
University of Maribor, Faculty of Logistics
Mariborska cesta 7, 3000 Celje, Slovenia
Phone: ++386 (0)3 428 5321; Fax: ++386 (0)3 428 5338
E-mail: matevz.obrecht@um.si

Bojan ROSI
University of Maribor, Faculty of Logistics
Mariborska cesta 7, 3000 Celje, Slovenia
Phone: ++386 (0)3 428 5310; Fax: ++386 (0)3 428 5338
E-mail: bojan.rosi@um.si

Tajda POTRČ
Slovenian National Building and Civil Engineering Institute (ZAG)
Dimičeva 12, 1000 Ljubljana, Slovenia
E-mail: tajda.potrc@zag.si

ISSN 1846-6168 (Print), ISSN 1848-5588 (Online)
ID: TG-20170513172848

Professional paper

BUILDING RESILIENCE THROUGH URBAN COMMONS: A POLICY RECOMMENDATIONS FOR ATOMIC SHELTER MANAGEMENT

Antonija BOGADI

Abstract: This paper presents set of arguments for incorporating urban commons as a way to increase resilience of the city. Vacant fallout shelters in residential neighborhoods are suitable case study, i.e. type of public place which could benefit from establishing commons management regime. Based on literature review on urban commons and site analysis, policy recommendations for developing urban commons on those sites are focused on needed actions from the local government and other stakeholders in "commons associations". Assigning bundles of rights to local user groups in order to stimulate self-organizing and long-term investments in active place management is a precondition for an urban common to succeed. The work presented here has implications for future studies of applicability of urban commons.

Keywords: fallout shelters; policy; resilience; urban commons

1 URBAN COMMONS IN THE RESILIENCE BUILDING OF CITIES

System's resilience is characterized by amount of change it can undergo while retaining the same controls on function and structure, and by its capacity of self-organization, learning, and adaptation. In the resilience discourse, key peculiarity for building resilience in complex systems is diversity management [1]. Diversity disperses risks, develops buffers, and diverse strategies from which humans can learn in situations when uncertainty is high. Diversity also helps by reorganization and renewal processes of disturbed systems [2] by allowing creativity and adaptive capacity to constructively deal with disturbance and change [1].

Analogously, if diverse groups of stakeholders, e.g. resource users from different ethnic and religious groups, scientists, community members with local knowledge, NGOs, and government officials, share management of a resource, it is stated in literature that they are making higher quality decisions, because stakeholders are more involved and can recognize better worth of the decisions [2, 3].

Nonetheless, group diversity can cause hardship for individuals to identify with the group, e.g. the greater the diversity in a group, the less integrated the group is likely to be, with higher level of dissatisfaction and loss of members [4].

Commons as a governing model which includes large spectrum of diverse stakeholders has been re-examined in last 25 years by scholars and practitioners. Until then economists and historians regarded the commons as a model exclusively tied to a feudal society. The reason for re-evaluation of that model is that it might offer a practical organizational model for todays' transitioning economy where "centralized command and control of commerce is capitulating to disturbed, laterally scaled, peer to peer production, where property exchange in market is becoming less relevant than access to sharable goods and services in networks, and where social capital is becoming more valued than market capital in modelling economic life" [5].

The literature review on urban commons shows that UCs are building urban resilience through [6]:

- Reducing potential social conflicts by offering arenas for management of cultural diversity, and therefore promoting cultural integration.
- UCs represent institutional re-development designs for cities to deal with crises (e.g. unemployment, economic recessions, underfunding of public area management).
- UCs represent institutional re-development designs for cities to deal with spatial changes such as when cities shrink or become too densely built.
- Long-enduring UCs can promote social - spatial memory in cities, important during periods of crises and/ or urban renewal and reorganization.
- UCs may provide economic benefits for local governments to manage urban public space by drawing upon civic voluntary management and therefore reduce economic vulnerability. There is a positive correlation between funding and management capability of areas under common management, suggesting that local governments with restricted financial capacities should consider voluntary site-management approaches like those offered by urban commons [6].
- Promote positive place making in cities, community empowerment and development [7], social integration, and democratic values [8].
- Case studies analysis of existing urban commons are showing that they promote social learning, in areas of gardening and local ecological conditions, learning about social organization, integration and participation, about the politics of urban space, and learning about social entrepreneurship [9].

Vacant fallout shelters in residential neighborhoods are suitable type of public place which could benefit from establishing commons management regime.

2 TYPOLOGY OF FALLOUT SHELTERS IN URBAN RESIDENTIAL NEIGHBORHOODS

Awareness of the fatal consequences of possible atomic explosions led to the construction of fallout shelters as the main typology of defense architecture during the Cold War in the former Yugoslavia.

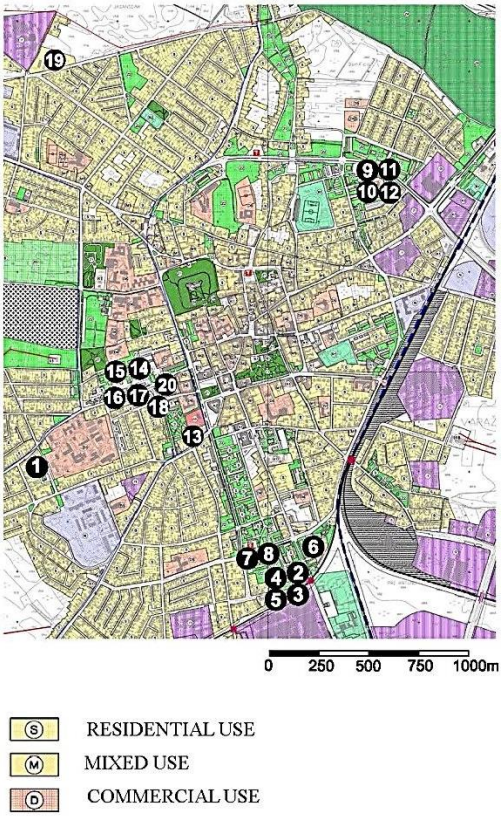

Figure 1 Location of fallout shelters in relation to land use types in Varaždin

Table 1 Fallout shelters built since 1965 to 1990 in Varaždin. The capacity of shelters calculated by one user per meter net area [10].

	Street	Net area (m^2)
1	Franje Galinca	150
2	Zagrebačka 13 - north	200
3	Zagrebačka 13 - south	200
4	Zagrebačka 15 - north	200
5	Zagrebačka 15 - south	200
6	Zagrebačka 73	300
7	Miroslava Krleže 1 (north)	200
8	Miroslava Krleže 1 (south)	200
9	Ruđera Boškovića 14c (north)	180
10	Ruđera Boškovića 14c (south)	180
11	Ruđera Boškovića 16 (north)	200
12	Ruđera Boškovića 16 (south)	200
13	Jalkovečka 10	100
14	Trakošćanska 14 (north)	200
15	Trakošćanska 14 (south)	200
16	Braće Radić 6	200
17	Braće Radić 31	100
18	Milkovićeva 3	100
19	Augusta Harambašića 32	250

With the development of modern weaponry and the ability to attack with a very short prior warning, an attack could happen at any time and in any place. There could not be much time for citizens to escape to other places, but only to the adjacent underground shelters. If the first wave of explosion was survived, further radioactive radiation would be equally deadly, so these shelters should support longer stays. For all of the stated reasons the construction of underground shelters in residential quarters was mandatory and it led to great changes in the urban landscapes (Tab. 1 and Fig. 1).

Mixing two different uses - military and housing - led to the development of a unique typology of fallout shelters in planned residential settlements built between the Second World War to 1990 (Figs. 3 and 4). Each residential building has its own underground shelter which is connected with underground hallways to a central shelter, above which the central public space is usually located. Atomic shelters have to be placed under the ground and protected by a layer of earth for better protection against radiation. These structures are hidden, cannot be seen from the pedestrian perspective, and the only indications of their presence are entrances, emergency exits, and ventilation pipes [10, 11], (Figs. 2 and 3).

Figure 2 Fallout shelter Ruđer Bošković in the center of residential quarters, with visible side entrances. A public square is on the roof of the shelter.

Figure 3 Fallout shelter Braća Radić in the center of residential quarters, with visible side entrances. A public square is on the roof of the shelter.

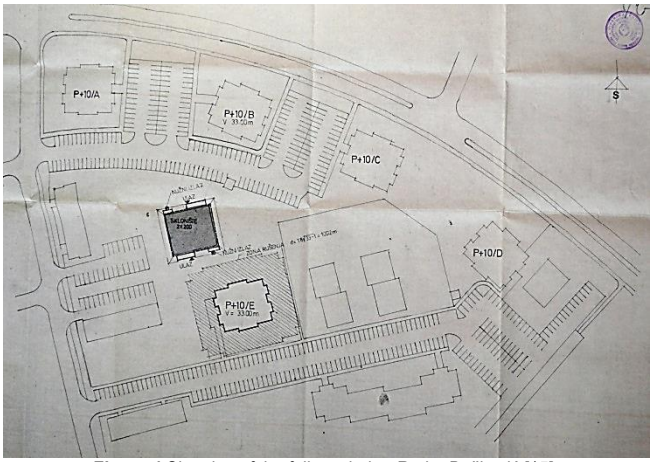

Figure 4 Site plan of the fallout shelter Ruđer Bošković [15].
The plan of the shelters is committed to their primary function. Shelters of the residential building are connected to the to the central room of the central shelter from which it is possible to access smaller accommodation rooms, sanitary facilities, water tanks, storages, etc. (Fig. 5).

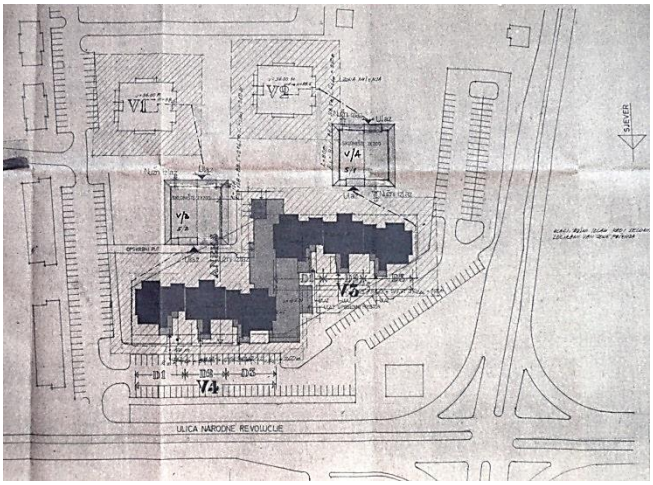

Figure 5 Site plan of the fallout shelter Miroslav Krleža [15].
The maintenance of shelters is financed by the City of Varaždin [12]. The primary function of atomic shelters is nowadays irrelevant. A few of the shelters today are used by non-profit organizations or are treated as storage spaces, but most of the potential that shelters provide due to their quality sites and their good construction status are largely neglected.

3 POLICY RECOMMENDATION FOR VACANT PUBLIC FALLOUT SHELTERS MANAGEMENT

This paper relies on the definition of urban commons as "physical spaces in urban settings of diverse land ownership that depend on collective organization and management and to which individuals and interest groups participating in management hold a rich set of bundles of rights, including rights to craft their own institutions and to decide whom they want to include in such management schemes" [6].

The main argument for managing fallout shelters and belonging parcels as urban commons is that governments may reduce maintenance and management costs by devolving management rights down to local user groups [6]. In those recommended institutional arrangements, governments retain their ownership, while assigning other rights to local user groups that will carry most of the costs related to maintenance and management. In that manner, urban commons are likely to enable a significant proportion of urban public space to be adequately used, maintained, managed and preserved.

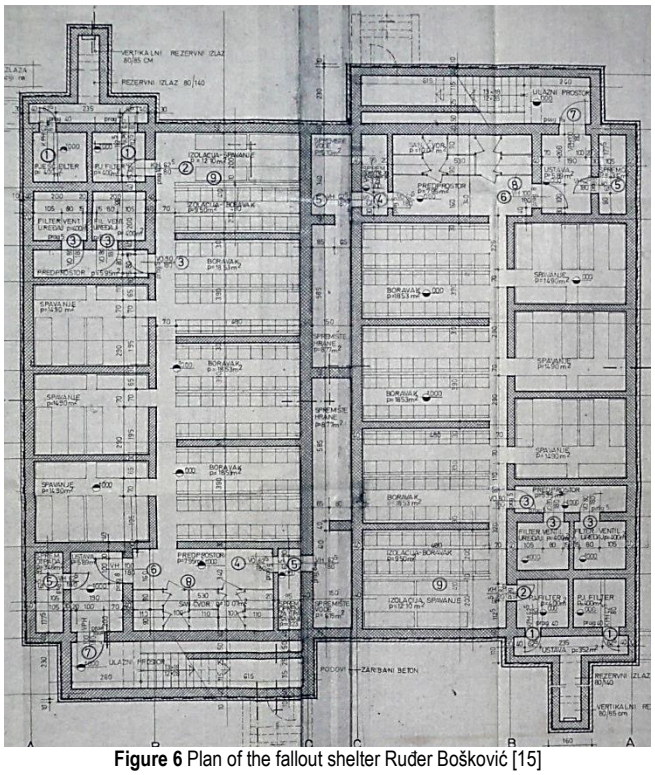

Figure 6 Plan of the fallout shelter Ruđer Bošković [15]

The critical feature of UCs rests on their practical management of land rather than on land ownership per se, implying that land used for urban commons may be owned by a number of potential owners, in this case by a local municipality.

The main condition for well-functioning urban commons is providing sufficiently stable property rights conditions in order to stimulate self-organizing, long-term investments in active place management. That is an obligation of local government and such incentives include the establishment of long-term leaseholds and incorporating urban commons in local development plans and strategies.

Participants in urban green commons are given critical bundles of rights by local government [13], including access rights, withdrawal rights, management rights, and exclusion rights to urban commons.

After property rights conditions and inclusion in local development plans are fulfilled, the design of the commons by the commons association is taking place. It is vital that government jurisdictions endorse the legitimacy of the rules established by the commons association.

Further recommendations for commons design are based on Elinor Ostrom's [13] "design principles" which are integral to every effective commons:

- Commons have to have clearly defined boundaries and "a commons association"; that is, it has to be clearly decided who (which individuals, groups, organizations, institutions, officials) is allowed to appropriate (in

further text: appropriators) from the commons and who is not.
- The time, place, technologies and quantity of the resources that can be used should be specified. Rules on amount of labor, materials, and money that can be allotted to the appropriation (urban common) should be precisely determined.
- Commons association needs to guarantee that those who are affected by the rules jointly and democratically determine those rules and their modifications over time.
- Commons association should ensure that those monitoring the activity on the commons are the appropriators of officials under an obligation to account to them.
- Appropriators who violate the rules should be gradually sanctioned by the other appropriators or officials accountable to the appropriators, and be guarded against overly vindictive punishment that questions their future participation and creates ill will in the community.
- Commons association has to design and practice procedures for prompt access to low cost private mediation to quickly resolve conflict among appropriators or between appropriators or public officials.

4 CONCLUSION

Main theme of the urban commons is that the people who know best how to govern their own lives are the community members themselves. If there are resources or services that are public, as in the case with fallout shelters in residential neighborhoods, and are best benefited by public access and use, then they are often best managed by the community as a whole.

Common property systems are also a beneficial option for local governments to consider when they lack funding for public space management [14], because they hold potential to reduce management and maintenance costs due to that they rely on volunteer-based engagement and on the self-interest of the participants.

This paper argues for adopting urban commons as a framework to restore vacant residential fallout shelters located in the valuable central areas in residential quarters, and it recommends diversity of institutional options for their arrangement in a city. Policy makers and planners should stimulate the self-development of UCs, and support their evolvement in urban areas through creating institutional space where urban residents are given management rights, while ownership rights are retained by the city.

5 REFERENCES

[1] Berkes, Fikret. "Can cross-scale linkages increase the resilience of social-ecological systems." RCSD International Conference, Politics of the Commons, Chiang Mai. 2003.

[2] Folke, Carl, Johan Colding, and Fikret Berkes. "Synthesis: building resilience and adaptive capacity in social-ecological systems." Navigating social-ecological systems: Building resilience for complexity and change 9.1 (2003): 352-387.

[3] Krasny, Marianne E., and Keith G. Tidball. "Civic ecology: a pathway for Earth Stewardship in cities." Frontiers in Ecology and the Environment 10.5 (2012): 267-273.

[4] Milliken, Frances J., and Luis L. Martins. "Searching for common threads: Understanding the multiple effects of diversity in organizational groups." Academy of management review 21.2 (1996): 402-433.

[5] Ribot, Jesse C., and Nancy Lee Peluso. "A theory of access." Rural sociology 68.2 (2003): 153-181.

[6] Colding, Johan, and Stephan Barthel. "The potential of 'Urban Green Commons' in the resilience building of cities." Ecological Economics 86 (2013): 156-166.

[7] Saldivar-Tanaka, Laura, and Marianne E. Krasny. "Culturing community development, neighborhood open space, and civic agriculture: The case of Latino community gardens in New York City." Agriculture and human values 21.4 (2004): 399-412.

[8] Shinew, Kimberly J., Troy D. Glover, and Diana C. Parry. "Leisure spaces as potential sites for interracial interaction: Community gardens in urban areas." Journal of leisure research 36.3 (2004): 336.

[9] Bendt, Pim, Stephan Barthel, and Johan Colding. "Civic greening and environmental learning in public-access community gardens in Berlin." Landscape and Urban planning 109.1 (2013): 18-30.

[10] Federal Secretariat for National Defence, 1987. Strategy national defense and social self Yugoslavia. Armed Forces Center for Strategic Research "Marshal Tito", Belgrade, 133

[11] Law on Protection and Rescue NN 174/04, 30 November 2004., Number: 01-081-04-3670 / 2, Zagreb

[12] National Protection and Rescue, 2010. Shelters Information on status and problems of shelter for people in the city of Varazdin, Regional Office for Protection and Rescue, Varazdin,

[13] Schlager, Edella, and Elinor Ostrom. "Property-rights regimes and natural resources: a conceptual analysis." Land economics (1992): 249-262.

[14] Authority, Greater London. Towards the London plan: initial proposals for the Mayor's spatial development strategy. Greater London Authority, 2001.

[15] State Archives Varaždin, City Council of Varaždin, file no. 06 - UPI - 1732/1979.

Author's contact:

Antonija BOGADI, lecturer
University North
Trg Zarka Dolinara 1
48000 Koprivnica, Croatia
antonija.bogadi@gmail.com

ISSN 1846-6168 (Print), ISSN 1848-5588 (Online)
ID: TG-20……..

14pt
14pt

ARTICLE TITLE ONLY IN ENGLISH (Style: Arial Narrow, Bold, 14pt)

14pt

Ivan HORVAT, Thomas JOHNSON (Style: Arial Narrow, Bold, 11pt)

11pt
11pt

Abstract: Article abstract contains maximum of 150 words and is written in the language of the article. The abstract should reflect the content of the article as precisely as possible. TECHNICAL JOURNAL is a trade journal that publishes scientific and professional papers from the domain(s) of mechanical engineering, electrical engineering, civil engineering, multimedia, logistics, etc., and their boundary areas. This document must be used as the template for writing articles so that all the articles have the same layout. (Style: Times New Roman, 10 pt, Italic)

10pt

Keywords: keywords in alphabetical order (5-6 key words). Keywords are generally taken from the article title and/or from the abstract. (Style: Times New Roman, 10 pt, Italic)

10pt
10pt

1 ARTICLE DESIGN
(Style: Arial Narrow, Bold, 10pt)

10pt

The article is written in Latin script and Greek symbols can be used for labelling. The length of the article is limited to eight pages of international paper size of A4 (in accordance with the template with all the tables and figures included). When formatting the text the syllabification option is not to be used.

10pt

1.1 General guidelines
(Style: Arial Narrow, 10pt, Bold, Align Left)

10pt

(First line indentation 5mm) The document format is A4 with 20 mm margins on all sides. A two column layout is used with the column spacing of 7 mm. The running text is written in Times New Roman with single line spacing, font size 10 pt, alignment justified.

Article title must clearly reflect the issues covered by the article (it should not contain more than 15 words).

Body of the text is divided into chapters and the chapters are divided into subchapters, if needed. Chapters are numbered with Arabic numerals (followed by a period). Subchapters, as a part of a chapter, are marked with two Arabic numerals i.e. 1.1, 1.2, 1.3, etc. Subchapters can be divided into even smaller units that are marked with three Arabic numerals i.e. 1.1.1, 1.1.2, etc. Further divisions are not to be made.

Titles of chapters are written in capital letters (uppercase) and are aligned in the center. The titles of subchapters (and smaller units) are written in small letters (lowercase) and are aligned left. If the text in the title of the subchapter is longer than one line, hanging indent of 0.7 mm is defined.

10pt

Typographical symbols (bullets), which are being used for marking an item in a list or for enumeration, are placed at a beginning of a line. There is a spacing of 10pt following the last item:

- Item 1
- Item 2
- Item 3

10pt

The same rule is valid when items are numbered in a list:

1. Item 1
2. Item 2
3. Item 3

10pt

1.2 Formatting of pictures, tables and equations
(Style: Arial Narrow,10pt, Bold, Align Left)

10pt

Figures (drawings, diagrams, photographs) that are part of the content are embedded into the article and aligned in the center. In order for the figure to always be in the same position in relation to the text, the following settings should be defined when importing it: text wrapping / inline with text.

Pictures must be formatted for graphic reproduction with minimal resolution of 300dpi. Pictures downloaded from the internet in ratio 1:1 are not suitable for print reproduction because of unsatisfying quality.

10pt

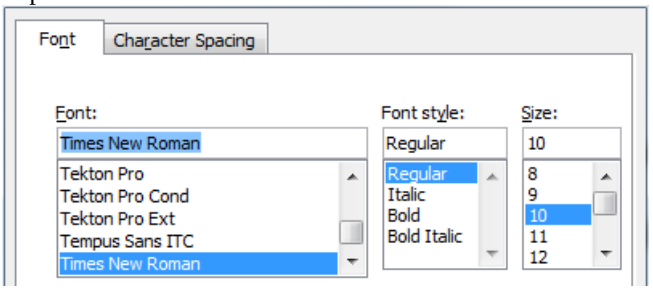

Figure 1 Text under the picture[1]
(Style:Arial Narraw, 8pt, Align Center)

10pt

The journal is printed in black ink and the figures have to be prepared accordingly so that bright tones are printed in a satisfactory manner and are readable. Figures are to be in color for the purpose of digital format publishing. Figures in the article are numbered with Arabic numerals (followed by a period).

Text and other data in tables is formatted - Times New Roman, 8pt, Normal, Align Center.

When describing figures and tables, physical units and their factors are written in italics with Latin or Greek letters, while the measuring values and numbers are written upright.

10pt

Table 1 Table title aligned center
(Style:Arial Narraw, 8pt, Align Center)

	1	2	3	4	5	6
ABC	ab	ab	ab	ab	ab	ab
DEF	cd	cd	cd	cd	cd	cd
GHI	ef	ef	ef	ef	ef	ef

10 pt

Equations in the text are numbered with Arabic numerals inside the round brackets on the right side of the text. Inside the text they are referred to with equation number inside the round brackets i.e. ".... from Eq. (5) follows ...." (Create equations with MS Word Equation Editor - some examples are given below).

10pt

$$F_{\text{avg}}(t,t_0)=\frac{1}{t}\int_{t_0}^{t_0+t}F\big(q(\tau),p(\tau)\big)\,\mathrm{d}\tau, \tag{1}$$

10pt

$$\cos\alpha+\cos\beta=2\cos\frac{\alpha+\beta}{2}\cdot\cos\frac{\alpha-\beta}{2}. \tag{2}$$

10pt

Variables that are used in equations and also in the text or tables of the article are formatted as *italics* in the same font size as the text.

Figures and tables that are a part of the article have to be mentioned inside the text and thus connected to the content i.e. „ … as shown in figure 1…" or „data from table 1…" and similar.

10pt

2 PRELIMINARY ANNOTATION

10pt

Article that is offered for publication cannot be published beforehand, be it in the same or similar form, and it cannot be offered at the same time to a different journal. Author or authors are solely responsible for the content of the article and the authenticity of information and statements written in the article.

Articles that are accepted for publishing are classified into four categories: original scientific papers, preliminary communications, subject reviews and professional papers.

Original scientific papers are articles that according to the reviewer and the editorial board contain original theoretical or practical results of research. These articles need to be written in such a way that based on the information given, the experiment can be repeated and the results described can be achieved together with the author's observations, theoretical statements or measurements.

Preliminary communication contains one or more pieces of new scientific information, but without details that allow recollection as in original scientific papers. Preliminary communication can give results of an experimental research, results of a shorter research or research in progress that is deemed useful for publishing.

Subject review contains a complete depiction of conditions and tendencies of a specific domain of theory, technology or application. Articles in this category have an overview character with a critical review and evaluation. Cited literature must be complete enough to allow a good insight and comprehension of the depicted domain.

Professional paper can contain a description of an original solution to a device, assembly or instrument, depiction of important practical solutions, and similar. The article need not be related to the original research, but it should contains a contribution to an application of known scientific results and their adaptation to practical needs, so it presents a contribution to spreading knowledge, etc.

Outside the mentioned categorization, the Editorial board of the journal will publish articles of interesting content in a special column. These articles provide descriptions of practical implementation and solutions from the area of production, experiences from device application, and similar.

10pt

3 WRITING AN ARTICLE

10pt

Article is written in the English language and the terminology and the measurement system should be adjusted to legal regulations, standards (ISO 80000 series) and the SI international system of units. The article should be written in third person.

Introduction contains the depiction of the problem and an account of important results that come from the articles that are listed in the cited literature.

Main section of the article can be divided into several parts or chapters. Mathematical statements that obstruct the reading of the article should be avoided. Mathematical statements that cannot be avoided can be written as one or more addendums, when needed. It is recommended to use an example when an experiment procedure, the use of the work in a concrete situation or an algorithm of the suggested method must be illustrated. In general, an analysis should be experimentally confirmed.

Conclusion is a part of the article where the results are being given and efficiency of the procedure used is emphasized. Possible procedure and domain constraints where the obtained results can be applied should be emphasized.

10pt

4 RECAPITULATION ANNOTATION

10pt

In order for the articles to be formatted in the same manner as in this template, this document is recommended for use when writing the article. Finished articles written in MS Word for Windows and formatted according to this template must be submitted using our The Paper Submission Tool (PST) (https://tehnickiglasnik.unin.hr/authors.php) or eventually sent to the Editorial board of the Technical Journal to the following e-mail address: tehnickiglasnik@unin.hr

The editorial board reserves the right to minor redaction corrections of the article within the framework of prepress procedures. Articles that in any way do not follow these

authors' instructions will be returned to the author by the editorial board. Should any questions arise, the editorial board contacts only the first author and accepts only the reflections given by the first author.

10pt

5 REFERENCES

10pt

The literature is cited in the order it is used in the article. Individual references from the listed literature inside the text are addressed with the corresponding number inside square brackets i.e. "… in [7] is shown …". If the literature references are web links, the hyperlink is to be removed as shown with the reference number 8. Also, the hyperlinks from the e-mail addresses of the authors are to be removed. In the literature list, each unit is marked with a number and listed according to the following examples (omit the subtitles over the references – they are here only to show possible types of references):

10pt

books:

[1] Franklin, G. F.; Powel, J. D.; Workman, M. L.: Digital Control of Dynamic System, Addison-Wesley Publishing Company, Massachusetts, 1990

[2] Kostrenčić, Z.: Teorija elastičnosti, Školska knjiga, Zagreb, 1982.

articles in journals:

[3] Michel, A. N.; Farrell, J. A.: Associative Memories via Artificial Neural Networks, IEEE Control System Magazine, Vol. 10, No. 3 (1990) 6-17

[4] Dong, P.; Pan, J.: Elastic-Plastic Analysis of Cracks in Pressure-Sensitive Materials, International Journal of Solids and Structures, Vol. 28, No. 5 (1991) 1113-1127

[5] Kljajin, M.: Prijedlog poboljšanja proračuna parametara dodira na primjeru evolventnih bokova zubi, Tehnički vjesnik/Technical Gazette, Vol. 1, No. 1,2 (1994) 49-58

articles published in conference proceedings:

[6] Albertsen, N. C.; Balling, P.; Laursen, F.: New Low Gain S-Band Satellite Antenna with Suppressed Back Radiation, Proc. 6th European Microwave Conference, Rome, September 1976, 14-17

[7] Kljajin, M.; Ergić, T.; Ivandić, Ž.: Izbor robota za zavarivanje uvjetovan konstrukcijom proizvoda, Zbornik radova - 3. međunarodno savjetovanje proizvodnoga strojarstva/3rd International Conference on Production Engineering CIM '95, Zagreb, November 1995, C-35 - C-41

links:

[8] http://www.sciencedaily.com/articles/w/wind_power.htm (Acessed:19.06.2012.)

10pt

10pt

Authors' contacts:

10pt

Full Name, title
Institution, company
Address
Tel./Fax,e-mail

Full Name, title
Institution, company
Address
Tel./Fax,e-mail